Aspects of quantum gravity in AdS_3/CFT_2

A dissertation for partial fulfillment
of the requirements for the degree of PhD
Pontificia Universidad Católica de Chile

Disseration zur Erlangung des
naturwissenschaftlichen Doktorgrades der
Julius-Maximilians-Universität Würzburg

vorgelegt von/submitted by

Ignacio A. Reyes

aus/from

Santiago de Chile

Würzburg, 2019

Eingereicht am/Submitted on:
bei der Fakultät für Physik und Astronomie, Julius-Maximilians-Universität Würzburg
Facultad de Física, Pontificia Universidad Católica de Chile

1. Gutachter / Reviewer: Prof. Dr. Johanna Erdmenger
2. Gutachter / Reviewer: Prof. Dr. Benjamin Koch
3. Gutachter / Reviewer: Prof. Dr. Max Bañados
4. Gutachter / Reviewer: Prof. Dr. Raimund Ströhmer
der Dissertation / of the Thesis

Vorsitzende(r) / Chair: Prof. Dr. Ansgar Denner

1. Prüfer / Examiner: Prof. Dr. Johanna Erdmenger
2. Prüfer / Examiner: Prof. Dr. Benjamin Koch
3. Prüfer / Examiner: Prof. Dr. Max Bañados
4. Prüfer / Examiner: Prof. Dr. Raimund Ströhmer
im Promotionskolloquims / in the Defense

Tag des Promotionskolloquims / Date of the Defense : 14.01.2019 / January 14th, 2019

Doktorurkunde ausgehändigt am / Doctoral degree granted on :

Abstract

The quest for finding a unifying theory for both quantum theory and gravity lies at the heart of much of the research in high energy physics. Although recent years have witnessed spectacular experimental confirmation of our expectations from Quantum Field Theory and General Relativity, the question of unification remains as a major open problem. In this context, the perturbative aspects of quantum black holes represent arguably the best of our knowledge of how to proceed in this pursue.

In this thesis we investigate certain aspects of quantum gravity in $2+1$ dimensional anti-de Sitter space (AdS_3), and its connection to Conformal field theories in $1+1$ dimensions (CFT_2), via the AdS/CFT correspondence.

We study the thermodynamics properties of higher spin black holes. By focusing on the spin-4 case, we show that black holes carrying higher spin charges display a rich phase diagram in the grand canonical ensemble, including phase transitions of the Hawking-Page type, first order inter-black hole transitions, and a second order critical point.

We investigate recent proposals on the connection between bulk codimension-1 volumes and computational complexity in the CFT. Using Tensor Networks we provide concrete evidence of why these bulk volumes are related to the number of gates in a quantum circuit, and exhibit their topological properties. We provide a novel formula to compute this complexity directly in terms of entanglement entropies, using techniques from Kinematic space.

We then move in a slightly different direction, and study the quantum properties of black holes via de Functional Renormalisation Group prescription coming from Asymptotic safety. We avoid the arbitrary scale setting by restricting to a narrower window in parameter space, where only Newton's coupling and the cosmological constant are allowed to vary. By one assumption on the properties of Newton's coupling, we find black hole solutions explicitly. We explore their thermodynamical properties, and discover that very large black holes exhibit very unusual features.

Kurzzusammenfassung

Die Suche nach einer vereinheitlichten Theorie zwischen Quantenmechanik und Gravitation ist von zentraler Bedeutung in der Hochenergiephysik. Trotz bahnbrechenden experimentellen Bestätigungen unserer Erwartungen aus der Quantenfeldtheorie und der allgemeinen Relativitätstheorie in der jüngeren Vergangenheit, bleibt die Frage nach einer vereinheitlichten Theorie unbeantwortet. In diesem Zusammenhang stellen störungstheoretische Aspekte quantenmechanischer schwarzer Löcher wohl eine der besten Anhaltspunkte dar, um diesen Ziel näher zu kommen.

In dieser Dissertation beschäftigen wir uns mit Merkmalen 3d-dimensionaler schwarzer Löcher im Anti-de-Sitter-Raum (AdS_3) und ihrem Zusammenhang zu (1+1)-dimensionalen konformen Feldtheorien (CFT_2) auf der Grundlage der AdS/CFT-Korrespondenz.

Wir untersuchen thermodynamische Eigenschaften schwarzer Löcher mit höherem Spin, insbesondere dem Fall von Spin 4. Hier zeigen wir, dass schwarze Löcher mit höheren Spin Ladungen im kanonischen Ensemble ein reiches Phasendiagramm aufweisen. Besonders bemerkenswert sind das Auftreten von Phasenübergangen des Hawking-Page-Typs, Phasenübergängen erster Ordnung zwischen schwarzen Löchern sowie eines kritischen Punktes zweiter Ordnung.

Ein weiterer Teil dieser Arbeit beschaeftigt sich mit vermuteten Zusammenhngen zwischen Bulk-Kodimension 1 Volumina und Komplexität in der CFT. Mittels Tensor-Netzwerken liefern wir konkrete Hinweise für die Korrelation zwischen diesen Volumina sowie der Anzahl an "Gates" in einem Quantenschaltkreis und legen ihre topologischen Merkmale dar. Zudem entwickeln wir, unter Verwendung des kinematischen Raumes, eine neue Formel anhand derer sich diese Komplexität direkt anhand von Verschränkungsentropien berechnen lässt.

Im Weiteren ändern wir unser Werkzeug und untersuchen Quanteneigenschaften schwarzer Löcher mittels Methoden der funktionalen Renormierungsgruppe basierend auf asymptotischer Sicherheit. Wir beschränken uns auf ein kleines Fenster im Parameterraum, in

welchen bloß Newtons Kopplungskonstante und die kosmologische Konstante variieren dürfen, und vermeiden hierdurch das Setzen einer beliebigen Skale. Eine einzige Annahme an die Eigenschaften der Newtonschen Kopplung, liefert uns explizite Lsungen schwarzer Löcher. Beim Untersuchen derer thermodynamischen Eigenschaften entdecken wir sehr ungewöhnliche Merkmale bei besonders großen schwarzen Löchern dieser Klasse.

Contents

Chapter 1

Introduction

1.1 The status of high energy physics today

The decade of 2010-2020 will pass to History as a memorable one for Physics. In less than ten years, two major experimental endeavours involving international cooperations have successfully achieved the purpose for which they were built for: the discovery of the Higgs boson in 2012 by Atlas and CMS at the LHC [1, 2], and the detection of of gravitational waves in black hole merging by LIGO [3, 4] in 2015. In both cases, the ideas ante ceded the facts, and by much. The existence of the Higgs boson was postulated in 1964 by Englert and Brout, and independently by Higgs [5–7]. On the other hand we have (almost fatefully) a century of gap: Einstein's paper predicting gravitational waves was published in 1918 [8]. These two are by far the most successful scientific theories in History.

On the one hand, we have quantum theory. Our present knowledge of the fundamental constituents of matter is the Standard Model (SM) of elementary particles. It is a renormalizable QFT in flat spacetime, containing as fundamental particles the leptons, the quarks, gauge bosons and the Higgs. It is based on two Symmetry principles. By requiring that all fields transform covariantly under the Poincare group (Lorentz transformations plus spacetime translations), we get a beautiful group-theoretic categorisation of particles in terms of two quantum numbers: mass and spin. The mass is understood as coming from the phenomenon of spontaneous symmetry breaking - the Higgs mechanics. Spin however has a much more geometric (and algebraic) origin: it is directly related

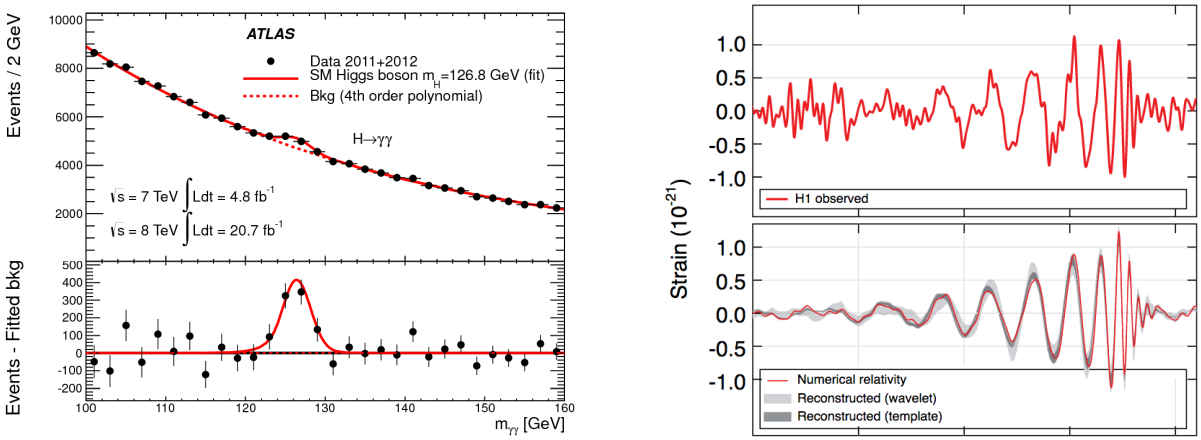

Figure 1.1: The two experiments of high energy physics of the decade. Left: the LHC detects the Higgs boson at around 125 GeV [1]. Right: LIGO signal, received in Hanford, Washington, of a gravitational wave coming from a black hole merger [3].

to the way in which the fields 'look different' when seen from a different frame of reference. Thus we have scalars, spinors and vectors. We will have much more to say about spin in Chapter 4. By requiring invariance under an internal symmetry, we also have the elegant structure of gauge theories build in it. In particular, the SM is built on a $SU(3) \times SU(2) \times U(1)$ gauge group acting on the different fields. Although it is considered an effective field theory (coming from some yet unknown more general framework) it has proven to be extremely accurate up to the 13 TeV achieved at the LHC.

On the other hand, we have General Relativity. By a simple but profound set of assumptions about the nature of space, time, rulers, clocks and light, Einstein was able to completely reform our notions of what gravity means. Instead of an action-at-distance, gravity is geometry. Einstein's equations,

$$G_{\mu\nu} = 8\pi G\, T_{\mu\nu} \tag{1.1}$$

are amongst the most complicated equations ever written in physics. They explain a vast class of phenomena. However, they reflect a remarkable elegant dynamic, as John Wheeler beautifully put it, "Spacetime tells matter how to move; matter tells spacetime how to curve" [9]. But the true richness of GR lies in its tremendous variety of applicability: from the perihelium of Mercury and the bending of light, to the theory of the Big Bang and the accelerated expansion of the universe, to the discovery of black holes and the recently measured gravitational waves.

In some sense, the two aforementioned experiments by LIGO and the LHC vividly reflect the situation in which high energy physics stands today. By separate, these two experimental evidences have given us spectacular tests of GR and QFT. But the principles behind these two theories belong, for the most of it, to two different bookshelves in the library of Physics.

But the quest for finding a unified description of both quantum mechanics and gravity is a long lasting dream in theoretical physics. Although by separate these two theories have been known for around a century, until now there has not been found a coherent scheme in which they can work together. This is not to say that no progress have been made. Indeed, much has been achieved.

It is against this background that we should understand why black holes have been (and will certainly remain) one of the key protagonists of this search. The study of black holes has dominated the field for several fundamental reasons. Since their theoretical prediction by Karl Schwarzschild in 1916 [10] until the early 1970s, it was believed that black holes belonged purely to GR, as cold dark objects from which nothing could escape. Therefore it came as a big surprise when Hawking, following the result from Bekenstein that black holes possess an entropy proportional to their area [11], showed in his series of seminal papers that black holes where in fact intimately connected to quantum mechanics and thermodynamics [12–15]. Two simple formulas materialised this relation:

$$S = \frac{A}{4G\hbar} \qquad , \qquad T = \frac{\kappa}{4\pi} \tag{1.2}$$

The first one is the Bekenstein-Hawking 'Area Law' for the entropy of a black hole. Until today, this formula remains one of the biggest riddles in quantum gravity. Although it provides an explicit formula for computing the entropy associated to a black hole, it tells us very little about what exactly are the microstates this multiplicity is supposed to be counting. We shall comment more on this issue in later chapters. The second one is the celebrated Hawking temperature. It asserts that black holes are in fact not black at all! By studying the behaviour of quantum fields in the vicinity of a black hole horizon, Hawking proved that an observer watching from far away will see the black hole emit black-body radiation at temperature given by (1.2). And even more, they proved that this entropy and temperatures are related via a first law of thermodynamics, where the

energy is given by the mass of the black hole,

$$dM = TdS \tag{1.3}$$

Last but not the least, Hawking further proved the famous Area theorem: in classical GR, the area of the event horizon of a black hole can never decrease. We have the second law of thermodynamics. These are remarkable discoveries, and it is fair to say that the quantum nature of black holes stands as the main foundation of our primitive understanding of quantum gravity. Whatever proposal for unification might be, it must be consistent with these findings.

But despite of these great successes, many deep questions remain about the implications of putting quantum theory and gravity together. Let us just mention a few. In quantum cosmology, the question of Cosmic inflation stands as one the key unsolved problems. Is inflation correct, and if so, what is the scalar particle (the 'inflaton') responsible for it? [16, 17]. Then there is the longstanding problem of the Cosmological constant or 'dark energy': the ratio between the 'natural' expected value of Λ from QFT and its measured value is roughly $\Lambda_{QFT}/\Lambda_{exp} \sim 10^{80}$ [18, 19], what has been dubbed as 'the worst theoretical prediction in the history of physics' [20].

Amongst the many challenges that quantum gravity involves, there is one particular direction that is most relevant for the purposes of this thesis. In recent years, there has been increasing efforts in finding new ways to address one problem: the black hole interior. Although the papers on which this thesis is based have not intended to tackle this problem directly, we will see along the way how our work is connected to this question. The interior of a black hole is mysterious for a variety of reasons. In the early days of GR, it was thought that the horizon was 'the end of spacetime'. Later it was discovered that the apparent singularity occurring there was merely a poor choice of coordinates, and that indeed one can shift to better coordinates and 'discover' much more of the manifold. However, the interior generically contains a catastrophe: an unavoidable spacetime singularity that leads to the breakdown of GR, and thus the predictability of the physics there. Many ideas have been proposed as 'resolutions' of the singularity problem, but to what extent they could be correct is far from being clear. We shall return to this point when discussing higher spin theories - it has been shown that the enlarged higher spin gauge symmetry could 'gauge away' singularities [21]. Of course, the Cosmic censorship conjecture [22] is

closely related to these ideas.

However the horizon itself is not devoid of controversy. Indeed, the last decade has seen a striking revival of old ideas, seen with a new light: the 'Information loss paradox' has sparked a lively debate on some very fundamental issues [23–26]. During the mid 1970s, there was a strong debate on wether the physical information that falls into a black hole is 'lost' or not to an outside observer. While some argued (most notably Hawking) that it was indeed lost, many others claimed that this could not be true for it would violate the principles of quantum mechanics. Although with the advent of the holographic principle (see below) the discussion was somewhat settled, the new findings of the last decade relating spacetime to entanglement have brought this issue back into the scene. In more modern language, the key question lies in the entanglement between the fields living inside and outside the horizon.

After the discovery of the Ryu-Takayanagi formula for holographic entanglement entropy [27](see below), it was realised that under certain circumstances, this could also be used as a tool to study the black hole interior. In particular, Maldacena and Hartmann [28] showed that, by considering the entanglement entropy of a two sided black hole, the minimal surfaces penetrate the interior and exhibited non-trivial time evolution. This was the spark that motivated Susskind [29] to study a property that will be of great importance in this thesis: **complexity**. In rough terms, Susskind's ideas was that in a maximally extended AdS black hole, there is a sense in which the Einstein-Rosen bridge (ER) - or wormhole - connecting the two sides is 'growing' in volume along time. He conjectured that this is dual to the growth of the *state complexity* of the dual boundary theory which is in a generalisation of an Einstein-Podolsky-Rosen state (EPR) or Bell state. Thus the acronym 'ER=EPR'. We will come back to this topic in Chapter 5.

Thus it seems that, regardless of the shape it might take, any major breakthrough in the study of the fundamental description of black holes will certainly require a modification of one or more of some well established notions of spacetime and quantum theory and the relation between them. Whether it's QFT that must adapt to GR or the other way around (or possibly some other ingredient not accounted for yet), one thing is clear: black holes have put our basic notions of physics at test.

1.2 The holographic principle and AdS/CFT

The Bekenstein-Hawking law for the entropy of a black hole (1.2), proportional to its area, was the starting point for many developments. In particular, it provided of a hint into what eventually came to be called the 'holographic principle'. The surprising thing about the area law is that, in usual thermodynamic systems like a gas, the entropy - which counts the logarithm of the number of accessible microstates giving the same macrostate - scales with the *volume* of the system rather than the area of the box where it is contained. It is as if the microstates of the interior would be projected as a hologram on to its boundary - the horizon.

Although quite vague, this principle was materialised very explicitly into what is known as the AdS/CFT correspondence or gauge/gravity duality (see Chapter 2). It was first proposed by Maldacena [30] in 1997 and since then has become a whole area of research on its own. Maldacena realised that within 10-dimensional string theory there exists some solutions containing D-branes hat had a very special property. If one takes a particular 'decoupling limit' one finds that the same physics should be described by two apparently very distinct theories. One is a type IIB supergravity living on $\mathrm{AdS}_5 \times S^5$. The other is a supersymmetric conformal cousin of QCD called $\mathcal{N} = 4$ Super Yang Mills (we shall explain all of this below). Moreover, the Super Yang Mills (SYM) theory lives on a flat Minkowskian background $\mathbb{R}^{1,4}$, which happens to be precisely the conformal boundary of the AdS_5 space. It looks as if the gauge theory was living 'on the boundary' of the supergravity theory, just as in the holographic principle of the black hole. The conjecture claims that these two theories are actually the same theory, written in very different variables. Having this duality at hand allows to explore the puzzles raised above from a new perspective, and we have learnt a great deal about perturbative quantum gravity in doing so in the last two decades.

This correspondence has passed a long series of non trivial checks, although it has not yet been rigorously proven. It has been generalised in many different directions which we shall not list here. We shall be interested in the lower dimensional version of it, that is not in $\mathrm{AdS}_5/\mathrm{CFT}_4$ but rather in $\mathrm{AdS}_3/\mathrm{CFT}_2$, which we review in the next chapter. And within that context, we shall focus on some specific aspects: its generalisation to include higher spin fields and understanding computational complexity. We will see that even in

such an apparently simple scenario, there are many things to learn about gravity and its relation to quantum theory.

One result that pioneered the introduction of quantum information theory into holography was the Holographic entanglement entropy formula by Ryu and Takayanagi [27]. This will be very important for some parts of this thesis, and we will review the proof in Chapter 3 and use it again in Chapter 5. In quantum theory, the most fundamental measure of bipartite entanglement is the **entanglement entropy**. Given a system with a Hilbert space that factorises into $\mathcal{H} = \mathcal{H}_A \otimes \mathcal{H}_B$, where $B = A^c$ is the complement, and given a density matrix ρ_{AB} in that space, the entanglement entropy between the subsystems A and B is computed as follows. First compute the reduced density matrix $\rho_A = \mathrm{Tr}_B \rho_{AB}$, and then calculate its von Neumann entropy (the quantum version of the classical Shannon entropy): $S_A = -\mathrm{Tr}_A (\rho_A \log \rho_A)$. In QFT, this is a very involved calculation, even in cases with high degree of symmetry. Thus it came as a great result, when Ryu and Takayanagi proposed, motivated by the Bekenstein-Hawking area law, that in holographic theories S_A is computed in a simple way. It is given by a quarter of the area of the minimal surface γ_{RT} that extends into the bulk, whose boundary coincides with the A/B interface at the asymptotic boundary (Fig. 1.2). A quantum information problem was converted into a geometrical one! We shall review this in more detail in Chapter 3.

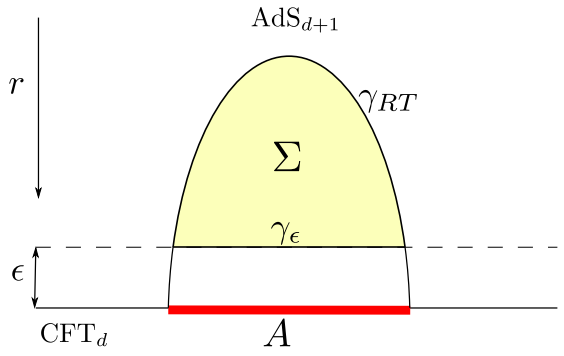

Figure 1.2: The Ryu-Takayanagi surface measures entanglement entropy $-\mathrm{Tr}\rho_A \log \rho_A$. Figure by R. Abt from [31].

1.3 Summary of this thesis and main results

We now briefly review more specifically the topics covered in this thesis. We introduce the key ideas, highlight the main results and comment on the new directions they suggest.

Chapter 3: Holographic Renyi entropies

We start by reviewing the original statement of the Ryu-Takayanagi conjecture. Next, we show the proof of Lewkowycz and Maldacena [32] of that formula, and explain its generalisation to Renyi entropies by Dong [33]. We then turn on to some applications of these prescriptions, and show how they can be used in practice, in particular to understand the phase diagram of the branched manifolds involved in the replica trick.

- We correct the Hawking-Page temperature to lowest order in the replica index $(n-1)$, for an arbitrary entangling region and dimension. It has a definite sign, implying that the temperature always increases (decreases) for $n > 1$ ($n < 1$).

- Working in a smallness expansion, we use the torus Renyi entropy from CFT_2 to find the modification to the modular group phase diagram. The possibility of new phase transitions is discussed.

- We match the CFT_2 thermodynamic Renyi entropy computed from the partition function, to the branched BTZ result, by integrating the area formula in the bulk.

Our analysis leaves many open questions regarding the thermodynamics of replicated manifolds. The possibility of an 'inverse' HP transition at low temperatures and of the HP 'disappearing' at certain replica index deserve further investigation. The most interesting open question is how to generalise the holographic Renyi entropies to non-holographic scenarios, which would lead to very interesting physical applications in real-world situations.

Chapter 4: Thermodynamics of Higher spin black holes

In Chapter 4 we study the physics of *higher spin black holes*. This does not mean a black hole with large angular momentum! It means a black hole that is embedded in a theory

with higher spin symmetry, i.e. interacting with fields of spin greater than two. A long standing question in both theoretical and experimental physics has been why haven't we detected particles of 'higher-spin' $s > 2$. Many beyond-Standard model theories seem to require their existence, but on the other hand no experimental evidence has been found. Is there some fundamental principle in Nature prohibiting their existence, or rather some technical or theoretical limitation? As we review below, in flat space *there is* an argument ruling them out: the theorems by Coleman-Mandula and Weinberg. However, these does not generically apply in curved spaces, such as our universe!

We study the case of black holes in AdS_3-like spacetimes interacting with fields of spin-3 and spin-4. Why AdS_3? Because it's simple. Higher-spin theories in higher dimensions are quite involved systems because in order to have a consistent theory one must couple an infinite number of higher spins together. However, in $2+1$ dimensions one can get away with a finite number of spins. Why black holes? Again, because of simplicity. Although extremely rich and still mysterious objects, in some sense black holes are surprisingly simple spaces. Moreover, in three dimensions they can be understood to a large extent by their topological properties.

In statistical mechanics, one must always specify in which ensemble one is working. The more familiar black holes have 'lower spin' charges and associated potentials: e.g. the mass is the spin-2 charge and temperature its conjugate variable. Similarly, higher-spin black holes carry additional charges Q_3, Q_4 which are conjugate to higher spin potentials μ_3, μ_4. We consider the grand-canonical ensemble, in which we fixed all the potentials of the system.

- We prove that the stability of these systems is not guaranteed, and in the grand canonical ensemble, a black hole whose highest spin potential is odd is unstable and will radiate all its higher spin charge away. Thus we consider solutions with spin-3 and spin-4 charges, which are guaranteed to be stable under certain assumptions.

- The main result is to exhibit the phase diagram of these black holes, Fig. 1.3. This is analogous to a T-P diagram in thermodynamics (intensive variables fixed).

- We discuss the existence of a first oder phase transition between black holes and the vacuum, known as the Hawking-Page transition.

- Next, within the phase space dominated by black holes, we find a first order transition between *different* black holes. It ends in a critical point, a second order phase transition, indicating that the thermodynamics of this system is indeed rich.

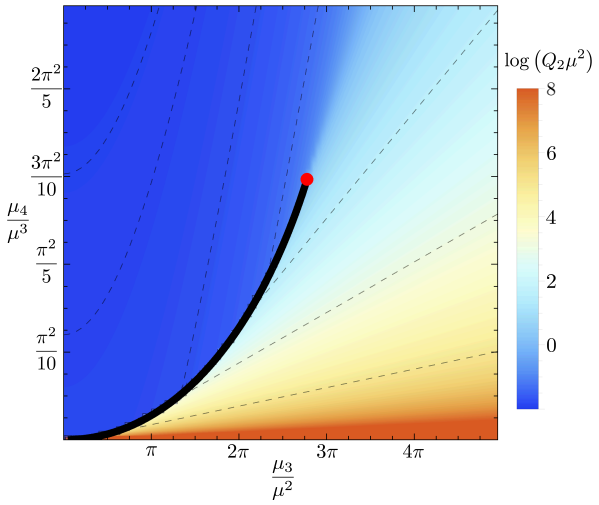

Figure 1.3: Phase diagram of higher spin black holes, for fixed spin-2 potential μ and varying spin-3 and spin-4 potentials. The color corresponds to the spin-2 charge value. It has a discontinuity along the solid line, ending on a second order phase transition. Figure from [34].

Many open questions remain. In the context of AdS/CFT, these higher spin theories on AdS_3 are conjectured to be dual to a specific kind of $1+1$ dimensional CFTs called 'coset minimal models'. Thus one should be able to describe the same physics purely from the boundary theory and find a precise matching. Also, although we focus on the spin-4 case, one should generalise this analysis for arbitrary spin-N fields, and moreover as we discuss below, extend it to *continuos* N.

Chapter 5: Holographic complexity and Tensor Networks

As we mentioned above, the problem of computational complexity is one of those topics coming from quantum information theory, that in recent years has seen a huge development in the gauge/gravity duality community. As we review in Chapter 5, this proposal introduces new concepts brought from quantum information and computer science into holography. In quantum computing, the central notion is the concept of a **quantum**

circuit. This consists of a set of initial data attached to wires which transmit them, on top of which one can apply **quantum gates**, a set of unitary operators acting on some number of wires. Then, given an input state and an output state, one can ask about its **complexity**: what is the minimal number of gates that we needed to turn the input into the output, given a set of allowed gates? When the input state is some initial state (wave-function or density matrix) and the output is the time evolution of it, this complexity is a function of time.

We mentioned above that in AdS/CFT, the entanglement entropy of the boundary is measured by certain minimal surfaces in the bulk. In an analogous manner, it has been argued that the complexity of the boundary state as a function of time is also captured by bulk observables. There are presently two competing proposals: 'Complexity=Volume' (CV) and 'Complexity=Action' (CA). The first one asserts that complexity is measured by the spacetime volume of a particular codimension-1 Cauchy slice anchored at the boundary. In the case of thermofield doubled states, this is closely related to the time growth of the 'size' of the Einstein-Rosen bridge in the maximally extended black hole spacetime. On the other hand, CA claims that complexity is given by the on-shell gravity action evaluated within a particular subset of the manifold known as Wheeler-de Witt patch.

Now there is a further proposal for complexity that has also gained much attention within the last few years: **subregion complexity**. This is very relevant for us, for it is on this quantity that we focused on in Chapter 5. As we mentioned above, the holographic dictionary states that the area of the Ryu-Takayanagi codimension-2 surface measures the entanglement entropy of the boundary theory. Then, it was proposed by Alishahiha [35] that the *volume* of the codimension-1 slice Σ **enclosed** by the RT surface should be capturing some form of complexity of the CFT (see Fig.1.2). However, to the best of our knowledge, no justification was given in the literature up to now about *why* should this quantity be associated with complexity. It is in this context that our work represents a progress in this direction.

In order to maximise simplicity, we consider AdS_3/CFT_2. The main result of our work was in providing an explicit and simple case in which we can understand why codimension-1 volumes in the bulk are indeed related to the complexity of a quantum

information problem on the boundary.

- By using the Gauss-Bonnet theorem in the bulk, we show that in $2+1$ pure gravity, subregion complexity is *topological*. We show that this implies, rather counterintuitively, that this complexity is independent of temperature.

- We interpret subregion complexity as the difficulty of a compression algorithm: to perform a unitary map of the reduced density matrix into the Hilbert space of smallest possible dimension.

- We generalise the construction of Random Tensor Networks [36] to the case of finite temperature, thus mapping the complexity to the magnetisation of the bulk Ising model, and confirm our analytic results by heat bath dynamics.

- We introduce the notion of 'mutual subregion complexity'. We show that it is UV-finite and measures the separability of the reduced density matrix.

- We provide a novel formula for bulk volumes using Kinematic Space, which allows to express complexity explicitly as an integral over the entanglement entropies.

- We use the MERA network and showed how to define the complexity there. This provides concrete evidence to link codimension-1 bulk volumes in AdS to a particular measure of complexity in the boundary.

One of the most interesting questions our work opens up is understanding exactly how is our calculation related to the original proposals for complexity measures. In our analysis, the bulk volume as a 'gate-counter' is very transparent and natural. With this in mind, one could guess that the codimension-1 volume proposed by Susskind should be also counting some number of gates. But exactly *which* gates is it counting, and how our compression-algorithm interpretation related to the complexity of time evolution is still not clear. We see that many exciting developments are still ahead.

Chapter 6: Black holes with running couplings in AdS_3

A different approach to quantum gravity is known as Asymptotic Safety, an idea originally proposed by Weinberg [37, 38]. The idea was that, although from dimensional

analysis gravity is not perturbatively renormalizable, it might be the case that it is **non-perturbatively** renormalizable. This cannot be in principle discarded, since the usual diagrammatic approaches fail as we go to strong coupling. The conjecture is that Einstein gravity hits a UV fixed point at finite couplings, instead of flowing to some ill defined curve in theory space. This implies that the gravity couplings, such as the Newton and cosmological 'constants' are not constants but are allowed to vary with the renormalization group scale k.

We consider an application of the above scenario, for the study of 2+1 AdS black holes within the 'Einstein-Hilbert truncation'. This means we restrict to curves in parameter space in which the only couplings flowing are G_k and Λ_k. Now, instead of solving the Wetterich equations directly, we follow the Brans-Dicke like approach of [39,40], where the goal is to study an 'improvement' of the classical Einstein-Hilbert action, by associating the scale with the spacetime location $k = k(x^\mu)$, which induces a spacetime dependence for the couplings $G = G(x^\mu), \Lambda = \Lambda(x^\mu)$. The key point of our approach is that we avoid the step of setting the scale $k(x)$ which is usually done in the literature by resorting to intuitive arguments. In fact, we ask a different question: whatever the solution to the Wetterich RG equation and the scale setting are, what class of running couplings actually satisfy the Einstein equations?

The main results of this section are the following:

- We analytically find the most general static spherically symmetric solution to pure 3d Einstein gravity that allow $G = G(r), \Lambda = \Lambda(r)$, under the assumption that the stress tensor induced by the RG flow saturates the null energy condition. They include pure AdS_3, and a generalisation of the BTZ solution.

- The improved BTZ solution develops a curvature singularity at the origin, which is consistent with the known properties of BTZ under matter perturbations.

- In certain regimes, these black holes have very peculiar thermodynamic properties. As the mass goes to infinity, the radius of the horizon and the temperature converge to finite values. Moreover, in this limit the entropy scales as the perimeter squared, instead of the usual area law.

The precise connection between our results from Asymptotic safety and AdS/CFT

require further investigation.

This thesis is organised as follows. In Chapter 2, we provide a brief review to the AdS/CFT correspondence. We describe its string theory origin, focusing on the AdS_5/CFT_4 example, and then discuss the salient properties of AdS_3/CFT_2, which is the one we will be concerned with. Chapter 3 is devoted to reviewing the holographic entanglement entropy formula by Ryu and Takayanagi together with its Renyi generalisations. We also provide some simple results on the phase diagram of the replica manifold. In Chapter 4 we introduce higher spin holography. We briefly review the Chern-Simons formulation and the coset constructions of the W_n algebras in the CFT. After these preludes, we show our work on the phase diagram of spin-4 black holes. Chapter 5 is devoted to holographic complexity. We begin by reviewing the holographic proposals, and then describe the two tensor networks that are relevant for our thesis: MERA and Random tensors. We then describe our work on subregion complexity from the gravity side, the tensor networks and the CFT using kinematic space. Finally, Chapter 6 explores, still in AdS_3, an alternative approach to quantum gravity, that of Asymptotic Safety. After reviewing the Wetterich equation, we explore the Einstein truncation of the renormalisation group equations, and describe black hole solutions in it. We discuss their thermodynamic and geometric properties. We end with some conclusions. In Appendix A we describe the construction of the hs[λ] algebra, relevant for the higher spin gravity.

Chapter 2 is partially based on [41], a review work done in collaboration with M. Bañados. The results of Chapter 3 are based on a soon to be published work, in collaboration with P. Fries. The contents of Chapter 4 are based on [34], done in collaboration with M. Bañados, G. During and A. Faraggi. The discussion of Chapter 5 is based on [31], work done together with R. Abt, J. Erdmenger, R. Meyer, Charles Melby-Thompson, C. Northe and H. Hinrichsen. The results of Chapter 6 follow [42], done in collaboration with B. Koch and A. Rincón.

Chapter 2

Introduction to AdS/CFT

2.1 A precursor: boundary terms and conditions

Before going into the details of holography, in this section we start by reviewing the importance of the boundary term analysis in gauge theories. To be very concrete, we discuss the problem of how to define the energy in a system with gauge symmetry. Although our aim is to focus on gravity, we shall frame the problem explicitly for $2+1$ Chern-Simons theory and end by going back to GR. This example is ideal since it shows clearly the role of the boundary conditions one chooses, and once this is done, how the boundary terms determine the value of the Hamiltonian. We emphasize that by itself this is not gauge/gravity duality yet, but these 'boundary issues' were one of the important precursors of the correspondence.

How does one define the energy of a black hole in general relativity? The first answer would be of course the Hamiltonian. However, the Hamiltonian of GR is given in the ADM decomposition by

$$H_0 = \int d^D x \left(N\mathcal{H} + N_i \mathcal{H}^i \right) \tag{2.1}$$

where N, N_i are Lagrange multipliers and $\mathcal{H}, \mathcal{H}^i$ are constraints that vanish if the Einstein equations are satisfied. Therefore, if we evaluate the Hamiltonian (2.1) on any metric satisfying the e.o.m., it is equal to zero. This could be reasonable for pure Minkoswki space, but how could it be true for a solution like a black hole? This problem was already realised by Dirac [43], but it was not until the work of Regge and Teitelboim [44] that a

satisfying explanation was provided. We shall not give a complete account of this story, but rather focus specifically on the problem of the energy.

With this in mind, let's dive into Chern-Simons theory and ask the same question. Consider with the usual CS action in 3 dimensions,

$$\frac{k}{4\pi}\int_{\mathcal{M}} \mathrm{Tr}\left(A\wedge dA+\frac{2}{3}A\wedge A\wedge A\right) \tag{2.2}$$

In order to make the Hamiltonian discussion clear, one performs a space + time decomposition $A_\mu=(A_0,A_i)$. This involves integrating by parts and dropping some boundary terms. One is left with the following action, which we will consider as our starting point:

$$I_{CS}[A]=\frac{k}{8\pi}\int_{\mathcal{M}} d^3x\ \epsilon^{ij}\,\mathrm{Tr}\left(A_i\dot{A}_j-A_0F_{ij}\right) \tag{2.3}$$

What are the equations of motion of this action? Let us find out by varying the action:

$$\begin{aligned}\delta I_{CS}&=\frac{k}{8\pi}\int d^3x\ \epsilon^{ij}\mathrm{Tr}\left(-\delta A_0F_{ij}+\delta A_i\dot{A}_j-\dot{A}_i\delta A_j-A_0\delta F_{ij}+\cancel{\frac{d}{dt}(A_i\delta A_j)}\right)\\&=-\frac{k}{8\pi}\int d^3x\ \epsilon^{ij}\mathrm{Tr}\left(\delta A_0F_{ij}+2\dot{A}_i\delta A_j+A_0\delta F_{ij}\right)\ ,\end{aligned} \tag{2.4}$$

where the time derivative vanishes since the initial/final configurations are held fixed, and we used the cyclic property of the trace. Moreover, it is direct to show that $\epsilon^{ij}\mathrm{Tr}\left(A_0\delta F_{ij}\right)=2\epsilon^{ij}\mathrm{Tr}\left[\partial_i\left(A_0\delta A_j\right)-D_iA_0\delta A_j\right]$, where D_i is the covariant derivative. Thus we obtain

$$\delta I_{CS}=-\frac{k}{8\pi}\int d^3x\ \epsilon^{ij}\mathrm{Tr}\left(\delta A_0F_{ij}+2\left(\dot{A}_i-D_iA_0\right)\delta A_j+2\partial_i\left(A_0\delta A_j\right)\right) \tag{2.5}$$

The first two terms give precisely the standard e.o.m. for CS, namely

$$\text{CS e.o.m.}\qquad F^a{}_{ij}=0\qquad,\qquad \dot{A}^a{}_i=D_iA^a{}_0 \tag{2.6}$$

The last term in (2.5) is a total derivative, which is the prototype of term that is assumed to vanish in many field theory discussions. However, in general it doesn't. Isolating this term and using Stoke's theorem, we have

$$\delta I_{CS}=\frac{k}{8\pi}\int(\text{e.o.m.})-\frac{k}{4\pi}\int dt\int_{r\to\infty}d\varphi\ \mathrm{Tr}\big(\left(A_0\delta A_\varphi\right)\big)\ , \tag{2.7}$$

Thus in order for the CS e.o.m. to be an extremum, we should pass the boundary term in (2.7) to the left hand side and this should define a new action:

$$\delta I_{CS}+\frac{k}{4\pi}\int dt\int_{r\to\infty}d\varphi\ \mathrm{Tr}\big(\left(A_0\delta A_\varphi\right)\big)=\frac{k}{8\pi}\int(\text{e.o.m.})\ . \tag{2.8}$$

But this is equivalent to a redefinition of the Hamiltonian in the action. Calling H_0 the 'naive' Hamiltonian $H_0 = \frac{k}{8\pi}\int \epsilon^{ij} A_0 F_{ij}$ coming from (2.3) - which is the CS version of the GR Hamiltonian (2.1) - the correct Hamiltonian must include an extra boundary term E,

$$H = H_0 + E \ , \tag{2.9}$$

whose variation we know,

$$\delta E = \frac{k}{4\pi}\int dt \int_{r\to\infty} d\varphi \ \mathrm{Tr}\big((A_0 \delta A_\varphi) \big). \tag{2.10}$$

This E is by definition the boundary term that makes the functional H or equivalently the action well-defined. We choose to call it E referring to 'energy', because it equals the value of H on any solution of the equations of motion, since the bulk piece H_0 is a constraint. We would now like to 'functionally integrate' (2.10) to find E. But since δE depends on the fields and their variations, we must now provide more information about the system's behaviour at the boundary.

Motivated by the black hole solution, let's take the chiral condition that $A_0 = A_\varphi$ as $r \to \infty$. Then, (2.10) becomes a total variation in δ,

$$\delta E = \frac{k}{4\pi}\delta \int dt \int_{r\to\infty} d\varphi \ \mathrm{Tr}\left(\frac{1}{2}A_\varphi^2\right) \ , \tag{2.11}$$

from where we obtain

$$E[A_\varphi] = \frac{k}{8\pi}\int dt \int_{r\to\infty} d\varphi \ \mathrm{Tr}\left(A_\varphi^2\right) \ , \tag{2.12}$$

With these boundary conditions, this is the correct energy of the system.

Finally, let's go back to the black hole. As we will review below, in the CS formulation the euclidean BTZ black hole is given by a specific A_φ, whose asymptotic value satisfies (the holomorphic and antiholomorphic sectors considered) $\mathrm{Tr}\left(A_\varphi^2\right) = \frac{8\pi}{k}M$, and euclidean time has period equal to one. Thus, we find that

$$E_{BTZ} = M \tag{2.13}$$

We conclude that although a naive look of the Hamiltonian of GR implied that black holes have no energy, a careful analysis of the boundary degrees of freedom gives the right answer.

2.2 Maldacena's AdS_5/CFT_4 conjecture

Let us start by simply stating Maldacena's proposal [30] to list the ingredients, and afterwards explain what it means. The conjecture claims that the following two theories are equal:

- $\mathcal{N} = 4$ Super Yang Mills in 3+1 dimensions, with gauge group $SU(N)$ and coupling g_{YM}.
- Type IIB superstring theory with string length $\ell_s = \sqrt{\alpha'}$ and coupling g_s on $\mathrm{AdS}_5 \times S^5$ with curvature radius L and N units of flux on S^5 of the F_5 form.
- The matching of the parameters on both sides is given by

$$g_{YM}^2 = 2\pi g_s \qquad , \qquad 2N g_{YM}^2 = \left(\frac{L}{\ell_s}\right)^4 \tag{2.14}$$

This is a weak-strong duality: if the effective t'Hooft coupling $\lambda = N g_{YM}^2$ of the gauge theory is very large this implies that the AdS radius L is much larger than the string length ℓ_s, so the background is very weakly curved. Conversely, if λ is very small we have a perturbative SYM theory, dual to a strongly coupled string theory.

The duality: D-branes equal p-branes

The key insight that led to Maldacena materialising his conjecture was a result by Polchinski [45] coming from superstring theory in 10 dimensions. He argued that two apparently different objects within string theory, namely **D3 branes** and **black 3-branes** where actually the same object, but in different regimes. This is very non trivial, since despite of the coincidence in names, D-branes are boundary conditions for open strings, while black $p-$branes are simply black holes in higher dimensions with planar horizons. It is not at all obvious that they should be related! This is also referred to as the 'open string vs closed string perspectives'. Following the exposition of [46, 47], the argument goes roughly as follows.

Open string story. String theory is not only a theory of strings. It also contains objects known as D-branes, which are higher dimensional branes where the open strings can be attached to in their endpoints. The D-branes also carry an action, known as the

Dirac-Born-Infeld action (DBI). If we consider the regime where the interaction between the closed and open strings is small, the effective action will be

$$S_{\text{eff}} = S_{\text{closed}} + S_{\text{open}} + S_{\text{int}} \tag{2.15}$$

where S_{int} refers to the open-closed string interaction. String theory contains in general an infinite tower of states given by the possible vibration modes of the strings. However, if we consider now the regime of **low-energy** $\alpha' \to 0$ (recall the mass of the string modes goes as $1/\alpha'$) string theory simplifies dramatically. What we get for the closed strings is a Lagrangian known as type IIB supergravity in 10 dimensions - essentially Einstein's theory (plus a dilaton ϕ) in higher dimension with some extra fermionic fields such that the theory has supersymmetry:

$$S_{\text{closed}} \sim \frac{1}{\alpha'^4} \int d^{10}x \sqrt{-g} e^{-2\phi} \left(R + (\partial\phi)^2 + \text{SUSY partners} \right) + \mathcal{O}(\alpha') \tag{2.16}$$

In this same regime, the open sector contains a gauge field (much like a gluon) of strength F that interacts with the dilaton and the D3 brane through the Dirac-Born-Infeld (DBI) action,

$$S_{\text{DBI}} \sim \frac{1}{\alpha'^2 g_s} \int d^4x \, e^{-\phi} \sqrt{-\det\left(\mathcal{P}[g] + 2\pi\alpha' F\right)} \tag{2.17}$$

where $\mathcal{P}[g]$ is the pullback of the metric to the worldvolume of the brane (the induced metric). Calling X^j the transverse coordinates to the brane (the remaining 6 dimensions), one can perform a Taylor expansion of (2.17) in α' and one finds,

$$S_{\text{open}} \sim \frac{1}{g_s} \int d^4x \left[\frac{1}{4} F^2 + \frac{1}{2} \partial^\mu X^j \partial_\mu X^j \right] + \text{SUSY partners} + \mathcal{O}(\alpha') \tag{2.18}$$

$$S_{\text{int}} \sim \frac{1}{g_s} \int d^4x \, \phi \, F^2 + \dots \tag{2.19}$$

This action is studied around a flat $\mathbb{R}^{1,9}$ background, since this is perturbation theory around flat space.

In the open part, we have a $U(1)$ gauge field kinetic term F^2 and a bunch of scalars X^j, plus their supersymmetric partners. If instead of one D3 brane we have a *stack* of N D3 branes, we get $SU(N)$ instead of $U(1)$, and the open action becomes exactly the famous $\mathcal{N} = 4$ Super Yang Mills theory in four dimensions, provided we identify

$$g_s \sim g_{YM}^2 \tag{2.20}$$

In the interaction, we see a vertex of one dilaton decaying to two gauge bosons.

The home-take message is that if you are an observer that lives on the brane and cannot see the transverse directions, the endpoints of the strings will effectively look as quark-like particles associated to a $U(1)$ field. And if instead of one D-brane you happen to live on top a *stack* of N D-branes, you will see instead an $SU(N)$ gauge theory. But along the transverse directions there will be a 10d supergravity decoupled from you, so we have schematically,

Open strings for $g_sN \ll 1$	$4d$ $\mathcal{N}=4$ SYM + $\mathbb{R}^{1,9}$ IIB SUGRA

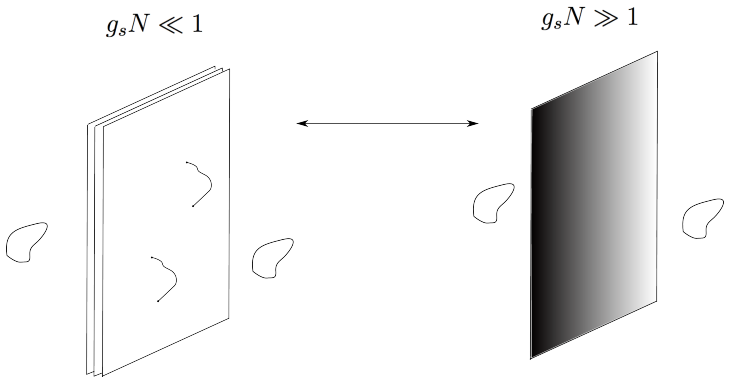

Figure 2.1: Left: at weak string coupling, the stack of D3 branes where the open strings produce an effective $\mathcal{N}=4$ SYM on the worldvolume. This picture is valid for perturbative λ. Right: at strong string coupling, we have black 3-branes in supergravity.

Closed string story. Polchinski noted that from a totally different perspective, $10d$ superstring theory also contains *another* kind of brane: the "$p-$branes" which were known for a very long time. A black $p-$brane is simply a supergravity solution in higher dimensions whose metric contains a planar horizon that looks like a brane. These are 'non-perturbative' solutions (just as any black hole is) related to the closed string sector, and valid when $g_sN \gg 1$. The SUGRA solution contains other fields, but the metric of the black 3-brane is

$$ds^2 = \frac{\eta_{\mu\nu}dx^\mu dx^\nu}{\sqrt{H(r)}} + \sqrt{H(r)}\left(dr^2 + r^2 d\Omega_5^2\right) \qquad , \qquad H(r) = 1 + \left(\frac{L}{r}\right)^4 \tag{2.21}$$

where $\mu,\nu = 0,\ldots,3$ are the worldvolume brane directions, $r = x^i x_i$ and Ω_5 spherical coordinates in the $i,j = 4,\ldots,9$ remaining transverse directions, and L is simply an

integration constant. Notice that as $r \to 0$ the metric is singular - this is due to a causal horizon and not a singularity. Now, Maldacena figured that the $\alpha' \to 0$ limit that we took in the open string picture actually corresponds to the $r/L \to 0$ limit in the p-brane picture, which is called the 'near-horizon region'. But in this regime, we clearly have $\sqrt{H(r)} \approx \left(\frac{L}{r}\right)^2$ and thus the metric reduces to

$$ds^2 = \left(\frac{r}{L}\right)^2 \eta_{\mu\nu} dx^\mu dx^\nu + \left(\frac{L}{r}\right)^2 \left(dr^2 + r^2 d\Omega_5^2\right) \tag{2.22}$$

Finally, if we change coordinates to $r = L^2/z$ - where the brane horizon stands at $z = 0$ now - we get

$$ds^2 = \left(\frac{L}{z}\right)^2 \left(dz^2 + \eta_{\mu\nu} dx^\mu dx^\nu\right) + L^2 d\Omega_5^2 \tag{2.23}$$

The first factor is precisely AdS_5 space with curvature radius L. The second is a 5-sphere of radius L. We found the SUGRA in $\mathrm{AdS}_5 \times S^5$. Finally, if we are far away from the horizon, $r/L \gg 1$ we recover flat 10d space in (2.21).

The home-take message from the closed strings regime is

Closed strings for $g_s N \gg 1$	IIB superstring thy. on $\mathrm{AdS}_5 \times S^5 + \mathbb{R}^{1,9}$ IIB SUGRA

The conjecture. Maldacena's audacious idea was the following. Strictly speaking, we only know that the SYM description is valid when $g_s N \ll 1$, while the $\mathrm{AdS}_5 \times S^5$ is valid in the opposite regime where $g_s N \gg 1$. But Polchinski showed that both pictures can be thought of as the same system in different regimes. So if we assume that the SYM description holds *all the way* up to the strong coupling regime, this means that SYM at strong coupling must possess an alternative description as gravity in $\mathrm{AdS}_5 \times S^5$. And the same the other way around. We will not dig deeper into the details of the derivation but from now on just take it for granted and review some implications.

One last comment is in order, regarding the matching of the symmetries on both sides. The $\mathrm{AdS}_5 \times S^5$ geometry has two important symmetries: the $SO(2,4)$ symmetry coming from AdS_5 and the $SO(6)$ coming from the 5-sphere[1]. Super Yang Mills is conformal and supersymmetric. In four dimensions, the conformal group is precisely $SO(2,4)$. The fields of the SYM theory, for the case of $\mathcal{N} = 4$, can be arranged into a multiplet possessing a $SU(4) \simeq SO(6)$. So both theories have identical symmetries.

[1]This is the isometry group of AdS. Recall that AdS_D is defined by embedding it into flat $D+1$-space, and defining the hyperboloid there, which clearly has $SO(2, D-1)$ as its symmetry group.

The 'holographic dictionary'

After Maldacena's paper containing the essential arguments, the conjecture was systematised into what is known as the 'holographic dictionary' that allows to translate the supergravity calculations into the conformal field theory ones. The most important entry of the dictionary was made precise by Witten [48], which initiated the way on how to extract useful information from the conjecture. The main idea is simple to grasp. Classical fields propagating in AdS will behave in a certain way at the asymptotic boundary. Then, specific modes of the fields will become *sources* and *expectation values* for the CFT defined on the boundary. Calling $Z_{grav}[\phi_0]$ the partition function of the supergravity or string theory in AdS computed with the boundary condition that the field ϕ asymptotes to the value ϕ_0, the conjecture is

$$Z_{grav}[\phi_0] = \langle \exp \int \phi_0 \, \mathcal{O}_\Delta \rangle_{CFT} \tag{2.24}$$

where the right hand side is simply the generating functional of the CFT with the function ϕ_0 turned on as a source for the operator $\mathcal{O}_\Delta$ of scaling dimension Δ is a definite function of the field data (e.g. the mass). In the $\alpha' \to 0$ limit, the string theory becomes classical supergravity, and we approximate the gravity partition function by the on-shell value of the gravity action in (2.24) by $Z_{grav}[\phi_0] = \exp(-I_{grav}[\phi_0])$. From here one can compute CFT correlation functions by taking functional derivatives,

$$\langle \mathcal{O}(y_1) \dots \mathcal{O}(y_n) \rangle_{CFT} = \frac{\delta^n Z_{grav}[\phi_0]}{\delta\phi_0(y_1) \dots \delta\phi_0(y_n)} \tag{2.25}$$

Let us quickly work with the simplest example: the two-point function for a massless scalar field ϕ propagating in AdS_{d+1}, following [46–48] (we have $\Delta(m=0) = d$). We must solve the e.o.m. of the field in the AdS background with the ϕ_0 boundary condition, plug it into the gravity action, and take some functional derivatives. We start from the boundary value problem: we wish to solve

$$\Box_{\vec{x},z}\phi(\vec{x},z) = 0 \quad \text{subject to} \quad \phi(\vec{x}, z \to 0) = \phi_0(\vec{x}) \tag{2.26}$$

We use the Green's function method. The solution will be

$$\phi(\vec{x},z) = \int d^d\vec{y}\, K(\vec{x},z|\vec{y})\phi_0(\vec{x}) \tag{2.27}$$

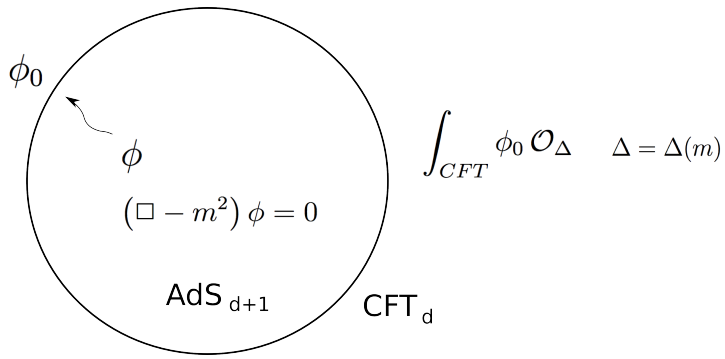

Figure 2.2: Sketch of the AdS/CFT dictionary: a scalar field of mass m propagates in the bulk, with asymptotic value ϕ_0. This becomes a source for an operator $\mathcal{O}_\Delta$ of the boundary CFT: its generating functional is computed by adding $\int \phi_0 \mathcal{O}_\Delta$ to the CFT action. The scaling dimension Δ of the operator is determined by the mass.

where $K(\vec{x}, z|\vec{y})$ is known as the *bulk-to-boundary propagator*, connecting a bulk point $(\vec{x}, z)$ with a boundary point $(\vec{y}, z = 0)$. The kernel is determined by the equation

$$\Box_{\vec{x},z} K(\vec{x}, z|\vec{y}) = \delta^d(\vec{x} - \vec{y}) \tag{2.28}$$

Using $\Box_{\vec{x},z} = 1/\sqrt{g}\partial_m\left(\sqrt{g}g^{mn}\partial_n\phi\right)$ and inserting the AdS metric in (2.23), we find

$$K(\vec{x}, z|\vec{y}) = C_d\left(\frac{z}{z^2 + (\vec{x} - \vec{y})^2}\right)^d \tag{2.29}$$

which in particular, as we go to the boundary $z \to 0$ becomes a delta function: $K(\vec{x}, z|\vec{y}) \to \delta^d(\vec{x} - \vec{y})$. C_d is a dimension-dependent constant. Now we insert this into the supergravity action, where things simplify. Since we only want the two-point function in the probe limit where the scalar only interacts via minimal coupling with the metric and doesn't backreact or interact with any of the other supergravity fields, it turns out that it suffices to consider the kinetic piece of the scalar,

$$I_{grav}[\phi_0] = \frac{1}{2}\int_{AdS} d^{d+1}x\sqrt{g}\partial_\mu\phi\,\partial^\mu\phi \tag{2.30}$$

$$= -\frac{1}{2}\int_{AdS} d^{d+1}x\sqrt{g}\phi\Box\phi + \frac{1}{2}\int_{AdS} d^{d+1}x\sqrt{g}\partial_\mu\left(\phi\partial^\mu\phi\right) \tag{2.31}$$

$$= \frac{1}{2}\int_{z=\epsilon} d^dx\ \sqrt{\gamma}\,\phi\,\vec{n}\cdot\vec{\nabla}\phi \tag{2.32}$$

In the first step we integrated by parts (retaining the boundary term!) and cancelled the first integral by the e.o.m. In the second term we used Stoke's theorem to rewrite it as

an integral over a regularised boundary - a slice of constant $z = \epsilon$ for very small ϵ. Here γ is the induced metric on that slice, and $\vec{n}$ its normal vector. The induced metric on this slice is easily computed from the AdS metric in (2.23) and gives $\sqrt{\gamma} = z^{-d}$, while the dot product yields simply $\vec{n} \cdot \vec{\nabla}\phi = z\partial_z\phi$. The derivative is evaluated by using (2.27) and (2.29), which give

$$z\partial_z\phi\,(\vec{x}, z) \underset{z\to\epsilon}{\longrightarrow} d\,C_d\,z^d \int d^d y \frac{\phi_0(\vec{y})}{|\vec{x} - \vec{y}|^{2d}} \tag{2.33}$$

Moreover, since $\phi \to \phi_0$ as we approach the boundary, the action is

$$I_{grav}[\phi_0] = \frac{dC_d}{2} \int d^d x\, d^d y\, \frac{\phi_0(\vec{x})\phi_0(\vec{y})}{|\vec{x} - \vec{y}|^{2d}} \tag{2.34}$$

Finally, we compute the two-point correlation function using the dictionary (2.25), and the final result is

$$\langle \mathcal{O}(\vec{x}_1)\mathcal{O}(\vec{y}_2)\rangle = -\frac{dC_d}{|\vec{x} - \vec{y}|^{2d}} \tag{2.35}$$

This result is quite remarkable. The falloff as $|\vec{x}-\vec{y}|^{2d}$ is exactly what we would expect to get if we were computing a two-point function in a conformal field theory, for operators of scaling dimension d! This is not a coincidence. Indeed, an analogous (although more involved) calculation can be done for the 3-point function

AdS/CFT has become an entire industry of theoretical physics. We shall not review it in generality any more. Instead, we turn now to a brief review of the case that will be of more importance for us.

2.3 $\mathbf{AdS_3/CFT_2}$

General relativity in $2 + 1$ dimensions,

$$\frac{1}{16\pi G} \int d^3x \sqrt{-g}\,(R - 2\Lambda) \tag{2.36}$$

is very peculiar. First, it has no gravitational waves, which follows from a simple counting of degrees of freedom (d.o.f.). In the Hamiltonian formulation, we have: the three d.o.f. coming from the metric g_{ij} at a space-like slice plus three from their conjugate momenta π_{ij}, but we also have to satisfy the three constraints $\mathcal{H} = 0 = \mathcal{H}^i$ (Einstein's equations), each of one carries an associate Lagrange multiplier which we fix at will (the choice of

coordinates). Thus, the physically meaningful (gauge invariant) d.o.f. are completely fixed and the Weyl tensor vanished identically: there are no gravitational waves. Moreover, all solutions must be maximally symmetric spaces of constant curvature: Minkowski, de-Sitter or Anti de-Sitter space. Finally, point masses experience no Newtonian attraction between them [49].

Although a naive look at this would regard this theory as trivial, it is in fact far from being so. Indeed, research in classical and quantum aspects of $2+1$ gravity has been extremely active in the last decades, the most prominent being asymptotically AdS_3 gravity. There are several reasons for this. For one, pure gravity in AdS_3 can be equivalently written as a Chern-Simons theory [50, 51](Chapter 4). Moreover, even within classical GR, AdS_3 has an 'enhanced' asymptotic symmetry algebra: the Virasoro algebra instead of $SO(2,2)$ which would be the naive guess [52]. Last but not the least, it possesses black hole solutions [53], which share many of the properties of their higher dimensional analogs, as well as a beautiful 'zoo' of topological cousins of it.

As it is well known, AdS space in any number of dimensions can be defined by solving an hyperboloid equation in an embedding space. In three dimensions, this means starting in $\mathbb{R}^{2,2}$,

$$ds^2 = -\left(dX^{-1}\right)^2 - \left(dX^0\right)^2 + \left(dX^1\right)^2 + \left(dX^2\right)^2 \tag{2.37}$$

Then AdS_3 is defined as the solution to

$$-\left(X^{-1}\right)^2 - \left(X^0\right)^2 + \left(X^1\right)^2 + \left(X^2\right)^2 = -L^2 \tag{2.38}$$

We stress that this has a $SO(2,2)$ as its isommetry group.

Since (2.38) contains closed time-like curves, one usually slightly modifies the geometry by considering its universal cover. In global coordinates, the metric of (the universal cover of) AdS_3 can be written in global coordinates as

$$ds^2 = -\left(1 + \left(\frac{r}{L}\right)^2\right) dt^2 + \frac{dr^2}{1 + \left(\frac{r}{L}\right)^2} + r^2 d\phi^2 \tag{2.39}$$

where $0 \leq r < \infty, -\infty < t < \infty, 0 \leq \phi < 2\pi$. Now because of the above arguments, all solutions to Einstein's equations with a negative cosmological constant must *locally* be AdS_3, so the only way of producing different solutions is by quotienting - 'cutting and gluing' along symmetry directions. The most prominent of such solutions is the BTZ

black hole, after Bañados, Teitelboim and Zanelli [53] (for more details see [54,55]). With mass M and angular momentum J, the metric is

$$ds^2 = -f(r)dt^2 + \frac{dr^2}{f(r)} + r^2\left(d\phi + N^\phi dt\right)^2 \tag{2.40}$$

where

$$f(r) = \left(-8GM + \frac{r^2}{L^2} + \frac{16G^2J^2}{r^2}\right)^{1/2} \quad , \quad N^\phi = -\frac{4GJ}{r^2} \tag{2.41}$$

As the Kerr solution, rotating BTZ has two horizons $r_\pm$, located at

$$r_\pm = 4GML^2\left(1 + \sqrt{1 - \left(\frac{J}{ML}\right)^2}\right) \tag{2.42}$$

Its Hawking temperature is given by

$$T = \frac{r_+^2 - r_-^2}{2\pi r_+ L^2} \tag{2.43}$$

and its Bekenstein-Hawking entropy is one quarter of its perimeter:

$$S = \frac{2\pi r_+}{4G} = 2\pi\sqrt{\frac{L}{8G}(ML + J)} + 2\pi\sqrt{\frac{L}{8G}(ML - J)} \tag{2.44}$$

Another important orbifold of AdS_3 are the 'conical defects'. These correspond to the solutions with a stress tensor coming from a point particle at the origin. These can be constructed by identifying the angle variable $\phi \sim \phi + \frac{2\pi}{n}$ for a given integer n, with the same metric (2.39). However, it is usually more comfortable to work in the same coordinates as before in (2.39), but modifying the line element to

$$ds^2 = -\left(\frac{1}{n^2} + \left(\frac{r}{L}\right)^2\right)dt^2 + \frac{dr^2}{\frac{1}{n^2} + \left(\frac{r}{L}\right)^2} + r^2 d\phi^2 \tag{2.45}$$

These actually correspond to BTZ solutions with $J = 0$ and $8GM = -1/n^2$, which are 'naked singularities' that fill the gap between the massless BTZ and AdS_3 for $n = 1$. We will encounter them again in this thesis.

The result of Brown and Henneaux was another of the important precursors of AdS/CFT. The main idea was, again, to consider the importance of the boundary conditions. One starts by choosing an asymptotic falloff for the fields at the boundary, that is physically reasonable for the problem at hand. Brown and Henneaux identified the following conditions, which allow finite shifts in the mass of the solution, but are constrained enough as

to have well defined diffeomorphisms at the boundary,

$$g_{tt} = -\frac{r^2}{L^2} + \mathcal{O}(1) \quad , \quad g_{t\phi} = \mathcal{O}(1) \quad , \quad g_{tr} = \mathcal{O}\left(r^{-3}\right)$$
$$g_{rr} = \frac{r^2}{L^2} + \mathcal{O}\left(r^{-4}\right) \quad , \quad g_{r\phi} = \mathcal{O}\left(r^{-3}\right) \quad , \quad g_{\phi\phi} = r^2 + \mathcal{O}(1) \tag{2.46}$$

Once the boundary conditions are fixed, we first ask what is the most general set of transformations (here diffeomorphisms) that preserve these conditions. One can show that these transformations are generated by the following vector field ξ^μ:

$$\xi^t = L\left(T^+ + T^-\right) + \frac{L^3}{2r^2}\left(\partial_+^2 T^+ + \partial_-^2 T^-\right) + \mathcal{O}\left(r^{-4}\right)$$
$$\xi^\phi = T^+ - T^- - \frac{L^2}{2r^2}\left(\partial_+^2 T^+ - \partial_-^2 T^-\right) + \mathcal{O}\left(r^{-4}\right)$$
$$\xi^r = -r\left(\partial_+ T^+ + \partial_- T^-\right) + \mathcal{O}(r^{-1}) \tag{2.47}$$

where the lightcone coordinates are given by $t/L \pm \phi$. The requirement that these diffeos preserve the Brown-Henneaux conditions (2.46) imply that $\partial_\pm T^\mp = 0$. These equations classify the set of transformations ξ^μ into two different two different categories, called **proper** and **improper** gauge transformations. Although all of them preserve the asymptotics, the proper gauge transformations do not change the physical state of the system, while the improper ones do. For example, all ξ^μ such that ξ^t have the same $T^\pm$ but differ only by terms $\mathcal{O}(r^{-4})$ are considered to be related by proper gauge transformations (they constitute "pure gauge"). But two fields that differ by their values of $T^\pm$ are said to be physically distinguishable. Since pure AdS has $T^\pm = 0$, the group of diffeomorphisms with non-zero $T^\pm$, modulo the proper gauge transformations, is known as the **Asymptotic symmetry algebra** of AdS_3.

Then, calling L_n and $\bar{L}_n$ the generators of the diffeos (2.47) with $T^\pm = e^{in(t/L\pm\phi)}$ (i.e. its Fourier modes), Brown and Henneaux showed that they satisfy the Virasoro algebra

$$[L_m, L_n] = (m-n)\,L_{m+n} + \frac{c}{12} m\left(m^2-1\right)\delta_{n+m} \tag{2.48}$$
$$[\bar{L}_m, \bar{L}_n] = (m-n)\,\bar{L}_{m+n} + \frac{c}{12} m\left(m^2-1\right)\delta_{n+m} \tag{2.49}$$
$$[L_m, \bar{L}_n] = 0 \tag{2.50}$$

with the central charge given by

$$c = \frac{3L}{2G} \tag{2.51}$$

This result was quite surprising at the time, since we must remember that the calculation was completely *classical*, in the sense that no quantum mechanics was involved. And remarkably, the algebra (2.51) is precisely the Virasoro algebra, which is the conformal algebra in $1+1$ dimensions, with a non vanishing central charge, which is an indication of a *quantum* field theory with conformal symmetry, rather than simply a classical conformal theory.

One of the simplest and most beautiful demonstrations of the holographic principle was worked out by Strominger [56], soon after the paper by Maldacena. Strominger's calculation is particularly nice, since it doesn't involve either string theory nor supersymmetry directly. The idea is to use the Cardy formula, which gives the universal result for the entropy of a CFT_2 for large values of the energy.

$$S(\Delta, \bar{\Delta}) = 2\pi\sqrt{\frac{c}{6}\left(\Delta - \frac{c}{24}\right)} + 2\pi\sqrt{\frac{c}{6}\left(\bar{\Delta} - \frac{c}{24}\right)} \tag{2.52}$$

where Δ and $\bar{\Delta}$ are the eigenvalues of the energy operators L_0 and $\bar{L}_0$ of the right and left moving sectors. The goal then is to compute the number of microstates associated to a BTZ of mass M and angular momentum J, in the large M regime, by using only CFT_2 techniques. The large M condition implies that $\Delta + \bar{\Delta} \gg c$. Using the Cardy formula, and replacing $\Delta, \bar{\Delta}$ in terms of M, J and the Brown-Henneaux central charge (2.46) and approximating, we have

$$S \approx 2\pi\left(\sqrt{\frac{c\Delta}{6}} + \sqrt{\frac{c\bar{\Delta}}{6}}\right) = 2\pi\sqrt{\frac{L}{8G}(ML + J)} + 2\pi\sqrt{\frac{L}{8G}(ML - J)} \tag{2.53}$$

which is exactly the BTZ entropy (2.44)!

We end with a comment on the validity of the duality. We saw above that there is an emergent CFT at the conformal boundary of AdS_3. However, we never specified *what* theory it was! In fact, there is an entire zoo of CFT_2 that have been extensively studied for decades. It turns out that to this question has not yet been settled, although there have been many conjectures. So, we know the symmetry algebra, but we do not know the Lagrangian. This is in contrast to Maldacena's example, where we have a very specific action in mind on both sides. Nevertheless, Hartmann, Keller and Stoica [57] have found the requirements that a CFT_2 must satisfy in order to have a 3d bulk dual. Consider the density of states. It is clear that any CFT_2 matches the 3d gravity results (BTZ entropy) for infinite temperature or equivalently for infinite energy, simply because of the

Cardy formula. What is special about holographic CFTs is that they also satisfy the Cardy formula all the way up to the lowest temperature that makes sense, namely the Hawking-Page transition. To be precise, they showed that

$$Z_{CFT}(\beta) = Z_{grav}(\beta) \tag{2.54}$$

iff two conditions are met:

$$c \gg 1 \tag{2.55}$$

$$\rho(\Delta) \leq \exp 2\pi\Delta \qquad \text{for} \quad \Delta < \frac{c}{12} \tag{2.56}$$

These are referred to as the 'sparseness conditions' on the spectrum.

Chapter 3

Holographic Renyi entropies

As we know, entropy is a key notion in many areas of knowledge. In classical information theory, the most important measure of information is the Shannon entropy [58]. Given a probability distribution $\{p_i\}$, its Shannon entropy is defined as

$$S = -\sum_i p_i \log p_i \tag{3.1}$$

Although the Shannon entropy provides very important information about the system, it is only one measure of the spectrum p_i. A generalisation of it which extract much more information are the Renyi entropies [59]. These carry an index $n \geq 0$ and $n \neq 1$, and are defined as

$$S^{(n)} := \frac{1}{1-n} \log \sum_i p_i^n \tag{3.2}$$

One nice property of the Renyi entropies is that they include several other well known measures as special cases. $S^{(0)}$ is commonly known as Hartley entropy, which measures the cardinality of the set. The Shannon entropy is recovered via the limit $\lim_{n\to 1} S^{(n)} = S$. The second Renyi entropy $S^{(2)}$ is sometimes referred to as 'collision entropy'. And the limit $n \to \infty$ is known as 'Min-entropy': $S^{(\infty)} = -\log \max_i p_i$. Of course, the existence of these limits depends in general on the analytic properties of the Renyi entropies, which is a subtle issue. For our purposes, we will from now on assume that the analytic continuation is well defined.

There exists a natural generalisation to the quantum case. We start with a density matrix ρ whose eigenvalues are interpreted as a probability distribution. Then, the natural

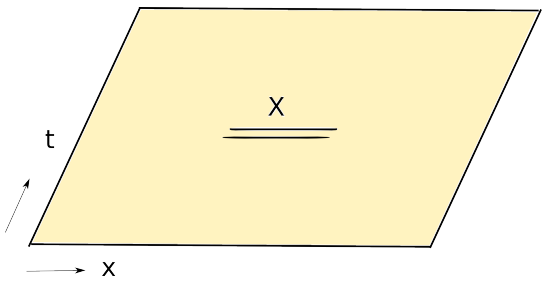

Figure 3.1: The entangling interval X in a single copy of the manifold $\mathcal{M}$.

extension of the Shannon entropy (3.1) is defined as the von Neumann entropy,

$$S = -\mathrm{Tr}\,(\rho \log \rho) \tag{3.3}$$

which is computed by diagonalising ρ. The quantum Renyi entropies are defined in the obvious way,

$$S^{(n)} = \frac{1}{1-n} \log \frac{\mathrm{Tr}\,(\rho^n)}{(\mathrm{Tr}\rho)^n} \tag{3.4}$$

where the denominator accounts for the normalisation.

For finite dimensional Hilbert spaces, the above calculations are in principle straightforward. The situation is much more delicate in QFT, which is the case we are interested. There exists different methods to perform actual calculations of these entropies, but we shall focus only in one: the Replica trick. Consider a QFT in euclidean signature in some d-dimensional manifold $\mathcal{M}$. We wish to compute the Renyi entropy of the reduced density matrix ρ_X on some co-dimension 1 'entangling' region X, see Fig. 3.1 in which we illustrate the $1+1$ dimensional case for simplicity.

The replica trick is particularly easy to grasp in the path integral formalism. A trace over states is simply given by a euclidean path integral coming from asymptotic times in the remote past and the far future. First we look for the reduced density matrix $\rho_X = \mathrm{Tr}_Y \rho$ where $Y = X^c$ is the complement. This requires to cut a small 'slit' at X at times $t_\pm$ immediately to the past and future of X as in the figure. Since this is a matrix, it has two free indices $(\rho_X)^i_j$ or equivalently, we get the matrix elements by projecting with $\langle \phi_- | \rho_X | \phi_+ \rangle$ where $\phi_\pm(x)$ are two states defined at the cuts. The reduced density matrix ρ_X is therefore defined as the path integral over the entire manifold $\mathcal{M}$, but keeping the values of the fields $\phi(t_\pm, x) = \phi_\pm(x)$ with $x \in X$ fixed, which becomes a functional of

$\phi_\pm(x)$:

$$\langle \phi_- | \rho_X | \phi_+ \rangle = \int_{\phi(t_\pm,x)=\phi_\pm(x)}^{\mathcal{M}} \mathcal{D}\phi \; e^{-I[\phi]} \tag{3.5}$$

Now we wish to take the trace over X of the $n-$th power of this matrix. In index notation, this amounts to

$$\mathrm{Tr}_X \left(\rho_X\right)^n = \left(\rho_X\right)^{i_1}_{i_2} \left(\rho_X\right)^{i_2}_{i_3} \left(\rho_X\right)^{i_3}_{i_4} \ldots \left(\rho_X\right)^{i_{n-1}}_{i_n} \left(\rho_X\right)^{i_n}_{i_1} \tag{3.6}$$

We can do the same in the path integral. Instead of working in $\mathcal{M}$, we consider the manifold $\mathcal{M}_n$, defined as shown in Fig. 3.2: we glue the t_+ edge of the $i-$th copy to the t_- edge of the $i+1$-th copy, all in a cyclic manner (with t_+ of the n is identified with t_- of the first). The manifold thus defined is an $n-$sheeted Riemann surface, which covers the initial manifold n times. The replica prescription instructs us to now compute the path integral in $\mathcal{M}_n$. This is accomplished by imposing cyclic boundary conditions at the edges in the path integrals: we impose $\phi^{(i)}_+(x) = \phi^{(i+1)}_-(x)$, where $\phi^{(i)}$ refers to the field variable in the $i-$th copy. Notice this puts a restriction on the space of fields that enter the path integral: they must be single valued in $\mathcal{M}_n$. This path integral is denoted by $Z[\mathcal{M}_n]$.

Thus we have

$$S^{(n)}(X) = \frac{1}{1-n} \log \frac{Z[\mathcal{M}_n]}{\left(Z[\mathcal{M}]\right)^n} \tag{3.7}$$

where the dependence on X in the right hand side is implicit in the definition of $\mathcal{M}_n$. The bottom line is that in QFT, the calculation of the Renyi entropies reduces to the evaluation of the path integral in a funny manifold $\mathcal{M}_n$.

As we mentioned before, the actual calculation of these partition functions is in QFT is generically quite involved. The best known example is, of course, two dimensional conformal field theories, because the large degree of symmetry allows to perform the calculation. This method is described in many excellent references, e.g. [60]. Since we wish to focus on the proof of the holographic RT formula and its generalisation to Renyi entropies, we will not review the field theory calculation here. Instead, in Section 3.1 we briefly review the Lewkowycz-Maldacena derivation of holographic entanglement entropies [32], and in Section 3.2 show some simple applications for the phase diagram of the replicated manifolds.

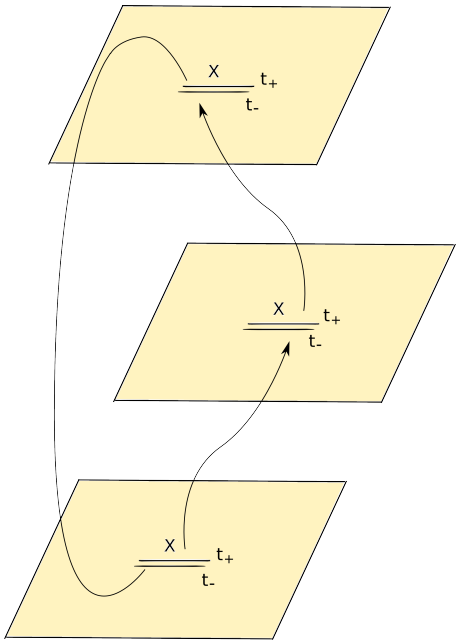

Figure 3.2: The replicated manifold $\mathcal{M}_n$. The copies are sewed cyclically, defining a Riemann surface.

3.1 Holographic entanglement entropy

We consider for simplicity the static case, where the bulk geometry is time independent. The Ryu-Takayanagi prescription is the following. We consider an entangling region X with boundary ∂X, defined on a surface of constant time on the conformal boundary of the asymptotically AdS space, as in Fig. 3.2. In the bulk, consider the set of all surfaces γ_X such that $\partial\gamma_X = \partial X$ and γ_X is homologous to X, i.e. that $X \cup \gamma_X$ define an 'interior' and 'exterior'. Then, S_X of the boundary is given by the area of the minimal surface,

$$S(X) = \min_{\gamma_X} \frac{\text{Area}(\gamma_X)}{4G} \tag{3.8}$$

Obviously, the RT formula (3.8) is inspired by the Bekenstein-Hawking formula. In fact, it is a generalisation of it, that reduces to the black hole entropy in a particular case. Although proposed in 2006, it was only in 2013 that it was finally proved by Lewkowycz and Maldacena [32], following the previous insight by Fursaev [61]. In 2016 Dong [33] provided the general argument for the static case in euclidean signature for the Renyi entropies. For simplicity, we review the proof of the entanglement entropy.

3.1.1 Derivation of holographic entanglement entropy

This argument is extremely elegant. It relies on three assumptions: 1) the semiclassical approximation (Gibbons-Hawking) of euclidean quantum gravity, 2) the AdS/CFT duality, 3) no spontaneous breaking of the replica symmetry. We start by doing the replica trick on the conformal boundary, as explained above. In gauge/gravity duality, this is nothing but a very special set of boundary conditions for the fields as they approach the asymptotic boundary $\mathcal{M}_n$. Then, provided these boundary conditions, one is supposed to solve the bulk Einstein equations, and find the saddle for those prescribed boundary conditions, call it $\mathcal{B}_n$, so that $\partial\mathcal{B}_n \sim \mathcal{M}_n$ (conformally equivalent). Once the bulk solution $\mathcal{B}_n$ is found, the partition function of the boundary $Z[\mathcal{M}_n]$ is computed according to AdS/CFT by the partition function in the bulk $Z[\mathcal{B}_n]$. In the semiclassical approximation $G_N \ll 1$, this is simply given by the on-shell action via the Gibbons-Hawking prescription,

$$Z[\mathcal{B}_n] \approx \exp\left(-I[\mathcal{B}_n]\right) \tag{3.9}$$

which replaced into the Renyi entropy (3.7) yields

$$S^{(n)} = \frac{1}{1-n}\log\frac{Z[\mathcal{B}_n]}{(Z[\mathcal{B}])^n} \tag{3.10}$$

$$= \frac{1}{1-n}\left(nI[\mathcal{B}] - I[\mathcal{B}_n]\right) \tag{3.11}$$

Now, the branched cover $\mathcal{M}_n$ possesses a discrete symmetry of cyclically permuting the n replicas. We assume that this symmetry is not spontaneously broken in the bulk. Since the gravity action (including all necessary boundary terms) is an integral of a local quantity, replica symmetry in the bulk means that we can consider the quotient bulk geometry

$$\hat{\mathcal{B}}_n := \frac{\mathcal{B}_n}{\mathbb{Z}_n} \tag{3.12}$$

and it will satisfy

$$I[\mathcal{B}_n] = nI[\hat{\mathcal{B}}_n] \tag{3.13}$$

Plugging into (3.10) we finally find

$$S^{(n)} = \frac{n}{1-n}\left[I[\mathcal{B}] - I[\hat{\mathcal{B}}_n]\right] \tag{3.14}$$

Notice that the two actions in (3.10) are exactly the same functional, but evaluated in different metrics. $\mathcal{B} = \mathcal{B}_1$ is simply the bulk whose conformal boundary is $\mathcal{M} = \mathcal{M}_1$ which was the original manifold, no replicas involved. On the other hand, $\mathcal{B}_n$ contains a codimension-2 conical defect somewhere, because it was obtained by the quotient (3.12) of a manifold that had a $\mathbb{Z}_n$ symmetry. Indeed, locus of the conical defect is the region of the original $\mathcal{B}_n$ that was a **fixed point** of the replica symmetry. This is essentially the same as when we produce a cone by quotenting a disc: the center of the disk is mapped to itself under the discrete symmetry, so the quotient (the cone) has a angle deficit around there. This conical defect is the prolongation into the bulk of the branch points located at ∂X on $\mathcal{M}$.

Now the task is to engineer the metric on $\hat{\mathcal{B}}_n$, with the desired conical defect. A convenient way of producing this geometry is by adding a brane term to the action $I' = I + I^{\text{brane}}$ where $I^{\text{brane}} = T_n A_n$, where $A_n = \int d^{d-1}y\sqrt{h}$ is a Nambu-Goto action for the area of the brane. Then the tension of the brane $T_n = (n-1)/4nG$ creates an opening angle of $2\pi/n$ around it. The desired metric is the solution to the new problem

$$\delta I' = \delta I + \delta I^{\text{brane}} = 0 \tag{3.15}$$

These are coupled equations: Einstein's equations for the metric on $\hat{\mathcal{B}}_n$ with a massive brane as a source, and the equation for the brane trying to minimise its area in the backreacted geometry. Equation (3.15) must be satisfied for any variation of the fields, so in particular it must hold when we consider a particular variation produced by varying the value of n, so that $\delta_n = \partial_n$. Of course, n was originally thought of as an integer (the number of replicas), but now that it's given by the brane tension, we take it to be continuous. This defined the analytic continuation.

Now we specify to entanglement entropy, by setting $n = 1+\epsilon$ with $\epsilon \ll 1$. From (3.15) we get, to first order,

$$\partial_\epsilon I' = \partial_\epsilon I[\hat{\mathcal{B}}_{1+\epsilon}] + \partial_\epsilon \left(\frac{\epsilon}{4G} A_{1+\epsilon}\right) \tag{3.16}$$

$$= \frac{I[\hat{\mathcal{B}}_{1+\epsilon}] - I[\hat{\mathcal{B}}_1]}{\epsilon} - \frac{A_1}{4G} + \mathcal{O}(\epsilon) \tag{3.17}$$

and thus we find the desired action,

$$I[\hat{\mathcal{B}}_{1+\epsilon}] = I[\mathcal{B}] + \epsilon \frac{A}{4G} \tag{3.18}$$

Finally, inserting this back into (3.14) we get the entanglement entropy as given by the RT formula:

$$S^{(1)} = -\frac{1}{\epsilon}\left[I[\mathcal{B}] - \left(I[\mathcal{B}] + \epsilon\frac{A}{4G}\right)\right] = \frac{A}{4G} \tag{3.19}$$

where A is the area of the minimal surface because of the equations of motion. Moreover, it is a probe brane since in the limit $n \to 1$ the tension T_n vanishes.

The above argument was nicely generalised by Dong [33] for finite values of n. The results is that the Renyi entropy satisfies

$$n^2\partial_n\left(\frac{n-1}{n}S_n\right) = \frac{A_n}{4G} \tag{3.20}$$

where A_n is the are of the backreacting brane as explained above.

We now turn to some simple applications of this formula, to understand how the Hawking-Page critical point depends on the replica index n.

3.2 Phase diagram of replicated manifolds

This section is based on still unpublished work done in collaboration with Pascal Fries. In [62], the authors investigated a similar problem by specifying $n = 2$.

As we saw in the previous Section, the calculation of entanglement entropies and in general Renyi entropies involve considering a branched cover of the original spacetime in question, and studying the backreaction of a codimension-2 brane on the background. The question we wish to address in this Section is how does the replica index n affect the Hawking-Page critical point. As we will see, this occurs because the actions of thermal AdS and the AdS black hole evolve *differently* with n, which causes a shift in the critical point as we move in n.

We start by briefly reviewing the Hawking-Page (HP) transition, which will also be important in future Sections. We work in arbitrary dimensions in the canonical ensemble, i.e. we start by fixing the euclidean time to have period $\tau \sim \tau + \beta$, where β is some fixed number. One fixes the asymptotic boundary conditions by giving the metric at the boundary $\partial\mathcal{B} = \mathcal{M}$. However, this needs not uniquely determine the interior solution, $\mathcal{B}$. The HP transition is the statement that there exists two exact solutions to the e.o.m.

at fixed β: thermal AdS ($\mathcal{B} = A$) and the AdS black hole ($\mathcal{B} = B$). Thus, the partition function, in the semiclassical approximation takes the form

$$Z(\beta) = \sum_{\mathcal{B}} e^{-I_{\mathcal{B}}(\beta,)} \sim e^{-I_A(\beta)} + e^{-I_B(\beta)} + \ldots = e^{-\beta F(\beta)} \tag{3.21}$$

The reason for this is that the gravitational action carries a factor of $1/G$, so that in the limit $G \to 0$ all but the classical solutions (which minimise the action if the variational principle is well posed) are exponentially suppressed.

Here I_{bulk} is assumed to include all correct boundary terms needed in order to extremize the action on the equations of motion, provided the boundary conditions. The usual HP temperature, call it β_1, is defined as the point where these two terms exchange dominance, i.e. the solution to the equation

$$\Delta I(\beta) \equiv I_B(\beta) - I_A(\beta) = 0 \quad \to \quad \beta = \beta_1 \tag{3.22}$$

Now let's do the same analysis for the replicated manifolds. The physics of the replica trick introduces two extra parameters: the entangling region X and the replica index n. Let us assume that the analytic continuation of both the AdS and BH solutions exist and are well defined for arbitrary (X, n). Moreover, again we focus on the region of phase space where all other saddles are subdominant. We denote by $I(\mathcal{B}, \beta, X)$ the on-shell action at temperature β for either of the saddles $\mathcal{B}_n = A_n, B_n$ (black hole and thermal AdS) defined by the entangling region X and index n. We now we define the critical point as the solution to

$$\Delta I[n, \beta, X] = I[B_n, \beta, X] - I[A_n, \beta, X] = 0 \tag{3.23}$$

This is one constraint on the set of variables (β, X, n), any of which we can think of functions of the other two, such that (3.23) is satisfied. But now we can express these in terms of the Renyi entropies using (3.10)

$$I[\mathcal{B}_n, \beta, X] = nI[\mathcal{B}, \beta] + (n-1)S^{(n)}(\beta, X) \tag{3.24}$$

Inserting (3.24) back into (3.23), it follows that the HP transition occurs at

$$\Delta I[n, \beta, X] = n\Delta I[\beta] + (n-1)\Delta S^{(n)}(\beta, X) = 0 \tag{3.25}$$

It is worth clarifying that the first term $\Delta I[\beta]$ has nothing to do with the replica trick, it is simply the difference in the on-shell actions of the black hole and thermal AdS in the usual analysis at a given temperature. It is the entropy term that carries the information about the entangling region X and number of replicas n. As we take $n \to 1$, the entropy contribution disappears, and we are left with $\Delta I[\beta] = 0$ which is the usual HP condition. It is the second term that modifies the transition temperature. In principle, one could simply solve (3.25). However, in practice the Renyi entropies are only known in very simple cases. Therefore, we will in the following resort to some approximations in order to grasp some of the physics. In the CFT, the HP transition is understood as the dual of the confinement-deconfinement transition in the gauge theory [63]. Although we have not investigated this here, it would be interesting to understand the meaning of the confining phases of the replicated manifolds.

3.2.1 Expansion around $n = 1$

In the vicinity of $n = 1 + \epsilon$, we can get a general result for the *variation* of the transition temperature. Recall β_1 is the usual HP temperature, i.e. the solution to (4.1), and now call $\beta = \beta_1 + \delta\beta$ the solution at $n = 1 + \epsilon$. Expanding (3.25) to lowest order in ϵ, we find

$$(1+\epsilon)\Delta I[\beta_1 + \delta\beta] + \epsilon \Delta S^{(1+\epsilon)}(\beta_1 + \delta\beta, X) = 0 \tag{3.26}$$

$$\Rightarrow \quad \Delta\partial_\beta I\Big|_{\beta_1} \delta\beta + \epsilon \Delta S^{(1)}(\beta_1, X) = 0 \tag{3.27}$$

where we used that $\Delta I[\beta_1] = 0$ by definition. Thus, we find

$$\delta\beta = -\epsilon \frac{\Delta S^{(1)}(\beta_1, X)}{\Delta\langle E\rangle(\beta_1)} \tag{3.28}$$

where $\partial_\beta I = -\partial_\beta \log Z = \langle E\rangle$ is the expectation value of the energy, so $\Delta\langle E\rangle$ is simply the difference the ADM masses of the two solutions, i.e. $\Delta\langle E\rangle = M(\beta)$ where M is the black hole mass for bulk dimensions $d \geq 4$. For $d = 3$, $\Delta\langle E\rangle = M(\beta) + 1$ due to the BTZ mass gap.

It is interesting to note that $\delta\beta$ has a definite sign: clearly $\Delta\langle E\rangle = M > 0$ and $\Delta S = S(\text{black hole}) - S(\text{AdS}) > 0$ also. This implies that $\delta\beta = -\frac{1}{T^2}\delta T < 0$ for $\epsilon > 0$, so the critical temperature *increases* (decreases) for $\epsilon > 0$ ($\epsilon < 0$) perturbatively in $n = 1+\epsilon$.

3.2.2 The AdS_3 case

In the case of 3d gravity, the Hawking-Page transition adopts a particularly beautiful form, as described by Maloney and Witten [64]. We consider the euclidean system in the canonical ensemble, with $\tau = (\theta + i\beta)/2\pi$ the modular parameter of the torus, where β is the inverse temperature and θ is the angular potential. The task is to find the transition locus in the complex τ plane. We first re-derive the phase diagram of [64] by the reasoning described above, since it will allow us to easily generalise this to the replicated spacetimes.

We start from the black hole partition function

$$Z = \sum_{M,J} \exp\left(-\beta H + i\Theta j + S(M,J)\right) \tag{3.29}$$

The entropy is

$$S(M,J) = 2\pi\sqrt{\frac{c}{6}}\left(\sqrt{\frac{M+J}{2}} + \sqrt{\frac{M-J}{2}}\right) \tag{3.30}$$

In these variables, the physical mass m is $8mG = M$ and the physical angular momentum $j = J/8G$, and c is the central charge.

From these equations, it is easy to show that by using the saddle point equations that the on-shell value of the action for the black hole is given by

$$\begin{aligned} I[B,\tau,\bar{\tau}] &= \beta m - i\Theta j - S = \frac{c}{12}\left(\beta M - i\theta J\right) - S \\ &= -\frac{i\pi c}{12}\left[\frac{1}{\tau} - \frac{1}{\bar{\tau}}\right] \end{aligned} \tag{3.31}$$

On the other hand, for thermal AdS, we have $M = -1, J = 0$, so its on-shell action is

$$I[A,\tau,\bar{\tau}] = -\frac{c}{12}\beta = -\frac{c}{12} i\pi\left(-\tau + \bar{\tau}\right) = \frac{c}{12} i\pi\left(\tau - \bar{\tau}\right) \tag{3.32}$$

The HP transition occurs when both exponentials in (3.21) are equal:

$$\Delta I(\tau,\bar{\tau}) = I[B,\tau,\bar{\tau}] - I[A,\tau,\bar{\tau}] \tag{3.33}$$

$$= -\frac{i\pi c}{12}\left[\frac{1}{\tau} - \frac{1}{\bar{\tau}}\right] - \frac{c}{12} i\pi\left(\tau - \bar{\tau}\right) \tag{3.34}$$

$$= -\frac{i\pi c}{12}\left(\frac{1}{\tau} + \tau - \frac{1}{\bar{\tau}} - \bar{\tau}\right) = 0 \tag{3.35}$$

which reduces to the unit circle

$$\tau\bar{\tau} = \frac{1}{(2\pi)^2}\left(\theta^2 + \beta^2\right) = 1 \tag{3.36}$$

The phase diagram is shown in Fig. 3.3 (figure from [64]), in the complex $\tau \sim \theta + i\beta$ plane. Although euclidean 3d gravity has many first order transitions, we are restricting to the HP, which corresponds to the segment of the unit circle. The grey lines indicate the fixed point of the modular group, i.e. the boundaries of the fundamental domains. The phase transitions lie on a subtesselation of it.

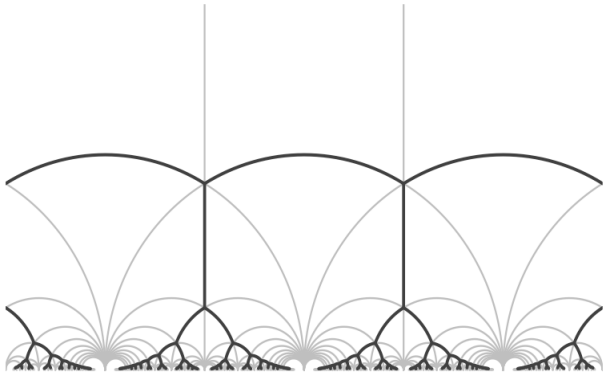

Figure 3.3: The phase diagram of 3d gravity in the complex plane of τ (figure from [64]). The solid black lines indicate first order phase transitions, where the unit circle corresponds to the HP.

In the next section, we study the analogous phase diagram for the replicated manifolds, and find to first order in a smallness expansion, how these lines are deformed.

Torus Renyi entropy: small interval expansion

We now consider the case of one interval on the torus. Although the general formula for the Renyi entropy is not known, there are expressions for the small interval expansion [65]. We shall work at the lowest non-trivial order in the length of the interval x, in the approximation that x is much smaller than both cycles of the torus. Furthermore, we restrict our attention to the holomorphic factor in the partition function, since the antiholomorphic analysis is completely analogous. Then, according to [65], the Renyi entropy to lowest non trivial order is given by

$$S^{(n)}(x) = \frac{c}{6}\left(1+\frac{1}{n}\right)\log\frac{x}{\epsilon} - \frac{1}{12}\left(1+\frac{1}{n}\right)\left(\langle T\rangle + \langle\bar{T}\rangle\right)x^2 \tag{3.37}$$

$$= \frac{c}{6}\left(1+\frac{1}{n}\right)\log\frac{x}{\epsilon} + \frac{1}{12}\left(1+\frac{1}{n}\right)2\pi i\left(\partial_\tau - \partial_{\bar{\tau}}\right)I(\tau,\bar{\tau})x^2 \tag{3.38}$$

where we have written the average energy in terms of the on-shell action of either solution.

The black hole - thermal AdS difference of Renyi entropies for a small interval is then

$$\begin{aligned}\Delta S^{(n)} &= \frac{1}{12}\left(1+\frac{1}{n}\right) 2\pi i \left(\partial_\tau - \partial_{\bar\tau}\right) \Delta I_1(\tau) x^2 \\ &= -\frac{1}{12}\left(1+\frac{1}{n}\right) 2\pi i x^2 \frac{i\pi c}{12}\left(\partial_\tau - \partial_{\bar\tau}\right)\left(\frac{1}{\tau}-\frac{1}{\bar\tau}+\tau-\bar\tau\right) \\ &= -\frac{1}{12}\left(1+\frac{1}{n}\right) 2\pi i x^2 \frac{i\pi c}{12}\left(2-\frac{1}{\tau^2}-\frac{1}{\bar\tau^2}\right)\end{aligned} \tag{3.39}$$

Plugging back into the HP equation,

$$\Delta I(\tau,\bar\tau) + \left(1-\frac{1}{n}\right)\Delta S^{(n)}(\tau,\bar\tau,x) = 0 \tag{3.40}$$

we have

$$\left(\frac{1}{\tau}+\tau-\frac{1}{\bar\tau}-\bar\tau\right) + \left(1-\frac{1}{n}\right)\frac{1}{12}\left(1+\frac{1}{n}\right) 2\pi i x^2 \left(2-\frac{1}{\tau^2}-\frac{1}{\bar\tau^2}\right) = 0 \tag{3.41}$$

or equivalently

$$\frac{1}{\tau}-\frac{1}{\bar\tau}+\tau-\bar\tau+i\delta\left(2-\frac{1}{\tau^2}-\frac{1}{\bar\tau^2}\right) = 0 \tag{3.42}$$

where $\delta = \left(1-\frac{1}{n^2}\right)\pi x^2/6$ is the smallness parameter. This of course reduces to the usual HP quadratic equation (3.36) when $n = 1$.

For $n > 1$, we plot in Fig. 3.4 the solutions to (3.42) in the complex plane of τ, where we have plotted the entire curves, but they should be thought as to end at a given point that we have not determined here and not very relevant for the discussion. The uppermost blue semicircle corresponds to the usual HP transition as in Fig. 3.3. The figure shows some very interesting features, although in this case we do not claim any decisive conclusion. For any $\delta > 0$, we see the appearance of a *new* critical line which is developing from the origin, and at around $\delta \approx 0.3$ the usual HP point disappears. However, both phenomena must be dealt with care, since it is possible that the approximation of the small interval is no longer valid in this regime. We leave this as a motivation for further study.

On the other hand the case for $0 < n < 1$ is even more interesting. For then $-\infty < \delta < 0$ is negative and unbounded, no matter what the size of the interval is. In Fig. 3.5 we plot the curves. The situation is clear from (3.42): as $\delta \to -\infty$, the usual HP line gets pushed towards infinity, whereas there appears a new HP line (the green curve in the

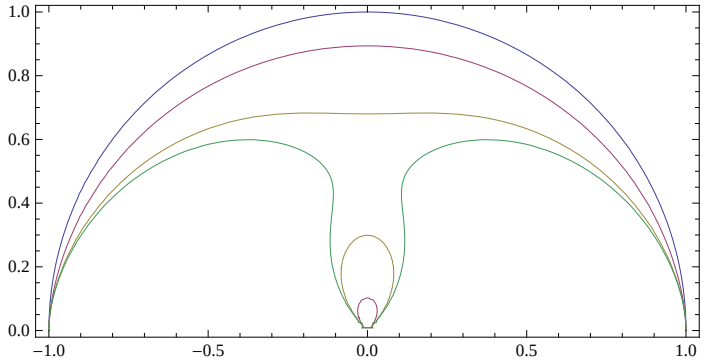

Figure 3.4: HP transition in the τ plane, for increasing values of δ in (3.42), for $\delta = 0, 0.1, 0.25, 0.32$.

plot), located at

$$2 = \frac{1}{\tau^2} + \frac{1}{\bar{\tau}^2} \tag{3.43}$$

This curve is an instance of the well known Lemniscate,

$$r^2 = \cos(2\varphi) \tag{3.44}$$

written in polar coordinates $\tau = r \exp(i\varphi)$.

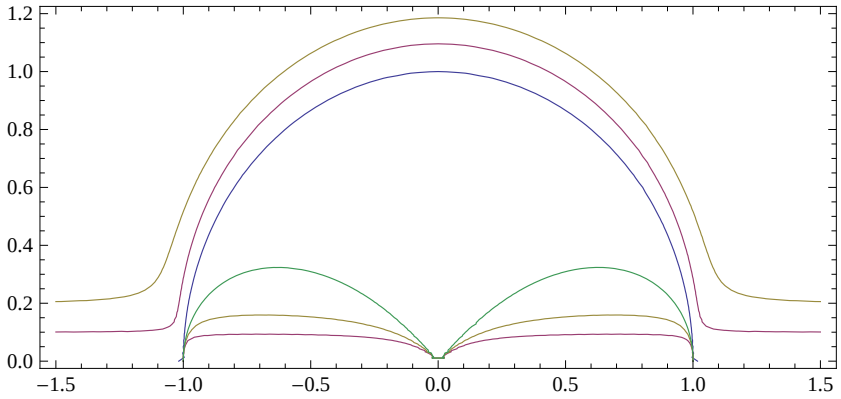

Figure 3.5: HP transition for $0 < n < 1$, for $\delta = 0, -0.1, -0.2, -2$. The lower curves converge to the green one as $n \to 0^+$.

As we see, we have found some interesting results which deserve further investigations. From the holographic dual point of view, these results are quite interesting. Recall that the Renyi entropy is related to the area of a massive backreacting brane attached to the boundary. The modification of the HP curve is related to the interaction between the brane and the horizon of BTZ.

Matching Renyi CFT to AdS

We close this section by performing a simple match of the thermal Renyi entropies computed directly from the CFT and the AdS sides. We work in the large central charge limit $c \to \infty$ and above the HP transition, and for simplicity we consider the non-rotating case. This can be readily generalised to higher dimensions and charges. By thermal Renyi entropy we simply mean that we take the entangling region to be the entire spacelike region in the CFT at a fixed time, in the CFT_2 this is simply a circle $X = S^1_{CFT}$. So we are working in the opposite limit as before, where X was very small with respect to the circle.

We start with the CFT side. We wish to compute the Renyi entropy of the full circle, but for that we must first take a look at the usual partition function in this regime. Due to modular invariance $\tau \to -1/\tau$ (here $\beta \to (2\pi)^2/\beta$) the torus partition function at high temperature $\beta \to 0$ has the symmetry

$$Z[\beta] = \text{Tr } e^{-\beta H} = \text{Tr } e^{-(2\pi)^2/\beta H} \tag{3.45}$$

But the last equality corresponds to very low temperature, in which case Z is dominated by the vacuum contribution. As it is well known, the Casimir energy in the torus is $E_0 = -c/12$, which comes from the vanishing Casimir energy on the complex plane. Therefore, the dominant contribution to the partition function is

$$Z[\beta] \approx \exp\left(\frac{c\pi^2}{3\beta}\right) \tag{3.46}$$

which of course matches exactly the BTZ saddle point approximation (3.31). Then, it is immediate to see that the Renyi entropy is given by

$$\begin{aligned} S^{(n)}(\beta) &= \frac{1}{1-n} \log \frac{\text{Tr } e^{-n\beta H}}{(\text{Tr } e^{-\beta H})^n} \\ &= \frac{1}{1-n} \frac{c\pi^2}{3\beta} \left(\frac{1}{n} - n\right) \\ &= \left(1 + \frac{1}{n}\right) \frac{c\pi^2}{3\beta} \end{aligned}$$

Since the usual thermal entropy is recovered for $n = 1$, we find that in this case, the Renyi entropy is actually proportional to the thermal entropy:

$$S^{(n)}(\beta) = \frac{1}{2}\left(1 + \frac{1}{n}\right) S^{(1)}(\beta) \tag{3.47}$$

We emphasise that this is in general **not true**. Indeed, one can by similar methods as shown here, prove that the CFT_3 problem does not satisfy this equality.

Let us now turn to the gravity side. To compute the Renyi entropy in the bulk, we follow Dong's recipe as explained in in Section 3.1.1. We are supposed to consider the same manifold as before (here the euclidean BTZ solution), but adding a tension-full brane whose boundary is attached to ∂X, the boundary of the entangling region. Next, we must solve the coupled equations of motion of the gravity+brane system, and finally compute the area of the brane.

This procedure simplifies in the particular case at hand. First, since we are in $2+1$ dimensions and the brane is always codimension-2, it is a tension-full string (or worldline). Furthermore since the entangling region $X = S^1_{CFT}$ is the entire circle in the CFT, $\partial X = \emptyset$ is the empty set, so the brane is no longer attached to the boundary. However, due to the homology condition, it must still wind once around the black hole. Due to spherical symmetry, the brane will lie at a constant radius r_b. Now, the e.o.m. for the brane imply that it must minimise its area in the backreacted geometry, which will only occur at the origin of the coordinates, which is the horizon in euclidean signature. We conclude that the brane will sit not at a finite distance but precisely at the horizon, $r_b = r_+$, creating a angle opening of $2\pi/n$ around it, instead of 2π as is imposed in the usual derivation of Hawking's temperature. It cannot shrink further since the BH interior does not exist in euclidean signature.

In the canonical ensemble, the presence of the conical defect does not modify the temperature, but rather the mass and location of the horizon. The solution to the coupled e.o.m. is simply

$$f(r) = -M + r^2 \quad , \quad \beta = \frac{4\pi}{n f'(r_+)} \tag{3.48}$$

It is convenient to write everything in terms of the horizon radius,

$$r_+^{(n)} = \frac{2\pi}{n\beta} \quad , \quad M = \left(\frac{2\pi}{n\beta}\right)^2 \tag{3.49}$$

The black hole 'shrinks' with increasing n. The area of the brane is

$$\frac{A_n}{4G} = \frac{\pi c}{3} r_+^{(n)} \tag{3.50}$$

Now we must integrate the holographic Renyi entropy equation (3.20), that is

$$n^2 \partial_n \left(\frac{n-1}{n} S_n \right) = \frac{A_n}{4G} \tag{3.51}$$

These is readily done and we obtain

$$\begin{aligned} \left(1 - \frac{1}{n}\right) S^{(n)} &= \int_1^n dm \, \frac{A_m}{4m^2} = \frac{\pi c r_+^{(1)}}{3} \int_1^n \frac{dm}{m^3} \\ &= \frac{1}{2} S^{(1)} \left(1 - \frac{1}{n^2}\right) \end{aligned} \tag{3.52}$$

which is precisely the CFT result (3.47).

Chapter 4

Higher spin holography in AdS_3/CFT_2

One of the most fundamental discoveries of physics during the XXth century was the concept of spin. Although initially discovered as an unexpected property of the electron passing through a magnetic field, with time we eventually understood that it is an intrinsic property of all particles we know in Nature. The role that spin has played in modern physics, particularly in as one of the key concepts providing a bridge between experimental physics and the mathematical area of group theory cannot be overestimated.

The road to understanding spin usually begins in undergraduate quantum mechanics courses by studying the role of $su(2)$ in non-relativistic quantum mechanics. Later, one learns that in relativistic classical and quantum field theory, spin is intimately connected to the *representations* of the Lorentz group. All fields in the Standard Model are assumed to be covariant under Lorentz transformations, as special relativity demands. The difference between different spins is simply the way in which we choose to *represent* the Lorentz group acting on these fields. We see that spin acts as an organising principle giving structure to our understanding of Nature.

In principle, particles exist with any value of integer or half-integer spin. Indeed, the theory of massless **free** higher spin fields is well understood. There is an algorithmic way of constructing such theories, put forward by Fronsdal [66]. Let us consider integer spins for simplicity. For each value s of the spin, we have a field with s indices that satisfies a certain second order differential equation of motion and has an associated gauge symmetry.

For example, for $s = 1, 2$ we have as examples the photon A_μ and the graviton $h_{\mu\nu}$:

$$s = 1 \quad \Box A_\mu - \partial_\mu \partial^\nu A_\nu = 0 \qquad \delta A_\mu = \partial_\mu \xi \tag{4.1}$$

$$s = 2 \quad \Box h_{\mu\nu} + \partial_\mu \partial_\nu h - \partial_\mu \partial^\sigma h_{\sigma\nu} - \partial_\nu \partial^\sigma h_{\mu\sigma} = 0 \qquad \delta h_{\mu\nu} = \partial_\mu \xi_\nu + \partial_\nu \xi_\mu \tag{4.2}$$

Following the same logic, one can study fields $\varphi_{\mu_1 \ldots \mu_s}$ that are symmetric in all the indices, that satisfy a corresponding e.o.m. (i.e. all possible contractions involving two derivatives with appropriate signs) and have a gauge symmetry given by $\delta \varphi_{\mu_1 \ldots \mu_2} = \partial_{(\mu_1} \xi_{\mu_2 \ldots \mu_s)}$. The fermionic construction follows the same lines, but one must contract using extra Dirac matrices. So we basically know how to deal with **free** theories of any spin. But we all know $s = 2$ has something special. Why have we detected only a handful of different spins within the SM, and only up to $s \leq 2$? In fact we know very well how to construct **interacting** theories with $s \leq 2$. The real problem comes we we wish to write down **interacting** theories involving $s \geq 3$. The problem? In flat space... they do not exist!

This subject has a long and complicated story, which we will not review in this thesis. Let us just comment on the main results. The main obstacle is the famous no-go theorem from Coleman and Mandula [67] and related work by Weinberg [68]. In brief, the question they were asking was wether it is possible to have a theory in which the generators of the spacetime symmetries (the Poincare group) don't commute with the generators of the gauge symmetries. In other words, wether we can have symmetries that mix both the spacetime and the internal transformations simultaneously. In short, the Coleman-Mandula theorem states that under some assumptions, the most general Lie algebra of the S-matrix must be a direct product of the Poincare algebra and the internal gauge algebra.

As pointed out by Weinberg [68], Lorentz invariance puts very strong constraints on the possible outcome of scattering processes in $3 + 1$ flat space. The argument is very nice since it doesn't rely on a particular Lagrangian. It only assumes invariance under the 'little group', together with the fact that for massless fields one can always take the *soft limit* (low momenta). By analysing what happens to the density matrix when we couple it to a massless spin-1 field, one can prove this implies that the **total** spin-1 (electric) charge of the incoming particles must be conserved during the interaction. The same reasoning for a spin-2 field (the graviton) implies that *gravity is universal*, i.e. that all particles couple to gravity with the same strength $\sqrt{G}$. This happens because the spin-2

field implies a 'larger' gauge invariance, so the conservation law is more stringent. But when we try a spin-3 field, we go too far: it implies that all individual momenta must be conserved during the process - no interaction at all!

This line of reasoning led people to believe for a long time that higher spin theories didn't exist at all. However, that was not the end of it. Vasiliev showed that, because the hypothesis of the theorems fail to hold in curved spaces, higher spin theories can still exist. In fact he showed precisely how to construct them explicitly in AdS space. Moreover, in $1+1$ dimensional flat spacetime there's a further caveat and the preceding arguments do not hold either. That's provides a perfect window for $\mathrm{AdS}_3/\mathrm{CFT}_2$ higher spin holography to work!

In this chapter, we have made a choice. We will not go deeper into the story of the subject. Instead, we choose to focus from now on in the specific scenario at hand, namely $\mathrm{AdS}_3/\mathrm{CFT}_2$, in order to explain in more detail the mechanism oh higher spin holography in this particular case.

4.1 The tensionless limit of AdS/CFT

As we discussed in Chapter 2, each side of the correspondence possesses two independent parameters. The mainstream philosophy has been traditionally to work in the $g_s \to \sim$ $g_{YM}^2 \to 0$ limit, but keeping $\lambda = N g_{YM}^2 = (L/\ell_s)^4 \gg 1$. The benefit of this approach is that, by using a theory we do understand well (classical supergravity weakly curved) we can gain some insight into aspects of the physics of a theory we do not understand very well (strongly coupled gauge theories). This means using gravity to understand gauge theories.

However, there's an alternative perspective: we could choose to use our knowledge about perturbative gauge theories to learn something about strongly curved quantum gravity. This requires now to work in the limit where $L \approx \ell_s$, meaning that the strings become 'long' with respect to the curvature scale and loose tension. But a long, tensionless string will vibrate in very low energy modes, i.e. from the target space point of view these excitations look like massless particles. But since the string vibration contains arbitrarily

higher spin modes, we will end up with a theory containing massless higher spin fields.

A systematic theory of higher spin gauge fields was first described by Fronsdal [66]. As we are already familiar with 'lower' spin theories, massless fields come with a gauge symmetry: the photon has spin 1 and is associated to a $U(1)$ symmetry, while the graviton has spin 2 and is associated to spacetime diffeomorphisms. Now a physical system with a symmetry will always be more constrained than the same system without that symmetry. Since each one of these new higher spin fields implies an additional symmetry, it follows that consistent higher spin theories must be very much constrained, so much so that for a long time it was believed that only *free* higher spin theories could exist. However, it was the work of Vasiliev [69] that proved that *interacting* higher spin theories can exist!

In the context of AdS/CFT, higher spin theories where first realised explicitly by Klebanov and Polyakov [70]. The idea is that, in the large N limit, a Vasiliev theory (including all infinite higher spins) in AdS_4 is dual to a *vector model* CFT_3. For a review see [71].

$$\text{Vasiliev theory in } AdS_4 \longleftrightarrow \text{O(N) vector model in } \mathbb{R}^{1,2} \tag{4.3}$$

Although very interesting by itself, we will not be concerned with it un this work. Rather, let's give a lighting review of the duality which we will be concerned with, that of AdS_3/CFT_2. The concrete form of the proposal was put forward by Gaberdiel and Gopakumar [72]. The idea is that a Vasiliev theory in AdS_3 is dual to a special kind of conformal field theory in $1+1$ dimensions called 'coset minimal models'.

$$\begin{array}{ccc} \text{HS gravity in } AdS_3 & & W_N, k \text{ minimal model coset } CFT_2 \\ \text{CS theory for } \mathrm{hs}[\lambda] \oplus \mathrm{hs}[\lambda] & \longleftrightarrow & \dfrac{su(N)_k \oplus su(N)_1}{su(N)_{k+1}} \\ \lambda = \dfrac{N}{N+k} \quad , & & \dfrac{3L}{4G} = c_{N,k} \end{array} \tag{4.4}$$

We will explain all the ingredients of this below. Here we anticipate that the HS theory in AdS_3 will be constructed as a Chern-Simons (CS) theory with Lie algebra $\mathrm{hs}[\lambda]$. In Appendix A we review the construction of $\mathrm{hs}[\lambda]$. For now, we should only keep in mind that $\mathrm{hs}[\lambda]$ is the generalisation of $sl(N,\mathbb{R})$ from $N \in \mathbb{Z}$ to continuos value, $N \in \mathbb{R}$. On the other hand, the CFT is constructed by taking two decoupled CFTs and 'removing' some of the elements of the algebra (represented by the quotient in (4.4)). The gravity

side has two parameters: the curvature radius L and a real number λ that parametrises 'how many' higher spin fields there are, while the CFT has a *level* k and the dimension N of its matrices.

4.2 AdS_3 as a Chern-Simons theory

In this section we briefly review the Chern-Simons formulation of pure gravity in AdS_3, highlighting the main properties that will be useful later to construct its higher spin cousins. As we already commented above, pure gravity in 2+1 dimensions is a topological theory. There are no gravitational waves, and point particles feel no Newtonian attraction. Moreover, there exists a plethora of beautiful different solutions to Einstein's equations, all differing by their global (or topological) properties. However, it still comes a surprise to lear that pure gravity in $2+1$ dimensions can be completely recast (at the classical level) as another three dimensional topological field theory: Chern-Simons. We start this section by reviewing this connection.

The bridge between 2+1 gravity in the metric formulation and Chern-Simons theory is provided by the vielbein (tetrad) formalism. The idea is that, instead of working directly with the metric components $g_{\mu\nu}(x)$, one defines at each event in space-time an object $e_\mu{}^a(x)$ such that

$$g_{\mu\nu}(x) = e_\mu{}^a(x) e_\nu{}^b(x) \eta_{ab} \tag{4.5}$$

The vielbeins tell us exactly what matrix takes locally $g_{\mu\nu}$ and turns it into a flat metric. While the metric is constructed explicitly in terms of a given coordinate system by use of the tangent vectors, the vielbeins are referred to as a 'non-coordinate' basis because they require no coordinate system to be defined.

In the metric formalism, the (Christoffel) connection plays a key role by 'correcting' the partial derivatives with respect to flat space, thus enabling to define a covariant derivative. In the vielbein formalism, this role is played by the *spin connection* $\omega_\mu{}^a{}_b(x)$. This object is defined exactly as one would expect: if we take a tensor but now written in its flat components, the spin connection must correct the partial derivative,

$$\nabla_\mu V^a_{\ b} = \partial_\mu V^a_{\ b} + \omega_\mu{}^a{}_c V^c_{\ b} - \omega_\mu{}^c{}_b V^a_{\ c} \tag{4.6}$$

This then fixes its relation to the Christoffel connection:

$$\omega_{\mu}{}^{a}{}_{b} = e_{\nu}{}^{a} e^{\lambda}{}_{b} \Gamma^{\nu}{}_{\mu\lambda} - e^{\lambda}{}_{b} \partial_{\mu} e_{\lambda}{}^{a} \tag{4.7}$$

The beautiful link between $2+1$ gravity and Chern-Simons theory was first discovered by Achucarro and Townsend [73], and subsequently developed further by Witten [74]. On the one hand side, we have the Einstein-Hilbert action

$$I_{EH} = \frac{1}{16\pi G} \int_{M_3} d^3x \, \sqrt{|g|} \, (R - 2\Lambda) \tag{4.8}$$

On the other hand, we have two independent Chern-Simons fields, each one valued in the algebra $sl(2,\mathbb{R})$, with their associated action

$$I_{CS}[A] = \frac{k}{4\pi} \int_{M_3} \mathrm{Tr} \left(A \wedge dA + \frac{2}{3} A \wedge A \wedge A \right) \tag{4.9}$$

The statement is that up to a boundary term, we have

$$I_{EH} = I_{CS}[A^{+}] - I_{CS}[A^{-}] \tag{4.10}$$

provided we make the identification

$$A^{\pm} = \omega \pm \frac{1}{L} e \quad , \quad k = \frac{L}{4G} \tag{4.11}$$

or equivalently

$$\omega = \frac{1}{2} \left(A^{+} + A^{-} \right) \quad , \quad e = \frac{L}{2} \left(A^{+} - A^{-} \right) \tag{4.12}$$

where the spin connection with two indices is defined via $\omega_{\nu}{}^{a} = \frac{1}{2} \epsilon^{abc} \omega_{\nu bc}$. Using this 'dictionary', the metric elements are obtained by

$$g_{\mu\nu} = \frac{1}{2} \mathrm{Tr} \left(e_{\mu} e_{\nu} \right) \tag{4.13}$$

where again the trace refers to the $sl(2,\mathbb{R})$ algebra (here we will only consider the fundamental representation).

What about the equations of motion? On the CS side, since A^{+} and A^{-} are independent, we have two sets of equations. It is easy to see that they are simply:

$$F^{\pm} = 0 \tag{4.14}$$

where F is the field strength,

$$F^{\pm} = dA^{\pm} + A^{\pm} \wedge A^{\pm} \tag{4.15}$$

So the CS connections are in fact flat! Does that mean that the theory is trivial? Of course not. Although locally 'trivial' in the sense that there are no *local* excitations (like gravitational waves), a theory with vanishing field strength is not necessarily trivial due to its *global* or topological properties. In fact, this is not related to the non-abelian nature of the $sl(2)$ algebra, but happens even for the abelian case. This is precisely the case behind the celebrated Aharanov-Bohm effect. In that context, the field strength - the electric field - is everywhere zero, but the remotion of a point (or a line) from spacetime changes the topology of the problem. This is precisely the same that's happening here, with the extra ingredient that we're looking at a non-abelian gauge symmetry, instead of the abelian $U(1)$ associated to the electric charge.

Although written in very different variables, the equations (4.14) are in fact very familiar to us. Adding and subtracting them, we have

$$F^{+} + F^{-} = 0 \tag{4.16}$$

$$F^{+} - F^{-} = 0 \tag{4.17}$$

Written in the metric variables, the first equation is simply

$$R_{\mu\nu} - \Lambda g_{\mu\nu} = 0 \tag{4.18}$$

that is simply Einstein's equations! The second one gives instead

$$\Gamma^{\mu}{}_{\nu\rho} - \Gamma^{\mu}{}_{\rho\nu} = 0 \tag{4.19}$$

This is the condition of having no *torsion* in spacetime, which is something that we assumed (implicitly) when solving Einstein's equations to get AdS_3 or BTZ.

We thus see that in the special case of three dimensions, one theory can be written equivalently in two very different languages. We emphasize here that this statement is true **on-shell**: although the e.o.m. are identical, this does not ensure that the quantization of both theories gives the same result. This is an entire topic by itself, and in this these we will not come back to it.

Having provided the dictionary relating the metric and the CS languages, it is natural to ask how do the particular *solutions* that we know on the gravity side look like from the CS perspective. Let us here for convenience use the complex coordinates $w^{\pm} = \phi \pm it$ to parametrise the boundary directions. The most general exact solution to pure gravity in three dimensions is [75]

$$ds^2 = d\rho^2 + 8\pi GL\left(\mathcal{L}^+ dw^{+2} + \mathcal{L} dw^{-2}\right)\left(L^2 e^{2\rho/L} + (8\pi G)^2 \mathcal{L}^+\mathcal{L}^- e^{-2\rho/L}\right) dw^+ dw^- \quad (4.20)$$

Although in general $\mathcal{L}^{\pm}(w^{\pm})$ can be arbitrary functions of the holomorphic/antiholomorphic coordinates, in this these we will restrict to the case of *constant* $\mathcal{L}^{\pm}$.

Now let's see how this looks on the CS side. We choose the following basis for both $sl(2,\mathbb{R})$,

$$L_{-1} = \begin{pmatrix} 0 & 1 \\ 0 & 0 \end{pmatrix} \quad , \quad L_0 = \frac{1}{2}\begin{pmatrix} 1 & 0 \\ 0 & -1 \end{pmatrix} \quad , \quad L_1 = \begin{pmatrix} 0 & 0 \\ -1 & 0 \end{pmatrix} \qquad (4.21)$$

The associated CS connections read

$$A^{\pm} = \left(e^{\rho} L_{\pm 1} - \frac{2\pi\mathcal{L}^{\pm}}{k} e^{-\rho} L_{\mp 1}\right) dw^{\pm} \pm L_0 d\rho \qquad (4.22)$$

The meaning of this is the following: take the space-time dependent $sl(2,\mathbb{R})$ matrices (4.22) and plug them into (4.12) to find e. Now take the matrix e and compute the metric elements using (4.13). This will give you exactly (4.20). One can of course also check that they are indeed flat connection, i.e. they satisfy the e.o.m. (4.14) $F^{\pm} = 0$.

The main message of this section is that in $2+1$ dimensions, a Chern-Simons theory for the algebra $sl(2,\mathbb{R})$ is (classically) equivalent to a theory of pure gravity, that is, a massless spin-2 field, the metric. The remaining part of this chapter is devoted to the question of

- What physics do we get if we replace $sl(2,\mathbb{R})$ by $sl(N,\mathbb{R})$ or its generalisation, hs[λ]?
- What form does the AdS/CFT correspondence take in this case?
- How does one define black holes in these theories, and what are their thermodynamic properties?

4.3 AdS_3 higher spin gravity

We saw in last section how pure gravity in AdS_3 is related to a CS theory for $sl(2)$. There exists an algorithmic way of constructing higher spin theories from it, developed by Campoleoni, Fredenhagen, Pfenninger and Theisen [76]. Instead of $sl(2)$, we take $sl(N)$ for integer N, or more generally hs[λ], both of which always contain $sl(2)$ as a subalgebra, thus ensuring that we have the gravitational field as before. This can be consistently done for any finite N, without the need to include the infinite Vasiliev tower of higher spins. Now, it turns out that there are different inequivalent ways of embedding $sl(2)$ into $sl(N)$, but we will not discuss this here. Instead, lets give an example. Suppose we take $sl(3)$, which has 8 generators: $L_n = L_{\pm 1,0}$ and $W_n = W_{\pm 2,\pm 1,0}$. The explicit representation of the algebra is not relevant here. The Lie brackets are

$$[L_m, L_n] = (m-n)L_{m+n} \quad , \quad [L_m, W_n] = (2m-n)W_{n+m} \tag{4.23}$$

$$[W_m, W_n] = \frac{1}{3}(n-m)\left(2m^2 + 2n^2 - mn - 8\right) L_{m+n} \tag{4.24}$$

The L_n are the generators of the spin-2 symmetry, while the W_n generate the spin-3 symmetry. Now, just as we are used to with other algebras like the $su(2)$ or the Lorentz algebra, it is customary to define linear combinations J^a and $T^{ab} = J^{(a}J^{b)}$ which are particularly useful. Then, the vielbein and spin connection take the form

$$e = e^a J^a + e^{ab} T^{ab} \quad , \quad \omega = \omega^a J^a + \omega^{ab} T^{ab} \tag{4.25}$$

Recall that J^a and T^{ab} are simply some particular 3×3 matrices. This is simply decomposing the 8 generators into $8 = 3 \oplus 5$ multiplets, similar as in quantum mechanics when we decompose $1/2 \otimes 1/2 = 3 \oplus 1$.

Just as we did with the metric (4.13), we can now define *higher spin fields* in a similar way. For instance, the spin-3 field is defined via

$$g_{\mu\nu\rho} \sim \mathrm{Tr}\left(e_{(\mu} e_\nu e_{\rho)}\right) \tag{4.26}$$

One way of seeing that this corresponds to what we would normally call a higher spin gauge theory (Fronsdal), is to look at its equations of motion. For any algebra, the e.o.m. of Chern-Simons theory are simply zero field strengths, but now for both the spin-2 and spin-3 components independently,

$$F^{\pm a} = 0 \quad , \quad F^{\pm (ab)} = 0 \tag{4.27}$$

Again, by adding and subtracting these equations, we get the spin-3 generalisation of the Einstein equations and the torsion free equations. Consider for instance the former,

$$F^+ + F^- = dA^+ + A^+ \wedge A^+ + dA^- + A^- \wedge A^- = 0 \tag{4.28}$$

In the absence of the spin-3 piece, this would simply be Einstein's equation in the vacuum, i.e. the dynamical equations for the spin-2 field. However, because of the extra spin-3 terms in (4.25), we see that when we take the commutators involved in $A^\pm \wedge A^\pm$, we will get terms involving the spin-3 fields $A^{\pm(ab)}$. These enter precisely as *sources* in the Einstein equations, so the spin-3 field is interacting with the metric. Moreover, consider the following spin-3 field configuration,

$$h_{\mu\nu\lambda} \sim e_{(\mu}{}^{ab}\bar{e}_{\nu a}\bar{e}_{\lambda)b} \tag{4.29}$$

where $\bar{e}$ are the values of the AdS_3 vielbeins. This is a linearised version of the full spin-3 field. Then, we can plug this into the equations of motion for the spin-3 field, namely

$$F^{+(ab)} + F^{-(ab)} = 0 \tag{4.30}$$

and what one finds are precisely Fronsdal's equations, on the fixed background of AdS.

Now what about the boundary? In Chapter 2 we reviewed the Brown-Henneaux result [52]: the asymptotic symmetry algebra for pure gravity in AdS_3 is two copies of the Virasoro algebra with central charge $c = 3L/2G$, which was an important precursor of holography. Indeed Bañados showed that this exercise was very natural in the CS language [75]. That's what happens if we take the Chern-Simons theory with gauge algebra $sl(2)\oplus sl(2)$. So what if we take $sl(N)$ or hs[λ]? This question was also answered by [76] and subsequently extended by others [77, 78]. The answer is, in ascending generality,

$$\begin{array}{rcl} & \text{Asymptotic symmetries} & \\ SL(2,R)\times SL(2,R) & \longrightarrow & \text{Virasoro}\times\text{Virasoro} \\ SL(N,R)\times SL(N,R) & \longrightarrow & W_N\times W_N \\ hs[\lambda]\times hs[\lambda] & \longrightarrow & W_\infty[\lambda]\times W_\infty[\lambda] \end{array}$$

4.4 $\mathbf{CFT}_2$ with higher spin symmetries

In the introduction to this chapter, we mentioned that in $3+1$ flat spacetimes dimensions, we cannot have theories with higher spin fields $s \geq 3$. They reason why we *will* consider them in this chapter is that these arguments do not hold in $1+1$ dimensions. This opens the door for the study of higher spin theories in low dimensions! We are all familiar with a spin-2 current: the energy-momentum tensor $T_{\mu\nu}$. However in general it is possible for a theory to possess conserved currents of spin higher than 2. The simplest examples are provided, of course, by free bosons and free fermions. We start by reviewing them quickly to get a grasp on what this means. Later, we turn into the more interesting *interacting* CFTs in $1+1$ dimensions. We loosely follow the exposition of Rajesh Gopakumar given at [79].

Higher spin current algebras: free bosons and fermions

Consider the well known free boson theory,

$$I_B = \int d^2z \, \partial\phi \, \bar{\partial}\phi \tag{4.31}$$

Now construct the following spin$-s$ object:

$$\mathcal{W}_B^{(s)}(z) \sim \sum_{j=0}^{s-2} a_{n,j} \partial^{s-j-1}\phi \partial^{j+1}\phi \tag{4.32}$$

This contains in total exactly s derivatives, implying this transforms as a spin s tensor. The $a_{n,j}$ are constants which are irrelevant for our discussion. By the e.o.m., this current is automatically conserved,

$$\bar{\partial}\mathcal{W}_B^{(s)}(z) = 0 \tag{4.33}$$

and is therefore conserved. Why is this object interesting? Well, given the OPE for the primary fields, i.e. the rules of how to contract the fields (or more properly their first derivatives), this will completely fix the OPE between the currents $\mathcal{W}$. That is a straightforward calculation, and the result is schematically

$$\mathcal{W}_B^{(s)}\mathcal{W}_B^{(s')} \sim \#\mathcal{W}_B^{s+s'-2} + \#\mathcal{W}_B^{s+s'-4} + \ldots + c_s\delta_{ss'} \tag{4.34}$$

Recall that in CFT we can always translate an OPE into an algebra satisfied by the Laurent modes. Well, it turns out that the algebra (4.34) has a name, and actually, we already know it! It is $W_\infty[\lambda = 1]$.

What about free fermions? As you would expect, a very similar construction is possible. In that case, the higher spin current is given by

$$\mathcal{W}_F^{(s)}(z) \sim \sum_{j=0}^{s-1} b_{s,j} \partial^{s-j-1}\bar{\psi}\partial^j\psi \tag{4.35}$$

and again, the OPE of the fields determines the OPE of the currents. Similarly, the algebra satisfied by (4.35) OPE again has a name, and we also know it, it's $W_\infty[\lambda = 0]$.

So we learnt two important lessons for the apparently harmless free bosons and fermions:

1. They possess higher spin currents which form known algebras, and they are **not** the same algebra.

2. They both involve W_∞: this means that the algebra only closes if we include **all** $s = 2, \ldots, \infty$. From the perspective of the higher spin theory, this makes these apparently 'simple' theories very complicated.

However from the HS theories in AdS_3 we learnt that the current algebra associated to $sl(N)$ closes *including only spins from* 2 *to* N. So in order to find the CFT dual of AdS HS theories, the key question now becomes: how do we construct interacting CFTs that have a **finite number** of conserved higher spin currents? The answer turns out to be the **Coset CFTs**! Unfortunately, this is a rather technical subject, but we will try to make it as down-to-earth as possible. The first step is to review the concept of an *affine* (or Kac-Moody) algebra.

Affine Lie algebras

In physis, affine Lie algebras usually appear as the algebra satisfied by conserved currents of some Lagrangian. In CFT, a current is defined a chiral fields $j(z)$ that has conformal dimension $h = 1$, and similarly for the anti chiral sector. Now suppose we have several currents labelled as $J_{(i)}(z)$, and the expand them in a Laurent series $J_i(z) = \sum_n z^{-(n+1)} J_{(i)n}$.

Then, one can show that after a simple redefinition of the components $J_{(i)n} \to J^i_n$ (a rotation and dilation of the currents), these satisfy the Kac-Moody algebra:

$$[J^i_m, J^\ell_n] = f^{ij\ell} J^\ell_{m+n} + km\, \delta^{ij}\delta_{m,-n} \tag{4.36}$$

This is an interesting equation. First, one notices that the f^{ijk} are actually the structure constants of some Lie algebra $\mathbf{g}$. They must be, because if we set $m = 0 = n$ in (4.36), we recover precisely the Lie algebra bracket. But now we have more: the second term is called the 'central extension' of level k, because the identity is in the center of any group. It is in this sense that the Kac-Moody algebra (4.36) is a 'affine' algebra denoted $\mathbf{g}_k$ - it is an extension of the $\mathbf{g}$ algebra defined by its structure constants.

A simple example is provided by the free boson (4.31). Consider the set of three currents given by $J(z) = i\partial\phi$ and the two vertex operators $J^\pm(z) =: e^{\pm i\sqrt{2}\phi} :$. By expanding in Laurent modes and doing the redefinitions mentioned above, the modes satisfy the algebra

$$[J^i_m, J^j_m] = i\sqrt{2}\epsilon^{ijk} J^k_{m+n} + m\delta^{ij}\delta_{m,-n} \tag{4.37}$$

The structure constants correspond to the algebra $su(2)$, and the level is $k = 1$. Therefore, we lear that the free boson has currents that satisfy a $su(2)_1$ affine algebra.

How do we get a more general $su(N)_k$ algebra? A well known option it the Wess-Zumino-Witten model (WZW). The WZW is a very important example for many reasons. For one, it is an interacting CFT_2 that is exactly solvable. It is also closely related to 3d Chern-Simons theory, although we will not review that here. Its action is

$$I_{WZW} = -\frac{k}{4\pi}\int_{\partial M} d^2z \mathrm{Tr}\left[\left(g^{-1}\partial g\right)\left(g^{-1}\bar\partial g\right)\right] - \frac{ik}{12\pi}\int_M d^3x\, \mathrm{Tr}\left[\left(g^{-1}\partial g\right)^3\right] \tag{4.38}$$

For our discussion, the only purpose of exhibiting the WZW action is to show an explicit example of a theory where a Kac-Moody algebra is realised. The symmetries of the WZW action satisfy precisely a Kac-Moody algebra. Therefore an action of the type (4.38) where $g \in su(N)$ would be a good example of any of the $su(N)_k$ terms appearing in the coset that we are concerned of.

The Sugawara construction

How to define a stress tensor if we have no metric? The concept of a stress tensor relies on that of a metric, either by viewing it as the Noether current generating global Poincare

symmetries or as the functional derivative of the action with respect to the metric. But in a topological field theory (such as WZW) there is no metric, so how do we define a stress tensor? This becomes even more relevant in the case of conformal field theories, since the very term 'conformal' refers to the stress tensor satisfying the Virasoro algebra.

Sugawara showed how to do this in a restricted case - if we are given the current algebra. Suppose that the only thing we know is that the currents satisfy an affine Lie algebra of the form (4.36). Then, Sugawara showed that the following objects

$$L_n^{Sug} \equiv \frac{1}{k+h^\nu} \sum_{a,n} : J^a_{n-m} J^a_m : \tag{4.39}$$

constitute the Laurent modes of a CFT stress tensor - indeed they satisfy the Virasoro algebra, with a central charge given by

$$c^{Sug} = \frac{k \dim(g)}{k+h^\nu} \tag{4.40}$$

In (4.39) h^ν is the dual Coxeter number, which depends on the algebra chosen. For the case of interest of $su(N)_k$ we have

$$c^{Sug}\left[su(N)_k\right] = \frac{k(N^2-1)}{N+k} \tag{4.41}$$

The coset construction: quotienting an algebra = gauging a field

Now that we have reviewed all the main ingredients, let's explain how to put them into the quotient

$$\frac{su(N)_k \oplus su(N)_1}{su(N)_{k+1}} \tag{4.42}$$

So we start from a theory that is simply the sum of two actions: e.g. a WZW at level k and a WZW at level 1, so the Lie algebra is $g = su(N)_k \oplus su(N)_1$. Now comes the important step - we form a coset: we choose a subalgebra h of g, in this case $h = su(N)_{k+1}$. Let us call K^a_n the generators of $su(N)_k$ and J^a_n the generators of $su(N)_1$. Then, it is easy to see that the generators of $su(N)_{k+1}$ take the form $M^a_n = K^a_n + J^a_n$. Here of course the K's and J's commute since they are independent algebras. We define the **coset algebra** as the set of all generators of the numerator (K's and J's) that commute with the generators of the denominator ($K+J$)'s.

From the physicist point of view, this quotenting actually corresponds to *gauging* the field g - we introduce extra terms coupling the original field to a new gauge field A valued in $h = su(N)_{k+1}$ with no kinetic term, and then declaring that field configurations related by gauge transformations are physically equivalent. This is completely analogous to what we do in Yang-Mills theories by replacing $\partial \to \partial + iA$, although a bit more involved since the action is non linear. To be specific, we add the following term to the action, involving a gauge field A and $\bar{A}$ interaction between

$$-\frac{k}{2\pi}\int d^2z \,\mathrm{Tr}\left[\bar{A}\left(g^{-1}\partial g\right) - A\left(\bar{\partial}g\right)g^{-1} + A\bar{A} - g^{-1}Ag\bar{A}\right] \tag{4.43}$$

where we have gauge the currents, i.e. $g^{-1}\partial g \to g^{-1}Dg$.

So we started with the sum of two CFTs, but then we quotiented by a particular subgroup, so is the resulting theory also a CFT? The answer if of course Yes! Why? Well, the symmetry algebra (4.42) contains many generators, and it is a simple exercise to show that the particular combination

$$\mathcal{L}_n \equiv L_n^{Sug}(K) + L_n^{Sug}(J) - L^{Sug}(K+J) \tag{4.44}$$

satisfies precisely the Virasoro algebra, with central charge

$$c_{N,k} = c_{N,k} + c_{N,1} - c_{N,k+1} = (N-1)\left[1 - \frac{N(N+1)}{(N+k)(N+k+1)}\right] \tag{4.45}$$

Finally we come to the main point of this whole construction. The quotenting process not only produces a Virasoro algebra, but in fact realises exactly what we were looking for: the coset theory contains higher spin currents, exactly up to spin N! As an example, the spin-3 generator is schematically of the form

$$\mathcal{W}^{(3)} \sim J^3 + J^2K + JK^2 + K^3 \tag{4.46}$$

with relative coefficients fixed by the condition that $[\mathcal{W}^{(3)}, J+K] = 0$ (due to the definition of the coset). So the result is exactly what we were looking for: the coset models with contain exactly one higher spin current $\mathcal{W}^{(s)}(z)$ per spin, and **only** for $s = 2, \ldots, N$. The current algebra closes within a finite number of spins!

The coset CFTs

$$\frac{su(N)_k \oplus su(N)_1}{su(N)_{k+1}}$$

contain higher spin currents for $s = 2, 3, \ldots, N$

One take-home lesson of this section is that, although it's very easy to find theories with infinitely many higher spin currents (in the sense that the algebra closes), it is actually quite hard to construct theories with a finite number of higher spins! This might be one reason why this area is often perceived as rather cryptic.

Finally we have all the ingredients to write down the Gaberdiel-Gopakumar conjecture in a concrete way.

$$\begin{array}{ccc} \text{HS gravity in } \mathrm{AdS}_3 & & W_N, k \text{ minimal model coset } \mathrm{CFT}_2 \\ \text{CS theory for } \mathrm{hs}[\lambda] \oplus \mathrm{hs}[\lambda] & \longleftrightarrow & \dfrac{su(N)_k \oplus su(N)_1}{su(N)_{k+1}} \end{array}$$

$$\lambda = \frac{N}{N+k} \quad , \quad \frac{3L}{4G} = c_{N,k}$$

Although this is the conjecture in full generality, in the next chapter we will restrict to the case of $\lambda = 4$, and thus work with $SL(4,R) \times SL(4,R)$, whose dual possesses a $W_4 \times W_4$ asymptotic symmetry algebra.

4.5 The phases of higher spin black holes

4.5.1 What is a higher spin black hole?

In Lorentzian signature, the most natural notion of a black hole comes from the study of spacetime horizons and causality in a manifold. The black hole region is defined as the set of events in spacetime from which signals will never reach a far away causal observer. Nonetheless, Hawking showed that the thermodynamic properties of black holes have a very natural interpretation from the euclidean path integral representation of gravity. This becomes even more transparent in the case of $2+1$ gravity, due to its topological nature.

There exists by now many derivations of Hawking's celebrated formula for the black hole temperature,

$$T = \frac{\hbar \kappa}{2\pi} \tag{4.47}$$

where κ is the surface gravity.

Since the CS theory is topological, there are no physically meaningful local quantities. If there were, we could always gauge them away. For instance, suppose we gave an

interesting profile for the gauge field A in some sufficiently small region in spacetime. Then, by simply performing a gauge transformation, we could always map this field to a non-interesting field since $F = 0$. The point is that, although possible locally, this cannot be done *globally*. Therefore, the only 'interesting' observables must be **non-local**, and the most obvious non-local object in gauge theory is a Wilson loop, which is by construction gauge invariant

$$\mathrm{Hol}_\Gamma = \mathcal{P} \exp \oint_\Gamma A \tag{4.48}$$

where Γ is some closed loop in the manifold. If Γ encloses a simply connected manifold and A is smooth in it, then the holonomy must be *trivial*, i.e. the resulting matrix must belong to the centre of the group. Now, the gauge group of the CS theory is $SL(2,R) \times SL(2,R)$, rather than the isometry group of AdS_3 which is $SL(2,R) \times SL(2,R)/\mathbb{Z}_2$. Both $\mathbb{1}$ and $-\mathbb{1}$ are in the center of the former, but not in the latter. In fact, the correct value of the holonomy around the temporal cycle is $-\mathbb{1}$, the minus sign coming from the spin structure of the CS theory, corresponding to the minus sign a fermionic particle picks around the cycle. We will use this property below. If instead, we take the gauge field along a non-contractible cycle, the holonomy will give some other value that is not in the centre and will not be very relevant in our discussion.

The topology of BTZ is that of a solid torus, since both euclidean time and the angular variable are periodic, whereas the radius coordinate is non compact. Thus, we have two interesting cycles in which to compute the Wilson loop, the angular and the temporal. Moreover, the $\mathcal{L}^\pm$ that give the BTZ metric are given by

$$\mathcal{L}^+ + \mathcal{L}^- = \frac{ML}{8\pi G} \quad , \quad \mathcal{L}^+ - \mathcal{L}^- = \frac{J}{8\pi G} \tag{4.49}$$

So let's study the holonomies of the BTZ solution (4.22) together with (4.49). Well, it turns out that by performing a gauge transformation

$$A^\pm = b^{\mp 1} a^\pm(w^\pm) b^{\pm 1} + b^{\mp 1} db^\pm \tag{4.50}$$

where $b = e^{\rho L_0}$ and $a^\pm(w^\pm)$ are holomorphic and antiholomorphic fields, we can actually gauge away the radial dependence of the connections $A^\pm$ and work with the simplified connections,

$$a^\pm = \left(L_{\pm 1} - \frac{2\pi \mathcal{L}^\pm}{k} L_{\mp 1} \right) dw^\pm \tag{4.51}$$

As we mentioned earlier, the BTZ modes $\mathcal{L}^{\pm}$ in (4.49) are simply constants, so evaluating the integrals is trivial. However we must remember here that in the euclidean formulation, the euclidean time variable does not range in a 'definite' interval, but rather $t \in [0, i\beta)$ where β is the inverse temperature. The holonomy around the temporal cycle, evaluated on a constant ϕ gives (using the matrices (4.21) explicitly):

$$\mathrm{Hol}_t(a^+) = \exp \oint dt \left(L_1 - \frac{2\pi \mathcal{L}^+}{k} L_{-1} \right) \tag{4.52}$$

$$= \exp \beta \left(L_1 - \frac{(2\pi)^2 \mathcal{L}^+}{k} L_{-1} \right) \tag{4.53}$$

$$= \exp \beta \begin{pmatrix} 0 & -\frac{2\pi\mathcal{L}}{k} \\ -1 & 0 \end{pmatrix} \tag{4.54}$$

and a similar expression for a^-. To evaluate the exponential, we first diagonalising the matrix to get

$$\mathrm{Hol}_t\left(a^+\right) = \exp\left(PDP^{-1}\right) = P \exp(D) P^{-1} \tag{4.55}$$

Next, we wish to impose that the diagonal matrix is $-\mathbb{1}$ as explained above, which will imply $\mathrm{Hol}_t = -\mathbb{1}$. The eigenvalues are simply $\lambda_{\pm} = \pm i\beta\sqrt{2\pi\mathcal{L}/k}$ which we then impose to be $\pm i\pi$. Finally we insert back $\mathcal{L}^+$ from (4.49). Following the same procedure for a^-, we get left and right temperatures,

$$\beta^{\pm} = \frac{L}{r_+ \pm i r_-} \tag{4.56}$$

The Hawking temperature is determined in terms of these as $\beta = \pi L \left(\beta^+ + \beta^-\right)$, that is

$$T = \frac{2\pi L^2 r_+}{r_+^2 - r_-^2} \tag{4.57}$$

which is precisely the BTZ temperature (2.43) as described in the Introduction. Thus we see that in the CS formulation, the themodynamics of the black hole can be defined

4.5.2 Canonical partition function and stability

Soon after black hole entropy [80, 81] and radiation [82] were discovered, Gibbons and Hawking [83] showed that these properties can be derived directly from the Euclidean gravitational action. Black holes are now understood as part of a thermodynamical system

with an associated semi-classical partition function

$$Z(\beta) = \sum_M e^{-\beta M + S(M)} \,. \tag{4.58}$$

For Schwarzschild black holes the entropy takes the famous value $S = \text{Area}/(4G) = 4\pi G M^2$ [1].

This partition function can be extended to more general black holes in various dimensions. Of particular interest in recent years has been a relatively new family of configurations, namely, three-dimensional black holes carrying higher spin charges [84].

In this thesis we study the thermodynamics of higher spin theories by emphasizing the role of the partition function (4.58). We uncover a rich structure with several interesting features: i) the existence of Hawking-Page transitions from black holes to the AdS_3 background; ii) discontinuous phase transitions among black hole states with different macroscopic properties (van der Waals-like); and iii) a second order transition and a critical point. For related work see [85–88].

We start by reviewing some applications of (4.58). The partition function is dominated by the configuration that minimizes the action

$$\Gamma_\beta(M) = \beta M - S(M) \,. \tag{4.59}$$

In a more general setup, Γ will depend on additional charges and chemical potentials. This function, related to the mean field free energy, encodes the thermodynamic structure of the gravitational system and will be our main tool to analyze its phases. Consider Schwarzschild black holes, for example. A quick look shows that $\Gamma_\beta(M)$ does not have a minimum at all; the value $M = \beta/(8\pi G)$ is a maximum, revealing the well-known instability of this system in the canonical ensemble.

The instability of Schwarzschild black holes can be cured either by putting the system in a box [89] or by adding a negative cosmological constant [15], the latter case leading to the celebrated Hawking-Page transition. It is instructive to understand this phenomenon from the point of view of the action (4.59).

In Figure 4.1 (left) we plot $\Gamma_\beta(M)$ for $3+1$ Schwarzschild-AdS black holes for different

[1] We work in natural units $\hbar = c = k_B = 1$.

values of β [2]. At high temperatures (burgundy curve, small β), there is a clear minimum satisfying

$$\beta = \frac{\partial S(M)}{\partial M}. \tag{4.60}$$

As the temperature drops, however, the solution to this equation ceases to be the global minimum of $\Gamma_\beta(M)$. For $\beta > \beta_c$, the AdS_4 background with $M = 0$ is the preferred state. This transition from the black hole dominated phase to the vacuum is called Hawking-Page transition. Notice that the minimum of $\Gamma_\beta(M)$ is continuous at $\beta = \beta_c$ but its derivative is not.

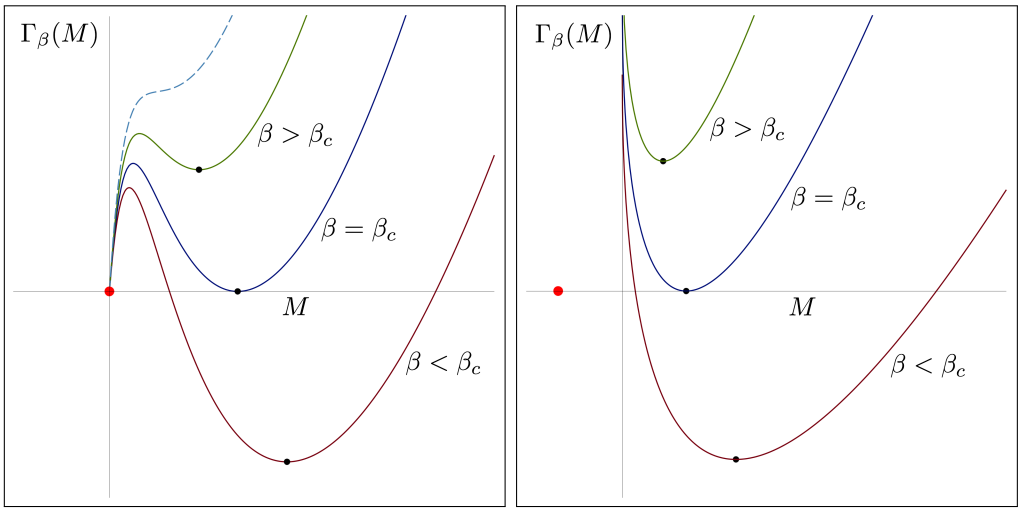

Figure 4.1: Hawking-Page transition in $3+1$ Schwarzschild-AdS black holes (left) and $2+1$ BTZ black holes (right). The red dots represent the AdS_4 ($M = 0$) and AdS_3 ($M = -1/(8G)$) ground states, respectively. The dashed curve has no local minima but plays no role in the analysis. Figure from [34].

The analysis for three-dimensional BTZ black holes is similar, except that the AdS vacuum is now a bound state separated from the black hole continuum by a mass gap. In Figure 4.1 (right) we plot $\Gamma_\beta(M) = \beta(M - M_{AdS}) - S(M)$ for three values of β [3]. For convenience we have shifted the action such that $\Gamma_\beta(M_{AdS}) = 0$. We see that a local

[2]The entropy of $3+1$ Schwarzschild-AdS black holes is $S(M) = \pi r_+^2(M)/G$, where $r_+(M)$ is the unique real solution to the equation $1 - 2GM/r_+ + r_+^2/\ell^2 = 0$. In particular, $S(0) = 0$; the AdS_4 vacuum has no entropy. The critical temperature is $\beta_c = \pi\ell$.

[3]The entropy of $2+1$ BTZ black holes is $S(M) = \ell\pi\sqrt{2M/G}$. In this normalization the AdS_3 vacuum corresponds to $M = -1/(8G)$. Of course, it carries no entropy. The critical temperature is $\beta_c = 2\pi\ell$.

minimum satisfying (4.60) exists for all temperatures but only for $\beta < \beta_c$ does this state have less action than AdS_3 space.

4.5.3 The higher spin grand canonical ensemble

We now move on to study the phase structure of three-dimensional higher spin gravity. This theory is topological in nature and does not have a known description in terms of metric fields ($g_{\mu\nu}$, $g_{\mu\nu\rho}$, etc.). Instead, it must be formulated as a Chern-Simons theory where the basic variables are $sl(N;\mathbb{R})$ ($N \times N$, real, traceless) matrices A_μ. In a radial gauge, and restricting to static and circularly symmetric configurations, one is left with two such matrices, A_t and A_φ, satisfying

$$[A_t, A_\varphi] = 0\,. \tag{4.61}$$

This is the remnant of the Chern-Simons equations of motion. We refer the reader to the extensive literature on this subject for more details.

The gauge invariant information carried by the fields is characterized by the $N-1$ charges

$$Q_n = \frac{1}{n}\mathrm{Tr}\left(A_\varphi^n\right)\,, \qquad n = 2\,,\ldots\,,N\,. \tag{4.62}$$

The possible values these charges can take depend on the spatial topology of spacetime. We shall consider two classes of solutions. First, there is the AdS_3 vacuum, for which the spatial topology is a plane and the cycle $\varphi \sim \varphi + 2\pi$ is contractible. As a consequence, the eigenvalues of A_φ are imaginary and quantized, so as to render a smooth field [4]:

$$\mathrm{Eigen}\left(A_\varphi^{AdS}\right) = \frac{i}{2}\left(N-1, N-3, \ldots, 1-N\right)\,. \tag{4.63}$$

The corresponding charges can be computed from (4.62). Notice that $Q_n^{AdS} = 0$ for odd n. For $N = 4$, which will be our main example, we find

$$Q_2^{AdS} = -\frac{5}{2}\,, \qquad Q_3^{AdS} = 0\,, \qquad Q_4^{AdS} = \frac{41}{16}\,. \tag{4.64}$$

The time direction is non-compact so the matrix A_t^{AdS} is only restricted by (4.61) and not by regularity. This is important. The residual freedom in A_t^{AdS} is just what is needed in

[4] The holonomy is $Pe^{\oint A_\varphi^{AdS}} = (-1)^{N-1}\mathbb{1}_{N\times N}$.

order to match the chemical potentials of AdS_3 to those of black holes (just like thermal AdS and Schwarzchild-AdS can both be put at the same temperature).

The second class of solutions we are interested in are black holes. The spatial topology in this sector is a semi-infinite cylinder, with the boundary at $r = 0$ corresponding to the horizon. This space is homeomorphic to the punctured disk. Since the cycle $\varphi \sim \varphi + 2\pi$ is not contractible, A_φ (and therefore Q_n) is left unrestricted. We take the eigenvalues of A_φ to be real for black hole configurations, in consistency with the definition given in [90] in a supersymmetric context. For $N = 4$ we parametrize the eigenvalues as

$$\begin{aligned}\text{Eigen}\,(A_\varphi) = \frac{1}{2}\,(&2\lambda_1 + \lambda_2, 2\lambda_1 - \lambda_2,\\ &-2\lambda_1 + \lambda_3, -2\lambda_1 - \lambda_3)\ .\end{aligned} \tag{4.65}$$

It follows that the black hole charges read

$$\begin{aligned} Q_2 &= 2\lambda_1^2 + \frac{1}{4}\lambda_2^2 + \frac{1}{4}\lambda_3^2\,,\\ Q_3 &= \frac{1}{2}\lambda_1\,(\lambda_2 - \lambda_3)\,(\lambda_2 + \lambda_3)\ ,\\ Q_4 &= \lambda_1^4 + \frac{1}{32}\left(\lambda_2^4 + \lambda_3^4\right) + \frac{3}{4}\lambda_1^2\left(\lambda_2^2 + \lambda_3^2\right)\ . \end{aligned} \tag{4.66}$$

In this sector, the matrix A_t is constrained by regularity to be [5]

$$\text{Eigen}\,(A_t) = \frac{1}{2}\,(N-1, N-3, \ldots, 1-N)\ . \tag{4.67}$$

This is because the time cycle $t \sim t + 2\pi$ is contractible in the black hole topology. Finally, black holes have an entropy given by [91–94]

$$S(Q) = \text{Tr}\,(A_t A_\varphi)\ . \tag{4.68}$$

For $N = 4$ this yields

$$S(\lambda) = \frac{1}{2}\,(8\lambda_1 + \lambda_2 + \lambda_3)\ . \tag{4.69}$$

We are now ready to display the grand canonical partition function [6] we aim to calculate:

$$Z(\mu_2, \mu_3, \ldots \mu_n) = 1 + \sum_{\left\{\substack{\text{black}\\ \text{holes}}\right\}} e^{-k\Gamma_\mu(Q)}\,, \tag{4.70}$$

[5] The absence of the factor of i in (4.67) is due to the Euclidean continuation. It reappears in the holonomy $Pe^{i\oint A_t} = (-1)^{N-1}\mathbb{1}_{N\times N}$.

[6] Higher spin gravity is actually described by two independent copies of the $sl(N)$ Chern-Simons action. Since the total partition function factorizes, we focus on one sector only.

where the action is

$$\Gamma_\mu(Q) = \sum_{n=2}^{N} \mu_n \left(Q_n - Q_n^{AdS}\right) - S(Q)\,. \tag{4.71}$$

The first term '1' in (4.70) corresponds to the AdS_3 bound state, whose contribution has been subtracted in (4.71) so that $\Gamma_\mu(Q^{AdS}) = 0$. The AdS charges have fixed values (for $N = 4$, see (4.64)). The sum is then taken over the spectrum of black holes, that is, over all charges consistent with real eigenvalues of A_φ. Also, for convenience we have factored out the coupling constant "k" (Chern-Simons level). This parameter is related to the central charge by

$$k = \frac{2\pi c}{N(N^2-1)}\,, \qquad c = \frac{3\ell}{2G}\,,$$

and is a measure of the number of degrees of freedom in the system. The steepest descent approximation is justified in the limit $k \sim c \to \infty$. The real parameters μ_n are chemical potentials conjugate to Q_n. See [91] for details on this. The case of pure gravity is recovered for $N = 2$ after identifying $\mu_2 = \beta/(2\pi l)$ and $Q_2 = 2GM$.

We emphasize that the study of the partition function (4.70) represents a well-posed problem on its own right, independent from its relation to Chern-Simons theories and higher spin black holes. In fact, this problem has striking similarities with the mean field description of some condensed matter systems such as liquid crystals [95–97].

Notice that, for any N, the charges Q_{2n} are always semi-positive while Q_{2n+1} have no definite sign. This explains why even N can yield a stable partition function but odd N cannot. Indeed, the action (4.71) is a polynomial of degree N in the eigenvalues of A_φ. Since the leading terms enter as $\Gamma_\mu(\lambda) = \mu_N Q_N(\lambda) + \cdots$, the conditions $N \in 2\mathbb{N}$ and $\mu_N > 0$ guarantee that $\Gamma_\mu(\lambda)$ is bounded from below. The sum (4.70) then converges. It turns out that $N = 4$ is the simplest, non-trivial, stable theory; $N = 2$ exhibits a Hawking-Page transition but no transitions between black hole states, and $N = 3$ is unstable. From now on we concentrate on $N = 4$.

In principle, the computation of (4.70) involves a sum over the charges Q_n. This is inconvenient because the entropy (6.39) has a very simple form in terms of the eigenvalues but not as a function of the charges themselves. Expressing S as a function of Q_n would involve inverting (4.66). Happily, this is not necessary. We shall now argue that the sum over charges can be traded for a sum over eigenvalues, up to logarithmic corrections that we discard in large k limit.

From (4.66) we find that the Jacobian for the change of variables $Q_n \to \lambda_i$ is

$$\left|\frac{\partial Q}{\partial \lambda}\right| = \frac{1}{32}\lambda_2\lambda_3\left(4\lambda_1+\lambda_2+\lambda_3\right)\left(4\lambda_1-\lambda_2+\lambda_3\right) \times \left(4\lambda_1+\lambda_2-\lambda_3\right)\left(4\lambda_1-\lambda_2-\lambda_3\right) . \tag{4.72}$$

We see that $\left|\frac{\partial Q}{\partial \lambda}\right| = 0$ happens precisely when two or more eigenvalues of A_φ coincide. In that case, A_φ is non-diagonalizable and the solution becomes extremal [90]. Of course, we restrict our attention to solutions bounded by extremal black holes; the points where the map $Q_n \to \lambda_i$ is not invertible are never touched. For orientation, recall that in the spectrum of 2+1 black holes, the angular momentum J is bounded by $-M < J < M$, with $J = \pm M$ corresponding to extremal solutions. The map $Q_n \to \lambda_i$ fails to be invertible at the extreme points $J = \pm M$. Going back to the general case, the domain of λ_i should lie within any of the "wedges" defined by the planes $\left|\frac{\partial Q}{\partial \lambda}\right| = 0$. Different wedges correspond to different branches of the inverse map $Q \to \lambda(Q)$ and have different entropy functions $S(Q)$. We will work in the wedge that includes the BTZ black hole ($\lambda_1 = \lambda_2 = \lambda_3 > 0$), for which all the factors in (4.72) are positive.

So, given a set of values for the chemical potentials μ_2, μ_3 and μ_4, we want to compute the values of λ_1, λ_2 and λ_3 that minimize the action $\Gamma_\mu(\lambda)$. This configuration will dominate the partition function (4.70). In particular, we would like to study the continuity of the λ_i obtained in this way as one varies μ_2, μ_3 and μ_4.

First, we have checked explicitly, within a wide range of chemical potentials, that the minimum of $\Gamma_\mu(\lambda)$ is never achieved by extremal black holes. The minimum either occurs for the AdS_3 groundstate, with $\Gamma_\mu(Q^{AdS}) = 0$, or it lies in the interior of the BTZ wedge [7]. We do not need to worry about extremal solutions.

4.5.4 The higher spin Hawking-Page transition

Next, we separate the region in the space of chemical potentials where black hole states dominate from the region where the AdS ground state is preferred. The interface between

[7] We have also checked that if one does not restrict the eigenvalues to any particular wedge, the global minimum of $\Gamma_\mu(\lambda)$ in the black hole sector is always found in the BTZ wedge and not in any other.

these two regions is defined by the equation

$$\min_{\left\{\substack{\text{black}\\\text{holes}}\right\}} \Gamma_\mu(Q) = \Gamma_\mu\left(Q^{AdS}\right), \tag{4.73}$$

and its graphical representation is shown in Figure 4.2.

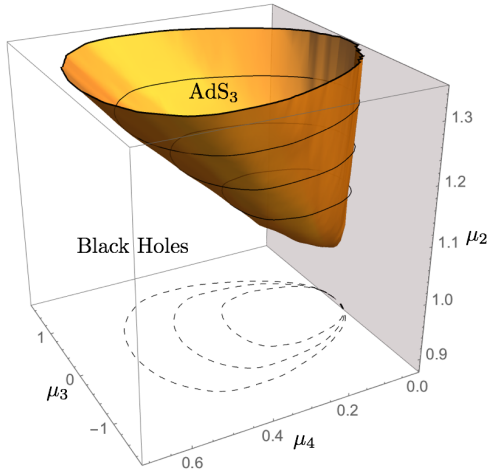

Figure 4.2: Hawking-Page surface for the $sl(4;\mathbb{R})$ theory. The minimum is located at $\mu_2 = 1$, $\mu_3 = 0$, $\mu_4 = 0$. This coincides with the critical temperature of $2+1$ BTZ black holes after identifying $\mu_2 = \beta/(2\pi\ell)$. Figure from [34].

The interior of the surface corresponds to the AdS dominated phase. Outside black holes dominate. Crossing this surface in any direction gives a first order Hawking-Page transition.

4.5.5 Transitions amongst black holes, critical point

Let us now concentrate on the region of black hole dominance and look for the global minimum satisfying

$$\frac{\partial \Gamma_\mu(\lambda)}{\partial \lambda_i} = 0\,. \tag{4.74}$$

(Recall that $\Gamma_\mu(\lambda)$ is built from (4.71) after using (4.66) to write the charges in terms of the eigenvalues, together with the expressions (6.39) for the entropy and (4.64) for the background charges). These equations can be simplified by setting $\mu_2 = 5\mu$ and rescaling $\mu_3 \to \mu_3\mu^2$, $\mu_4 \to \mu_4\mu^3$ and $\lambda_i \to \lambda_i/\mu$. The μ dependence then drops out from (4.74), reducing the black hole thermodynamics to a two dimensional phase diagram.

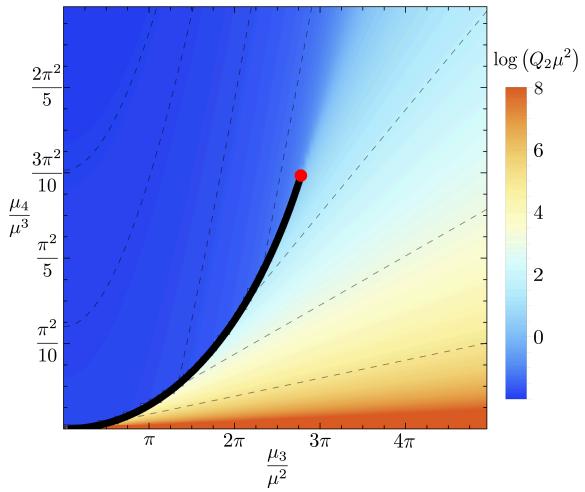

Figure 4.3: Phase diagram of the $N = 4$ system, with the second order critical point in red and the first order critical line in black. The complete diagram is symmetric with respect to the vertical axis. $\mu = \mu_2/5$. Figure from [34].

Figure 4.3 shows the phase diagram for the charge Q_2. Similar results are obtained for the other two charges. One observes that from the origin stems a critical line across which the system exhibits a first order phase transition between two macroscopically different black hole states. The line ends at a critical point (in red). We now show that at the critical point a second order phase transition takes place in which the minima of $\Gamma_\mu(\lambda)$ become degenerate.

For systems with a single order parameter a critical point occurs when the first, second and third derivatives of the free energy vanish. The simplest generalization to the case with multiple order parameters is to demand that the Hessian matrix has one null eigenvalue, with the rest being strictly positive. Calling v^i the corresponding normalized eigenvector, we further require that the third derivative of $\Gamma_\mu(\lambda)$ along v^i vanishes. Thus, in addition to (4.74), the critical point must satisfy

$$v^j \frac{\partial^2 \Gamma_\mu(\lambda)}{\partial\lambda_i \partial\lambda_j} = 0\,, \quad v^i v^j v^k \frac{\partial^3 \Gamma_\mu(\lambda)}{\partial\lambda_i \partial\lambda_j \partial\lambda_k} = 0\,. \tag{4.75}$$

To ensure that we still have a minimum, the fourth derivative along v^i should be positive. Following this approach we find that the $N = 4$ higher spin theory exhibits two mirror

critical points, the first of which is located at

$$\begin{aligned} &\mu_2 = 5\,\mu\,, && \lambda_1 = \frac{0.3299}{\mu}\,, && v^1 = -0.2061\,, \\ &\mu_3 = 8.7184\,\mu^2\,, && \lambda_2 = \frac{0.0854}{\mu}\,, && v^2 = 0.0349\,, \\ &\mu_4 = 2.9299\,\mu^3\,, && \lambda_3 = \frac{1.0259}{\mu}\,, && v^3 = -0.9779\,, \end{aligned} \tag{4.76}$$

and corresponds to the one displayed in Figure 4.3. The second point (not shown in Figure 4.3) is obtained by exchanging $\lambda_2 \leftrightarrow \lambda_3$ ($Q_3 \to -Q_3$) and $\mu_3 \to -\mu_3$, which is a symmetry of the action (4.71). The values of the charges and the entropy at the critical points can be computed directly from (4.66) and (6.39). One can check that in the range $1.0886 < \mu < 6.3591$ the second order phase transition takes place inside the Hawking-Page surface and is therefore not relevant. The endpoints of this interval correspond to the intersection of the critical point with the Hawking-Page surface.

The phase diagram "μ_3-μ_4" is qualitatively similar to a "P-T" diagram for a liquid-gas transition. Therefore, a Van der Waals-like equation of state is expected to describe the different phases. Figures 4.4 and 4.5 are the analog of plotting 'isotherms' in a "P-V" diagram for a liquid-gas system. A drastic change in the derivatives $\partial\mu/\partial Q$ is observed when crossing the critical line. Thus, we could identify the different regions as a 'liquid' phase, in which the black holes are highly sensitive to any change in the charges, and a 'gaseous' phase, characterized by considerably smaller values of $\partial\mu/\partial Q$.

It is important to notice that the phase transitions always occur between black hole states with $Q_4 \neq 0$, as seen explicitly in the "μ_4-Q_4" diagram (figure 4.5). This fact guarantees that the solutions between which the system is transitioning have the same asymptotic (UV, far from the horizon) structure [8]; it is the spin of the highest spin charge that sets the value of the AdS radius and the central charge. As argued in [88], the corresponding asymptotic symmetry algebra for $N = 4$ is a $\mathcal{W}$-algebra associated to the $(2, 1, 1)$ non-principal embedding of $sl(2)$ in $sl(4)$.

4.5.6 Conclusions and future directions

In this thesis we have studied the thermodynamic phase space properties of $sl(N;\mathbb{R})$ higher spin black holes. We have identified the even-N theories as those having well-

[8] We thank one of the referees for pointing out this issue.

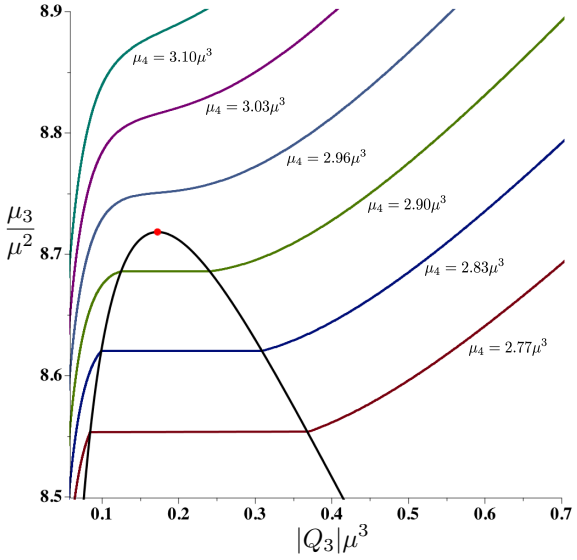

Figure 4.4: μ_3 - Q_3 diagram with iso - μ_4 curves. Figure from [34].

defined (finite and stable) partition functions in the ensemble under consideration. These theories exhibit Hawking-Page transitions, just like any black hole coupled to a negative cosmological constant. Moreover, we find first order phase transitions between different higher spin black holes, as well as a second order transition and a critical point.

Our work left many interesting future directions to pursue. On the gravity side, an obvious question is to generalise our method to consider $sl(N, \mathbb{R})$, and, more interestingly, to hs[λ]. In principle, we see no fundamental impediment to achieve this goal.

On the other hand, our thesis was mainly concerned with the gravity side of the duality. So a very intriguing direction would be to understand how to extract the same phase diagram, but working directly with the higher spin CFT. Where exactly the CFT partition function do we find the information of the relevant saddles that we see in gravity?

Even for the $N = 4$ case at hand, there remain some interesting lines to explore. For instance, we only discussed the grand canonical ensemble, in which we fix all the potentials. But how does the phase diagram change if we change the ensemble? This is in general a non-trivial question which can have interesting physics behind. For example, it is well known that black holes carrying electric charge (i.e. spin-1 charge) behave very differently if we fix the electric potential, or the electric charge [98]. In the latter case, this includes a second order phase transition but with anomalous critical exponents.

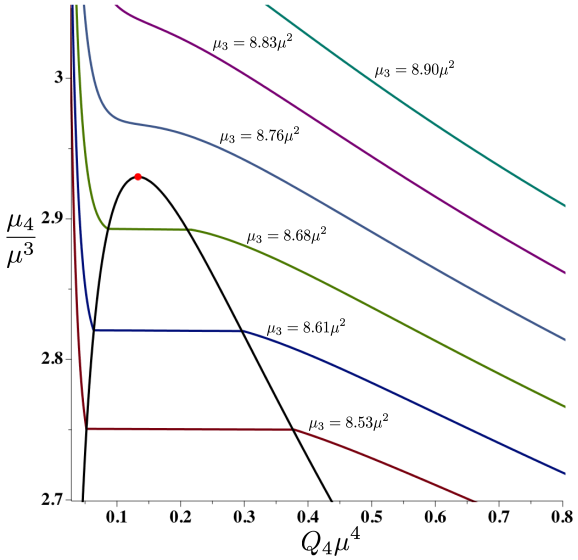

Figure 4.5: μ_4 - Q_4 diagram with iso - μ_3 curves. Figure from [34].

Another point worth mentioning for the $N = 4$ case is very existence of a second order phase transition. This of course implies that the system possesses an *emergent* conformal symmetry at that point. Understanding the meaning of this extra Virasoro symmetry (which is of course not originated in the Virasoro defining the CFT) would be very interesting.

Chapter 5

Complexity from Tensor Networks in holography

The Ryu-Takayanagi formula reviewed in Chapter 3 has opened an entire new subarea in high energy physics. By providing a link between the geometry of the bulk spacetime and the entanglement structure of the boundary theory, it suggested that there could be entire field of physics underlying its mechanics: (quantum) **information theory**. Although entanglement entropy has received by far most of the attention, in recent years some other concepts have also been the subject of intense study.

One such quantity is **computational complexity**. The original motivation by Susskind [29] was the following. In a generic quantum theory, in the process of time evolution the system will eventually thermalise, and quantities such as the entanglement entropy of any subregion will stop growing and saturate. However, it was known due to the results of Nielsen [99,100] that even in that regime, the wavefunction continues to move non-trivially in the Hilbert space for a much longer time, implying that the computational complexity keeps growing. Does AdS/CFT capture this phenomenon? And if so, how? This will be the topic of this chapter.

5.1 Computational Complexity and its holographic proposals

In order to understand the notion of complexity in holography, we first need to review what it means in quantum mechanics. This requires to introduce some notions from information theory.

First let's review what the idea of a **circuit** is. Actually, this is a very old concept that comes from computer science. The main difference between classical and quantum circuits is the class of gates that we are allowed to use. A circuit consists of a set of initial data (let's say classical bits or qubits), each of one is transmitted via a wire, and a set of *gates* that can act on those channels. By taking the initial data as an input, we act on it by a given sequence of gates and this will produce some final output. In Fig. 5.1 we see a simple example.

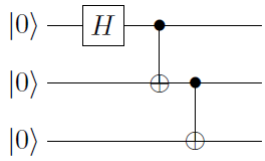

Figure 5.1: A simple 3-qubit circuit. First the Hadamard gate is applied, followed by a par of cNOT.

Here we read the circuit from left to right. We see two very frequently used gates: H and cNOT. The Hamard gate H acts on a single qubit, and in the basis $|0\rangle, |1\rangle$ it takes the form

$$H = \frac{1}{\sqrt{2}} \begin{pmatrix} 1 & 1 \\ 1 & -1 \end{pmatrix} \tag{5.1}$$

The usefulness is of course that, given a basis state, it produces superpositions of states with equal probability. In the circuit, after H is applied, we see two successive applications of the controlled-NOT (cNOT) gate. By itself, the NOT gate is a single-qubit gate that corresponds to the $\oplus$ symbol and is simply equal to the Pauli matrix X,

$$X = \begin{pmatrix} 0 & 1 \\ 1 & 0 \end{pmatrix} \tag{5.2}$$

The reason for the name NOT is that X is the quantum analog of the classical NOT gate: it the input is $|0\rangle$ it gives $|1\rangle$ and viceversa - so it returns the 'opposite' of the input. Now, the controlled-NOT in the figure is the prototype for multi-qubit gates. In this case, it is a 2-qubit gate that has one *control* qubit (the upper one) and a *target qubit* (the bottom one). The function of the gate is the following: if the if the control qubit takes the value 0, then the target qubit is flipped. Otherwise it is untouched. In matrix language, we can represent it like this: choose the 2-qubit basis in this order: $\{|00\rangle, |01\rangle, |10\rangle, |11\rangle\}$, where the first qubit corresponds to the control and the second to the target. Then, the cNOT gate looks like this

$$\text{cNOT} = \begin{pmatrix} 1 & 0 & 0 & 0 \\ 0 & 1 & 0 & 0 \\ 0 & 0 & 0 & 1 \\ 0 & 0 & 1 & 0 \end{pmatrix} \tag{5.3}$$

This is a very simple example to grasp the key ideas of quantum circuits. Of course, this an entire field in computer science and quantum information theory which is indeed extremely interesting. Now, one important concept is that of a **universal set of gates**. In both classical and quantum computing, this is roughly defined as a set of gates such that *any* possible operation on the computer can be achieved by a finite sequence of gates within that set. Of course, strictly speaking this is impossible since the set of gates in uncountable, whereas the number of finite sequences of a finite set of gates is countable. Thus, technically one always asks wether it is possible to approximate any given state to a finite tolerance. There are many interesting results about universality. For example, an important theorem by Kitaev one states that the set $\{\text{Hadamard}, \text{cNOT}, \text{phase}, \pi/8\}$ is universal [101]. We shall encounter again the question of the set of gates when we discuss Tensor Networks and our results on compression complexity.

Having introduced the general idea of quantum circuits, we are in better shape to define the notion of **computational complexity**. In rough term, complexity captures how 'difficult' it is to perform a given task. Now, in information theory there are many different notions of complexity. In this section, we are interested in the following definition. Suppose we are given a set of n qubits, an initial reference state $|\psi_i\rangle$, a final state $|\psi_f\rangle$ and a finite universal set of gates $\{g_j\}$. The g_j are unitaries are some collection of matrices in

$SU(2^n)$ (the space of all possible allowed operations). Then, complexity is defined as the minimal number of applied gates needed within the set that will produce the final state starting from the initial reference:

$$|\psi_f\rangle = U|\psi_i\rangle \tag{5.4}$$

where $U = \ldots g_2 g_1$. Since we assume the gate set is universal, the existence of at least one circuit that implements U is guaranteed. However, this circuit might be very far from optimal for it could include various redundancies, etc. The question is to find what is the minimum number of operations we need, using the allowed gates, to produce the unitary U.

Some clarifications are in order. This form of complexity contains a large degree of arbitrariness. First, it clearly depends on the reference state in a way that is hard to quantify. Moreover, it depends on the choice of gates: given a particular set, if we add gates to it, the complexity cannot increase, since there are now new operations allowed that weren't available before. In particular, if we allowed for the set of *all* arbitrary-qubit gates, the complexity of any state would be equal to one, since one could always find a gate complicated enough that did the job in a single shot. Of course that would be meaningless from both the theoretical and practical point of view. In reality, computers work on the basis of a few 'simple' gates (which can be made more precise). The art of this science is to construct circuits that achieve what we want, using only this restricted set of gates.

There exist relatively few known results on complexity. It is a young field that is just in its infancy. How is it then, that a concept coming from information science made its way to AdS/CFT? Here the work of Nielsen [100,102] was fundamental. He asked the question: "What is the minimal size quantum circuit required to exactly implement a specified n-qubit unitary operation, U, without the use of ancilla qubits?" [100]. He showed that a lower bound is given by the minimal geodesic length between U and the identity, where the metric is computed via a Finsler metric on $SU(2^n)$. Thus, he provided the means of *geometrizing* complexity, which opened the way for the application of differential geometry technology to tackle a question about quantum information.

In particular, they considered the question of the *evolution* of complexity along time. Given a Hamiltonian in quantum mechanics, and given an arbitrary initial state $|\psi(0)\rangle$,

then what is the complexity (as defined above) of the wavefunction $|\psi(t)\rangle = e^{-iHt}|\psi(0)\rangle$? Under some assumptions, they were able to prove using the geometrical approach that a lower bound for the complexity scales *linearly* with time. Now comes the holographic story. Since the discovery of the Holographic entanglement entropy formula, there was a very strong focus on studying the time evolution of entanglement. However, Susskind proposed that 'Entanglement is not enough' [29]. Why? Susskind argued [29, 103, 104] that since this should hold for general quantum systems (such as CFTs) and moreover it remains to be valid even long after a system thermalises. So, if we start with a holographic system out of equilibrium (say some black hole which we perturb in some way), it will take some time to reach the thermal limit, and complexity will be increasing along that process. However, once it already reached equilibrium, the entanglement entropies in the bulk stabilise and stop growing. Therefore he proposed that there must be another observable in the bulk that captures the complexity of the boundary state.

The proposals are simpler to formulate for thermofield doubled states (TFD) in the CFT, which are dual to maximally extended AdS black hole solutions [28]. Consider a thermal state density matrix

$$\rho = \frac{1}{Z}\sum_i e^{-\beta E_i}|E_i\rangle \tag{5.5}$$

This is a mixed state. A **purification** of the state corresponds to a pure state in an extended Hilbert space, such that, when the extension is traced out, we recover the state (5.5). The TFD is a particularly useful purification, in which the extra Hilbert space is simply the copy of the first one. Calling the eigenstates in the copy space $|E'\rangle$, we choose the particular pure state

$$|TFD\rangle \equiv \frac{1}{\sqrt{Z}}\sum_i e^{-\beta E_i/2}|E_i\rangle|E_i'\rangle \tag{5.6}$$

The AdS/CFT interpretation of this state is depicted in Fig.**??**. There are two asymptotic, disconnected, conformally flat boundaries (left and right). Although there's no interaction amongst them, the quantum state is entangled, as can be seen explicitly in (5.6).

The first proposal is the so called 'complexity=volume'. Susskind argued [29] that the complexity of $|TFD(t)\rangle$ should equal the spacetime volume of a codimension-1 slice on the bulk, whose asymptotic time coincides with the boundary time. More precisely, start by fixing the time t in the right boundary, and time $-t$ in the left boundary(recall

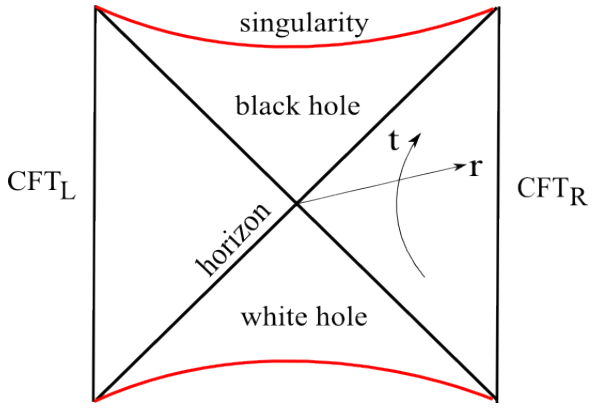

Figure 5.2: The TFD state (5.5) on the two disconnected (but entangled) CFT boundaries is dual to the maximally extended AdS black hole bulk solution.

they evolve in opposite directions on both sides). Now define a Cauchy slice such that it's 'anchored' at those times at the boundary. Now, one can vary the slice at will, keeping the condition that it stays spacelike. This defines a min-max problem, when we compute the induced volume of the slice. The conjecture states that the volume of the maximal volume slice is dual to the complexity of the boundary state, see Fig.**??**

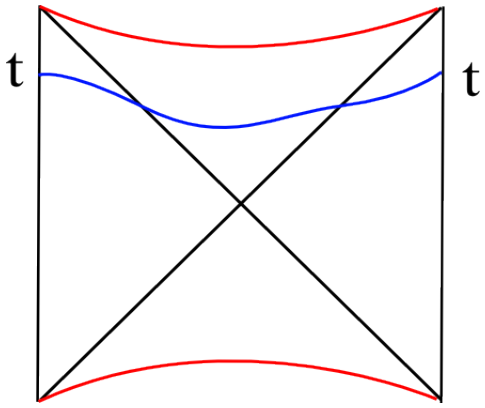

Figure 5.3: Susskind's complexity=volume proposal: one looks for the bulk slice that has maximum (Lorentzian) volume.

These are the conjectures for the bulk. What about the boundary? Is it possible to match these results to some actual CFT calculation of the complexity of the time evolved state? This question has been addressed by several groups in recent years. The main progress has been done for the special case of gaussian states in QFTs [105]. Probably the best understood example is the case of the free massive boson. The essential physics

of this problem is captured by that of two coupled harmonic oscillators. This system has a ground state, which has non-trivial entanglement between the two oscillators. Now, as a reference state, it is natural to take an unentangled state. Next one must specify what is the set of unitary quantum gates that are allowed. This choice is of course arbitrary (as the reference state), but a natural choice made in [105] was to choose simple operations with the position and momentum operators, for example $U = \exp(i\epsilon x_i p_j)$ which corresponds to 'shifting x_j by ϵx_i', thus introducing entanglement between the two oscillators. In this way they were able to compute, by using Nielsen's geometric approach described above, the computational complexity of the target state. Other relevant developments have applying the Fubini-Study metric as a measure of complexity [106], and understanding the UV divergent structure of complexity [107].

5.2 Tensor networks for holography

The recent developments in Tensor Networks have gained much attention in the holography community, due to their close connection to quantum information and numerical quantum lattice models. In this section, after briefly reviewing the basics, we discuss the two tensor networks we use in our work: the Multi-Entanglement-Renormalization-Ansatz (MERA) [108] and the Random Tensor Networks (RTN) [36].

Tensor networks were developed originally as algebraic variational tools (ansatz) to numerically find the ground states of local Hamiltonians. In sharp contrast to classical computing, quantum computing is far more **complex**: given a set of n classical bits, it requires n bits to completely specify the state of the system, because a classical string of data can only be in one state at a time. On the other hand, a system of n qubits requires a much larger 2^n classical bits to specify the state, namely all the values of the coefficients $C_{i_1 \ldots i_n}$

$$|\psi\rangle = \sum_{\{i\}} C_{i_1 \ldots i_N} |i_1 \ldots i_n\rangle \tag{5.7}$$

because the wavefunction can in general be an arbitrary linear superposition of the tensor product basis. If the problem at hand is to diagonalise a Hamiltonian of a lattice of say 100 sites, the complexity of this problem is already out of reach of any present or near future classical computer. The great insight that led to tensor networks is that, although

the size of the Hilbert space grows exponentially with the number of degrees of freedom, if we are interested only in the ground state and small perturbations around it, it might be possible to 'restrict' the numerical search into a much smaller region of the Hilbert space. Therefore, the strategy is to make an *educated ansatz* of how the ground state should look like, and then run a numerical algorithm to find the minimal energy state.

The first tensor network developed in this way is called Matrix-Product-State (MPS). This ansatz is particularly useful for finding ground states of $1+1$ dimensional quantum spin models (a typical example is the 1d quantum Ising model). The MPS ansatz for n qubits reads

$$|\Psi\rangle = \sum_{i_1,\ldots,i_n} \mathrm{Tr}\left(A_{i_1}\ldots A_{i_n}\right)|i_1\ldots i_n\rangle \tag{5.8}$$

where A_{i_j} are complex square matrices, all of local dimension χ.

Tensor networks are very frequently represented diagrammatically, see Fig.5.4. A tensor $M_{\mu_1\ldots\mu_j}$ is depicted as a vertex or node with j legs attached to it. Two tensor connected by a single line indicates that this particular index is being summed over, whereas free legs are physical input/output data. The range χ over which a particular index i_j runs ($i_j = 1, 2, \ldots, \chi$) is called the 'bond dimension' χ and is not shown in the graph, which is related to the entanglement of the state.

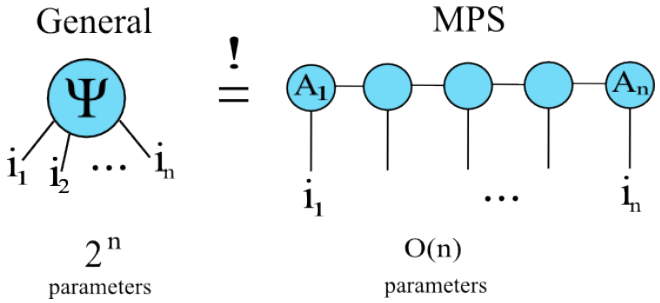

Figure 5.4: The common diagrammatic representation of a tensor network, here an MPS. Each node represents a tensor, and its legs represent the indices.

An explicit example of a MPS wavefunction is the Greenberger-Horne-Zeilinger (GHZ) state for n particles,

$$|GHZ\rangle = \frac{1}{\sqrt{2}}\left(|0\rangle^{\otimes n} + |1\rangle^{\otimes n}\right) \tag{5.9}$$

This is constructed using matrices all of local bond dimension $\chi = 2$, that is $i_j = 0, 1$, and the seed matrices

$$A_0 = \begin{pmatrix} 1 & 0 \\ 0 & 0 \end{pmatrix} \quad , \quad A_1 = \begin{pmatrix} 0 & 0 \\ 0 & 1 \end{pmatrix} \tag{5.10}$$

Inserting this into the MPS wavefunction (5.8), one obtains (5.9).

Multi-Entanglement-Renormalization-Ansatz (MERA)

The problem that motivated Vidal to introduce the MERA network was that of finding the RG flow of quantum states in systems with high degree of entanglement [108]. One starts with a given state $|\Psi\rangle$ and performs the Wilson-Kadanoff idea of block spinning two pairs of sites. Now, the ground state $|\Psi\rangle$ of a CFT is highly entangled: the entanglement entropy of a subregion of x sites scaling as $\log x$. Vidal realised that, if we naively apply only block spinning, the averaging procedure in each RG step causes the short-range entanglement (say between nearby qubits) to get mixed with the entanglement at the subsequent layers, and produces an entanglement spectrum that is not the one exhibited by a CFT ground state. Thus, he proposed to add an extra layer of unitaries at each step, before the block spin takes place, such that it *removes local entanglement* first, and then we block. Repeting this procedure, we get a network that looks like Fig. 5.5. The squares with four legs represent the **disentanglers**, which are 2-qubit gates. An example of such a gate would be U such that $U|00\rangle = (|00\rangle + |01\rangle)/\sqrt{2}$.

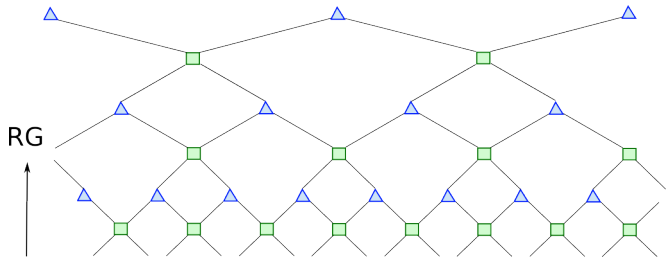

Figure 5.5: MERA network: the free bottom legs correspond to the physical degrees of freedom (e.g. spins on a 1d chain), which are then flowed through layers of disentanglers (squares) and isometries (triangles). This produces a final state at the upper layers.

Each triangle with 3 legs represents a block-spin or isometry. As it stands, it is not a unitary map (it's not even a square matrix), but it can be made unitary by attaching to it

a fourth leg with some prescribed state, typically $|0\rangle$. With that addition, MERA can be viewed alternatively as a quantum circuit that starts in the *upper layer* with a completely unentangled state such as $|000\ldots0\rangle$ and maps it unitarily by running the circuit from top to bottom. Given a specific Hamiltonian, one then numerically optimises the exact gates by running a sweeping algortithm [108], which produces an approximation of the ground state.

The reason why MERA became so popular in the AdS/CFT community was an observation by Swingle [109]. Swingle noted that in MERA, the circuit direction acts as a renormalisation scale, in striking similarity as what happens in holography. Moreover, the entanglement entropy of an interval on a given boundary state produced by a tensor network is bounded from above by the minimum number of 'cuts' of any line crossing the circuit connecting the interval endpoints, see Fig. 5.6. This defines 'geodesics' γ in the network, where the length of one leg cut is given by the local bond dimension of that link. But due to the scale invariant geometry of MERA, the length of the minimal-cut line $|\gamma|_{min}$ scales precisely as $\log n$, where n is the number of lattice sites of the subinterval whose entropy we are computing.

$$S \leq |\gamma|_{min} \log \chi \qquad\qquad |\gamma|_{min} \approx \log(n) \tag{5.11}$$

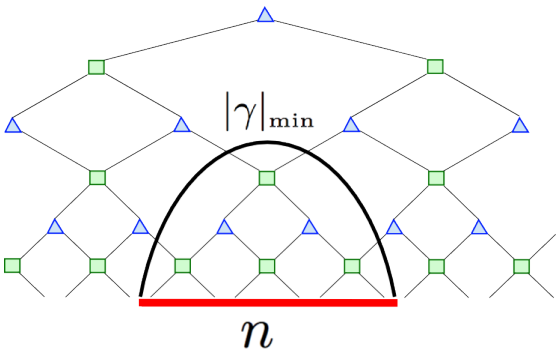

Figure 5.6: Minimal cut line or 'geodesic' in MERA.

Although it is a bound, this formula has a striking similarity with the Ryu-Takayanagi prescription for AdS_3 reviewed in Chapter 3. This has led to a variety of developments in the field [110–114].

Random tensor networks

Observables of the random tensor networks of [36] are defined by averaging over tensor network states built from random tensors living on a fixed graph. The main result of their work is that, in a tensor network lattice with a boundary, the average value of the second Rényi entropy of a subregion A, $\overline{\mathrm{tr}(\rho_A^2)}$, can be expressed as the partition function Z_A of an Ising model whose boundary conditions are determined by A. The temperature of the Ising model vanishes as the bond dimension D becomes large, in which case the Ryu-Takayanagi surface manifests as a domain wall in the spin system. In this picture, the subregion complexity of A is mapped to the magnetization of the Ising model.

Let us briefly review their construction. The network lives on a graph Γ, with boundary consisting of dangling edges $\partial\Gamma$. Each edge e of a vertex x has associated to it a vector space $\mathcal{H}_e$. We assume all $\mathcal{H}_e$ to have fixed dimension D. The tensor at vertex x is a unit vector $|V_x\rangle \in \mathcal{H}_x = \bigotimes_{e\in\partial x} \mathcal{H}_e$, whose probability distribution is invariant under unitary transformations of $\mathcal{H}_x$. An edge $\langle xy\rangle$ attaching x to y corresponds to projection onto a maximally entangled state $|xy\rangle$ in $\mathcal{H}_{xy}\otimes\mathcal{H}_{yx}$. The result is a state

$$|\Psi\rangle = \left(\bigotimes_{\langle xy\rangle}\langle xy|\right)\cdot\left(\bigotimes_{x\in\Gamma}|V_x\rangle\right) \tag{5.12}$$

in the boundary Hilbert space $\mathcal{H}_\partial = \bigotimes_{e\in\partial\Gamma}\mathcal{H}_e$, to which we can associate a density matrix $\rho = |\Psi\rangle\langle\Psi|$.

Given $A\subset\partial\Gamma$, we can use the swap trick to write the second Rényi entropy of A as

$$e^{-S_2(A)} = \frac{\mathrm{tr}\big[(\rho\otimes\rho)\cdot\mathcal{F}_A\big]}{\mathrm{tr}\big[\rho\otimes\rho\big]} = \frac{Z_1}{Z_0}\,, \tag{5.13}$$

where the trace is over $\mathcal{H}_\partial\otimes\mathcal{H}_\partial$, and $\mathcal{F}_A$ is the swap operator reversing the order of the tensor product in the subspace $\mathcal{H}_A$.

The average value of $\rho\otimes\rho$ is found by integrating over $|V_x\rangle$. It can be evaluated by noting that it is linear in $|V_x\rangle\langle V_x|\otimes|V_x\rangle\langle V_x|$, hence all we require is the average

$$\overline{|V_x\rangle\langle V_x|\otimes|V_x\rangle\langle V_x|} = \frac{I_x+\mathcal{F}_x}{D(D+1)} \tag{5.14}$$

where I_x and $\mathcal{F}_x$ are the identity and flip operators, respectively, on $\mathcal{H}_x\otimes\mathcal{H}_x$. Expand this into a sum over terms involving either I_x or $\mathcal{F}_x$, and define a spin variable s_x which is 1 (-1) if the term contains I_x ($\mathcal{F}_x$). We further introduce a boundary function h_x equal

to -1 for $x \in A$, and 1 otherwise. For large bond dimension we can approximate

$$\overline{S_2(A)} = -\log \frac{\overline{Z_1}}{\overline{Z_0}}\,, \tag{5.15}$$

where $\overline{Z_{0,1}}$ are now expressed as partition functions

$$\overline{Z_1} = \sum_{\{s_x\}} e^{-\mathcal{A}[\{s_x\},\{h_x\}]}\,, \quad \overline{Z_0} = \sum_{\{s_x\}} e^{-\mathcal{A}[\{s_x\},\{h_x=1\}]}\,. \tag{5.16}$$

The explicit form of the statistical Hamiltonian $\mathcal{A}$ was derived in [36], and (up to constant shift) takes the form

$$\mathcal{A}[\{s_x\}] = -\frac{1}{2}\log D\left(\sum_{\langle xy\rangle} s_x s_y + \sum_{x\in\partial\Gamma} s_x h_x\right); \tag{5.17}$$

this is an Ising model on Γ, whose boundary spins are held fixed to the values $\{h_x\}$. As is well known, the most probable configuration consists of the domain wall separating two regions of opposite spins that has smallest possible length. This domain wall coincides with the RT surface.

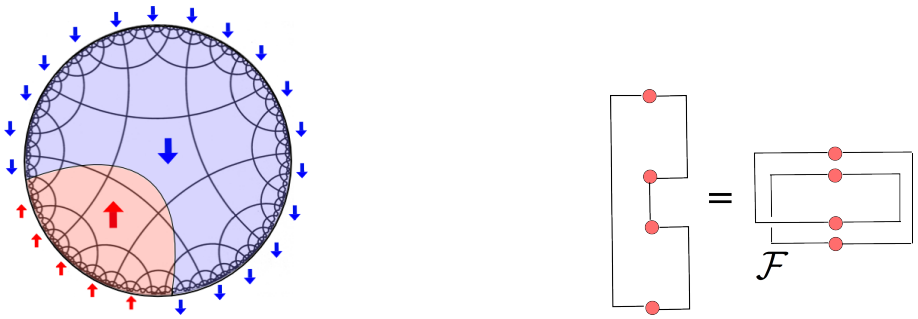

Figure 5.7: Left: Ising model resulting from a RTN on a tesselation of $\mathbb{H}^2$. The domain wall mimics the RT surface. Right: representation of the swap trick used in the derivation.

5.3 Compression complexity from topology in $\mathrm{AdS}_3/\mathrm{CFT}_2$

This section is based on [31], in joint collaboration with R. Abt, J. Erdmenger, H. Hinrichsen, Charles Melby-Thompson, R. Meyer, and C. Northe.

We consider subregion complexity within the $\mathrm{AdS}_3/\mathrm{CFT}_2$ correspondence. We rewrite the subregion volume proposal, according to which the complexity of a reduced density

matrix is given by the spacetime volume contained inside the associated Ryu-Takayanagi (RT) surface, in terms of an integral over the curvature. Using the Gauss-Bonnet theorem we evaluate this quantity for general entangling regions and temperature. In particular, we find that the discontinuity that occurs under a change in the RT surface is given by a fixed topological contribution, independent of the temperature or details of the entangling region. We offer a definition and interpretation of subregion complexity in the context of tensor networks, and show numerically that it reproduces the qualitative features of the holographic computation in the case of a random tensor network using its relation to the Ising model. Finally, we give a prescription for computing subregion complexity directly in CFT using the kinematic space formalism, and use it to reproduce some of our explicit gravity results obtained at zero temperature. We thus obtain a concrete matching of results for subregion complexity between the gravity and tensor network approaches, as well as a CFT prescription.

5.3.1 Introduction

Since the proposal of Ryu and Takayanagi [60, 115] that entanglement entropy in a holographic conformal field theory (CFT) is measured by the area of minimal surfaces in asymptotically AdS spacetimes, the connection between the AdS/CFT correspondence [30] and quantum information has seen many exciting developments. In recent years, these ideas have found applications ranging from tensor networks [109] and quantum error correcting codes [116, 117] to the emergence of spacetime [118].

One research topic that is receiving increasing attention is the notion of complexity [119]. Roughly speaking, the complexity of a pure quantum state is the minimal number of gates of any quantum circuit built from a fixed set of gates that produces this state from a given reference state. Complexity was first studied within the framework of the AdS/CFT correspondence in the context of time-dependent thermal state complexity, which was proposed to be dual either to the volume of the Einstein-Rosen bridge [103], or the action of a Wheeler-DeWitt patch [120]. Recently, additional insight has been gained into both proposals from more detailed holographic studies [107, 121, 122].

The present work is concerned with the *subregion complexity* of the reduced density matrix of a finite subregion A. While the area of the Ryu-Takayanagi (RT) surface γ_{RT} of

A is known to give the entanglement entropy of A [115], it was proposed in [35, 123, 124] that the subregion complexity should correspond to the volume of the co-dimension 1 region Σ enclosed by γ_{RT} and the cutoff surface (fig. 5.8). Other recent proposals relate bulk volumes to *Fisher information* [125] and *fidelity susceptibility* [126–129].

The particular object of study of this work is the behavior of subregion complexity in $\mathrm{AdS}_3/\mathrm{CFT}_2$. We study a slightly different quantity than [35]: we define the subregion complexity of A to be the integral over Σ of the scalar curvature R,

$$\mathcal{C}(A) \equiv -\frac{1}{2}\int_{\Sigma} R\, d\sigma\,. \tag{5.18}$$

The minus sign accounts for the negative curvature of asymptotically AdS spaces.

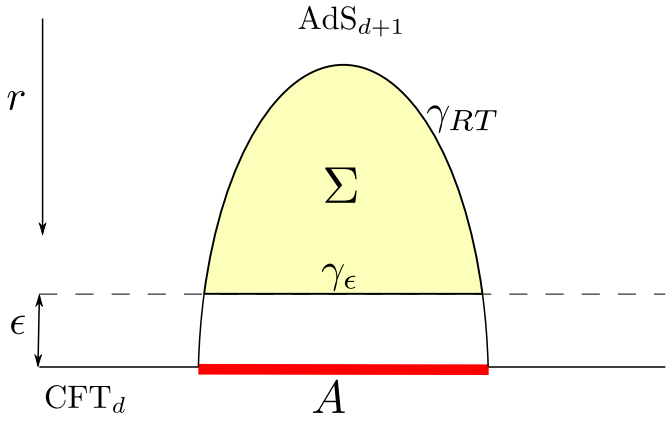

Figure 5.8: The subregion complexity is computed from the regularized volume contained in the region Σ, enclosed by γ_{RT} and the segment γ_ϵ of the cutoff surface. Figure by R. Abt from [31].

The examples studied in the present work have constant spatial curvature, so that our definition coincides with the proposal in [35]. However, the definition in (5.18) has several advantages. On the one hand, it is particularly natural in AdS_3, as the resulting quantity is dimensionless without introducing an *ad hoc* scale. On the other hand, we will see below that, due to the appearance of $\int_\Sigma R$ in the Gauss-Bonnet theorem, the quantities of primary interest to us are determined purely by topological data. For this reason we may refer to the subregion complexity as defined by (5.18) as topological complexity. Finally, the idea of defining the subregion complexity as an integral over a local *complexity density* proportional to the scalar curvature is conceptually interesting on its own.

The aim of this article is to develop and compare three complementary points of view on subregion complexity in AdS_3/CFT_2: within gravity, using tensor networks, and its computation using CFT quantities. Our approach has two main foci. The first is the study of transitions and temperature dependence of subregion complexity from both the point of view of gravity and of tensor networks. On the gravity side, the Gauss-Bonnet theorem yields an elegant result: when the total length of the entangling region is held fixed, the subregion complexity (5.18) varies only by discrete jumps determined purely by the topology of Σ. This holds true for any number of entangling intervals at both zero and non-zero temperature, and for variations of temperature as well as the shape of the entangling region. In the latter case the change in complexity during topological transitions of the Ryu-Takayanagi surface is in particular independent of temperature. While the two-interval subregion complexity was originally computed in [130], the computation for arbitrary numbers of intervals at both zero and non-zero temperature is new.

In the context of tensor network/AdS proposals, we interpret the subregion complexity as the complexity of the map that optimally compresses the reduced density matrix of A. Using the map between random tensor networks and the Ising model proposed in [36], by numerical simulations we reproduce the qualitative behavior at the transitions observed in gravity. Our numerics reproduce to a good approximation the temperature independence of the subregion complexity as measured by the volume under the Ryu-Takayanagi-surface, as well as the jump in subregion complexity when the Ryu-Takayanagi surface undergoes a topological transition for large boundary interval sizes.

Our second focus is the computation of subregion complexity within CFT_2. In continuum CFT we cannot compute complexity from first principles, because a satisfactory definition of complexity in QFT is not yet available. (See however [105, 106, 131, 132] for recent work in this direction.) Here we seek to approach this problem from a different angle by outlining the definition of a quantity using the kinematic space formalism of [133] which, in the case of CFT_2 with a holographic dual, we expect to reproduce the holographic subregion complexity for states sufficiently close to the vacuum. We apply our prescription to compute the complexity of the vacuum when the entangling region is the entire spatial boundary, and find that it matches the gravitational computation. As the kinematic space measure is built from entanglement entropy, this suggests that

complexity can be recovered from entanglement entropy, at least for states sufficiently close to the vacuum.

The chapter is organized as follows. In section 5.3.2 we consider the subregion complexity of an arbitrary number of entangling regions for locally AdS_3 solutions. We obtain explicit expressions from the proposal (5.18) for these geometries. In section 5.3.3 we study subregion complexity from the viewpoint of tensor networks. In section 5.3.4 we use the kinematic space formalism of [133] to define a quantity in CFT_2 that, when a weakly curved gravitational dual exists, coincides with the subregion complexity. Our conclusions are summarized in section 5.5.

5.3.2 Subregion complexity from gravity

We begin with the computation of the subregion complexity (5.18) in asymptotically AdS spacetimes of constant spatial curvature. Using the Gauss-Bonnet theorem, we derive a simple and general expression for the subregion complexity of any collection of intervals and for arbitrary geometries of constant spatial curvature. We illustrate this formula in detail for the specific cases of vacuum AdS, static BTZ black holes, and conical defect geometries. In vacuum AdS we illustrate this formula in the case of the two-interval subregion complexity originally computed in [130], while in black holes and defect geometries we focus on the mass dependence of single interval complexity. In general, we find that the jump in complexity that occurs when the dominant Ryu-Takayanagi surface undergoes a transition comes "quantized" in integer multiples of a fixed value, independent of geometric parameters of the background such as interval size or black hole temperature.

We work on constant time slices of asymptotically AdS_3 solutions. One first fixes an entangling region A at the boundary, whose RT surface consists of geodesic(s) connecting its endpoints. As usual, one places a cutoff slice γ_ϵ near the boundary for regularization. As depicted in fig. 5.8, this defines a compact two dimensional manifold Σ with boundary $\partial\Sigma = \gamma_{RT} \cup \gamma_\epsilon$.

The Gauss-Bonnet theorem allows us to express the topological subregion complexity (5.18) in a simple form:

$$\mathcal{C}(A) = -\frac{1}{2}\int_\Sigma R\, d\sigma = \int_{\partial\Sigma} k_g ds - 2\pi\chi(\Sigma)\ , \tag{5.19}$$

where χ is the Euler characteristic of Σ and ds is the line element along $\partial\Sigma$. The geodesic curvature k_g, defined in (5.21) below, measures how much the curve $\partial\Sigma$ deviates from a geodesic. If $\partial\Sigma$ is piecewise smooth, then $\int_{\partial\Sigma} k_g ds$ is the sum of the integral along the smooth portions of $\partial\Sigma$, plus the sum of the corner angles at its turning points (where k_g has delta function singularities).

We now compute (5.19) for entangling regions on AdS_3, BTZ black holes and the conical defects. The time slices of these solutions have constant curvature $R = -\frac{2}{L^2}$, where L is the AdS radius.

Zero temperature (AdS)

Consider first a set of two entangling intervals of lengths x_1 and x_2 in the vacuum state of a CFT_2, which is dual to global AdS_3 (fig. 4.3) with metric

$$ds^2 = -f(r)dt^2 + \frac{dr^2}{f(r)} + r^2 d\phi^2 \ , \tag{5.20}$$

with $f(r) = 1 + \left(\frac{r}{L}\right)^2$ and $\phi \sim \phi + 2\pi$. We choose $l_{\rm CFT}/r$ as our defining function, corresponding to a CFT metric $ds^2_{\rm CFT} = l^2_{\rm CFT}(-L^{-2}\, dt^2 + d\phi^2)$, and hence a CFT spatial circle of length $2\pi\, l_{\rm CFT}$.

The entanglement entropy of the two subregions is known to exhibit a transition between two configurations depending on a conformal ratio of their sizes and separation [134, 135]. In standard analogy with statistical mechanics we refer to such competing configurations as "phases". In particular, while the entanglement entropy is continuous across a transition, its first derivative jumps (this is, however, smoothed out at finite c). On the CFT side, this transition can be explained as the exchange of dominance between the s and t channels in the four point function of the twist fields. On the gravity side, this corresponds to the two different ways of connecting the interval endpoints by geodesics (see fig. 4.3). In these two configurations, referred to as phase I and phase II, the total length of the corresponding geodesics is generally different. The RT prescription states that the actual entanglement entropy is given by the configuration for which this length is minimal, meaning that the transition occurs at the point where lengths in both phases coincide. Interestingly, we find that the volume of Σ exhibits a discontinuity at the transition.

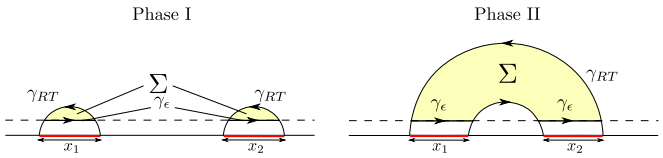

Figure 5.9: The two phases of a system with two subregions. For phase I, Σ is the union of the colored regions. Figure by R. Abt [31].

We now apply eq. (5.19) to compute the subregion complexity in phase I. Here Σ is the union of two disjoint regions. Since the Euler characteristic is additive, we obtain $\chi(\Sigma) = 2$, since each region is topologically like a disk.

Next we compute the integral of the geodesic curvature around the smooth parts of $\partial\Sigma$. Since the geodesics γ_{RT} do not contribute, we only have to integrate along γ_ϵ, which is a segment of a circle at radius $r = Ll_{\text{CFT}}/\epsilon \equiv r_\epsilon$ with $\epsilon \ll l_{\text{CFT}}$. For a constant time slice of a metric of the form (5.20), it is easy to show that the geodesic curvature along a circle of radius r is simply

$$k_g = \left|\frac{Du}{ds}\right| = \frac{\sqrt{|f(r)|}}{r}\,, \tag{5.21}$$

where u is the unit vector tangent to the curve. For asymptotically AdS spaces, where $f(r) \to \left(\frac{r}{L}\right)^2$ as $r \to \infty$, we obtain

$$\int_{\gamma_\epsilon} k_g ds = \frac{\sqrt{|f(r_\epsilon)|}}{r_\epsilon} \int_{\gamma_\epsilon} ds = \frac{x_1 + x_2}{\epsilon} + \mathcal{O}(\epsilon)\,, \tag{5.22}$$

where x_1 and x_2 denote the lengths of the intervals. Finally, the contributions coming from the corner angles between γ_{RT} and γ_ϵ have to be taken into account. Since γ_{RT} is known to terminate perpendicularly at the boundary [60], any joint of γ_{RT} with γ_ϵ contributes with a term of $\pi/2$ to (5.19) when $\epsilon \to 0$. Summarizing all contributions, the subregion complexity for two disjoint intervals of length x_1 and x_2 is simply given by

$$\mathcal{C}_I(\{x_1, x_2\}) = \frac{x_1 + x_2}{\epsilon} - 2\pi\ . \tag{5.23}$$

Similarly we can compute the subregion complexity in phase II, the only difference being that the Euler characteristic is now $\chi(\Sigma) = 1$:

$$\mathcal{C}_{II}(\{x_1, x_2\}) = \frac{x_1 + x_2}{\epsilon}\,, \tag{5.24}$$

Since both phases differ by a constant topological term

$$\Delta\mathcal{C} = \mathcal{C}_{II} - \mathcal{C}_{I} = 2\pi\,, \tag{5.25}$$

the subregion complexity exhibits a discontinuous jump at the transition, although the entanglement entropy is continuous. This was already computed in [130] by direct integration of the volume form.[1]

The generalization to an arbitrary number of entangling intervals is straightforward. Consider a set of q disjoint intervals of length x_i in the vacuum state of a CFT_2 (see fig. 5.10). Depending on their configuration, γ_{RT} can take many possible forms, giving rise to various phases. Applying once again the Gauss-Bonnet theorem, each corner angle contributes $\pi/2$, hence the subregion complexity is given by

$$\mathcal{C}(\{x_i\}) = \frac{x}{\epsilon} + \pi q - 2\pi\chi\,, \tag{5.26}$$

where $x = \sum_{i=1}^{q} x_i$ is the total entangling length on the boundary of the q intervals, and χ the total Euler characteristic.

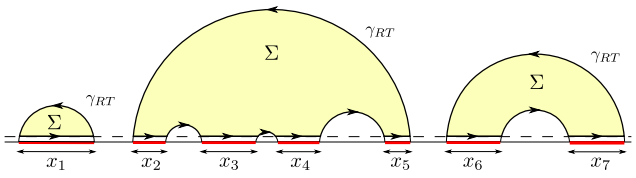

Figure 5.10: Example of a configuration of RT surfaces for a several entangling intervals ($q = 7$) in the vacuum. Figure by R. Abt [31].

At any transition of γ_{RT}, all contributions to (5.19) remain the same except that the Euler characteristic χ changes, thus

$$\Delta\mathcal{C} = -2\pi\Delta\chi\ . \tag{5.27}$$

This is the first main result of this section: if the entangling intervals are varied while the sum of their lengths is held fixed, then subregion complexity varies discretely in multiples of 2π. We shall see below that the same is true for a finite temperature state.

[1] In [128] hyperbolic polygons lying in spatial slices of AdS_3 were considered in context of holographic complexity. The Gauss-Bonnet theorem was consulted to confirm their computations. Our prescription (5.19) reproduces their findings as a special case.

In particular, the subregion complexity of the entire time slice of AdS_3 is obtained when a single entangling region covers the entire boundary circle. Setting $q = 0$ (no corner angles) we obtain the result

$$\mathcal{C}\,(\text{circle}) = 2\pi \left(\frac{l_{\text{CFT}}}{\epsilon} - 1 \right) , \tag{5.28}$$

which will be derived in terms of CFT quantities in sec. 5.3.4.

Finite temperature and conical defects

We now consider a single interval of length x in a CFT_2 on a circle at finite temperature T. This is dual to the BTZ black hole [53], where the metric is again of the form (5.20), but now with

$$f(r) = -M + \left(\frac{r}{L} \right)^2 , \tag{5.29}$$

where M is the black hole mass (in units of $8G_N = 1$) which is related to the temperature by $T = L\sqrt{M}$. It is well known that $M > 0$ corresponds to black holes while $M = -1$ reproduces AdS_3. The geometries for $-1 < M < 0$ correspond to conical defects in AdS, i.e. naked singularities with no horizon.

In the presence of a black hole γ_{RT} is known to exhibit two different phases a and b, as shown in fig. 5.11, provided that the entangling region is larger than half of the boundary perimeter. In phase b the geodesic γ_{RT} remains homotopic to the entangling region, while in phase a it is given by the geodesic of the complement plus a surface wrapping around the horizon of the black hole. Again the physically realized phase is the one where the entanglement is minimal. For low temperatures the black hole is small so that $\gamma_{RT,b}$ is shorter than $\gamma_{RT,a}$ while for large temperatures it is the other way round. Both phases are separated by a transition point $M = M^*$ where the entanglement in both phases coincides.

The calculation of the subregion complexity in each phase is analogous to the vacuum case. Indeed, in phase a the result is identical to that of a single interval in the vacuum, namely

$$\mathcal{C}_a(x) = \frac{x}{\epsilon} - \pi , \tag{5.30}$$

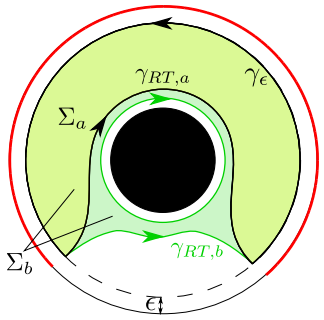

Figure 5.11: The two phases a and b of γ_{RT} for a single interval (red line) in the presence of a black hole. Figure by R. Abt [31].

independent of the mass of the black hole. Thus, our second main result is that the topological nature of the subregion complexity (5.18) implies it is independent of temperature. Although the entanglement entropy has a strong temperature dependence (γ_{RT} changes with the black hole size), it changes in precisely such a way as to leave the volume inside constant. Note that this is not true in higher dimensions, and is due to the fact that the BTZ geometry is locally isometric to AdS_3.

As we lower the mass, the black hole gets smaller, until we hit the phase transition and pass to phase b, as shown in fig. 5.12. The geodesic curvature of the horizon vanishes, and so all contributions to (5.19) remain unchanged except for the Euler characteristic, which is now $\chi(\Sigma_b) = 0$, as Σ_b is topologically an annulus. Therefore the corresponding complexities differ by

$$\Delta\mathcal{C} = \mathcal{C}_b - \mathcal{C}_a = 2\pi\,, \tag{5.31}$$

as derived earlier in [130] by direct integration.

As we continue reducing the temperature, we hit massless BTZ (extremal), and pass to the 'naked singularity' sector. Solutions with negative M correspond not to black holes, but to solutions of Einstein's equations when we place a point particle of mass M at the origin. This generates a conical defect geometry, where the deficit angle is $2\pi(1-\sqrt{-M})$. There is no horizon, and the curvature is still $R = -\frac{2}{L^2}$ everywhere except at the origin, where it has a Dirac delta peak.

The entanglement entropy for conical defects in AdS_3 was studied in [136]. We now consider their subregion complexity. When the horizon disappears at $M = 0$, it would seem that the topology of Σ changes since it would no longer have any hole. However,

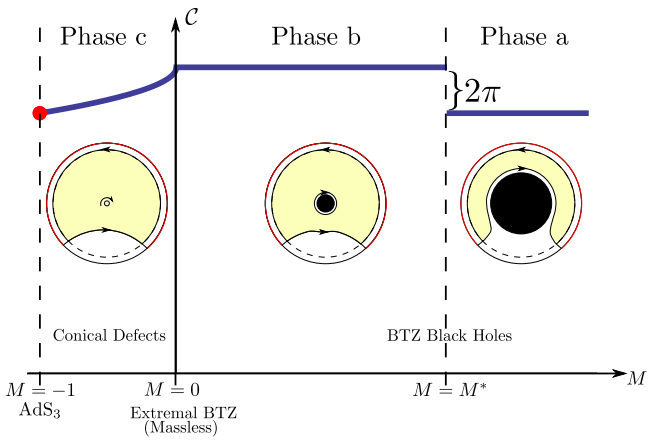

Figure 5.12: Subregion complexity as function of the black hole mass, for a fixed entangling region. Figure from [31].

it remains the same: given that there arises a singularity at the origin, and in order to be consistent with the homology condition for the RT surface, one must remove an infinitesimal disk around the singularity, compute the subregion complexity, and finally take the disk radius to zero. This introduces another boundary, whose geodesic curvature is again given by (5.21) but now with $f(r) = -M + \left(\frac{r}{L}\right)^2$. The integral around the disk is

$$\oint k_g ds = 2\pi\sqrt{f(r)} \underset{r\to 0}{\longrightarrow} 2\pi\sqrt{-M} \quad , \; M < 0 \; . \tag{5.32}$$

All other contribution to (5.19) remain the same, so the subregion complexity for the naked singularity is

$$\mathcal{C} = \frac{x}{\epsilon} + \pi - 2\pi\sqrt{-M} \quad , \; M < 0 \tag{5.33}$$

For $M = -1$ the AdS vacuum is recovered where (5.33) reduces to (5.30), and the subregion complexity again approaches the same value as in phase a.

To summarize, for a single entangling region of a given size we find three different phases depicted in fig. 5.12. Although the entanglement entropy varies non-trivially with temperature in all phases, the Gauss-Bonnet theorem ensures that the subregion complexity in phase a and b are constant, exhibiting a jump of 2π at the transition. This changes once we cross to the conical defect sector, in which a naked singularity appears which causes the subregion complexity to vary smoothly.

Finally, the subregion complexity for q intervals at finite temperature is again analogous to (5.26), and the natural generalization of (5.33) for the conical defect case.

5.3.3 Tensor networks

The aim of this section is to suggest a physical interpretation of the holographic subregion complexity discussed in section 5.3.2 by defining an analogous quantity for tensor networks, and to illustrate for a particular class of tensor networks that this quantity has the same qualitative behavior found in section 5.3.2.

The advantage of this approach is that tensor networks are equipped with a natural notion of complexity, allowing us to define subregion complexity explicitly for a certain class of tensor network states. Motivated by this definition, we compute subregion complexity in random tensor networks via numerical simulations of the Ising model realization of the second Rényi entropy derived in [36]. Our simulations reproduce the qualitative behavior found in section 5.3.2 for the subregion complexity in CFT at finite temperature.

Subregion complexity for tensor network states

The first goal of this section is to define an analogue of the holographic subregion complexity for network states. This quantity roughly measures the difficulty of building the reduced density matrix. The remainder of this section will investigate the properties of this definition in the particular case of random tensor networks.

We begin by briefly reviewing the definition of complexity and its relation to tensor networks. Complexity is an information-theoretic quantity that can be defined as follows.[2] Starting with a Hilbert space $\mathcal{H}$ with a decomposition into local units, one chooses a set $\{U_i\}$ of quantum gates, *i.e.,* unitary operators acting locally on $\mathcal{H}$. The complexity of an arbitrary unitary operator U is the minimal number of gates required to represent U by a product of U_i's. The complexity of a state $|\Psi\rangle$ in $\mathcal{H}$ — or a density matrix, which can be understood as a state in $\mathcal{H} \otimes \overline{\mathcal{H}}$ — is then the smallest complexity of all unitary maps sending a fixed reference state $|\Psi_0\rangle$ to $|\Psi\rangle$.

A useful definition of complexity in continuum field theory is currently unavailable. A sharper picture is, however, provided by tensor network states [137]. It is known that some tensor networks are relevant to CFT: the Multi-scale Entanglement Renormalization Ansatz (MERA) is a tensor network known to accurately approximate CFT ground states [138]. These networks live on discretizations of hyperbolic space, and, as a result,

[2]References, and a geometric approach to this problem, can be found in [99].

many statements from holography have a natural realization in such states. In particular, their entanglement entropies are bounded from above by the RT formula [109]. Other networks can satisfy tighter bounds, for example the quantum error-correcting codes of [117], where it was shown that, for a single entangling interval, the discretized Ryu-Takayanagi formula holds exactly.[3]

As observed in [139], the 'complexity=volume' conjecture is naturally realized in tensor network constructions by associating a fixed spatial volume to each tensor. In this picture, one drops the focus on the fixed Hilbert space $\mathcal{H}$, working instead with maps between two Hilbert spaces that are built out of tensors. We still require the tensors (gates) to act locally, but the output dimension is now allowed to be smaller than the input dimension. The subnetwork of tensors Σ connecting the (discretized) RT surface to the boundary entangling region A can be interpreted as defining a map $\imath_A$ from $\mathcal{H}_{RT}$, the Hilbert space of the legs cut by the RT surface, to $\mathcal{H}_A$, the Hilbert space of region A. The RT surface is characterized by the property that it has the *smallest* Hilbert space for any cut through the tensor network bounded by ∂A, and the number of tensors $\mathcal{C}(\imath_A)$ measures the complexity — with respect to tensors of a given size and locality — of the corresponding map. In general, the resulting tensor network may not be the map with the smallest number of tensors, so that this number only constitutes an upper bound on complexity.

We define subregion complexity $\mathcal{C}_A$ to be $\mathcal{C}(\imath_A)$. For certain networks — for example, for A a single interval on the boundary of a perfect tensor network [117] — the reduced density matrix ρ_A can be recovered directly from $\imath_A$, so that $\mathcal{C}_A$ describes the complexity of ρ_A itself. In general, we expect that at large central charge the complexity of building ρ_A is well parametrized by $\mathcal{C}_A$.

Our main interest in this section is the behavior of $\mathcal{C}_A$ under transitions in the (discretized) RT surface. Some tensor networks, such as the perfect tensor networks of [117], are guaranteed to exhibit discretized versions of the jumps in complexity observed in section 5.3.2. A more interesting illustration is given by random tensor networks [36], in which the RT formula is satisfied only in the limit of infinite bond dimension. Using

[3]This paper applied the Gauss-Bonnet theorem to hyperbolic tesselations to make a distinct but related computation, whose aim was to quantify multipartite entanglement associated to a partition of the whole system into several components.

numerical simulations, we will see in what follows that the qualitative behavior of the transitions is preserved at finite bond dimension.

Ising model reproducing the subregion complexity for BTZ black holes

The analogy of Ryu-Takayanagi surfaces and domain walls of an Ising model suggested in [36] assumes a constant bond dimension D, meaning that all coupling constants $J_{x;y}$ in the corresponding Ising Hamiltonian $H = -\frac{1}{2}\sum_{<x,y>} J_{x;y} s_x s_y$ take the same value $J_{x;y} = J$ and that $\beta_{\text{Ising}} \to \infty$ in the limit of a large central charge. In this setup the bulk geometry is taken into account by arranging the tensors (Ising spins) in such a way that their geodesic distance is constant. However, such regular tessellations are only known for few special cases as, for example, the hyperbolic plane. In particular, we are not aware of a regular equidistant tessellation of the bulk geometry in presence of a BTZ black hole.

To circumvent this problem, we suggest here that the bulk geometry can also be taken into account for any arrangement of the Ising spins by assigning non-constant couplings in such a way that the energetic cost of domain walls reproduces the correct geodesic length. In the following we consider the example of a non-spinning BTZ black hole, reproducing the transition between the phases a and b illustrated in fig. 5.11. The generalization to other examples is straight forward.

To reproduce the transition in the BTZ case, we first map the standard coordinates (r, ϕ) in a constant-time slice of the metric (5.20),(5.29) to conformal coordinates (η, ϕ) with $\cos\eta = T/r$ defined on a rectangle $\eta \in [0, \pi/2), \pi \in [-\pi, \pi)$, turning the metric into

$$ds^2 = \sec^2(\eta)\left(L^2\, d\eta^2 + T^2\, d\phi^2\right). \tag{5.34}$$

In these coordinates, the black hole horizon and the conformal boundary correspond to $\eta = 0$ and $\eta = \pi/2$.

Next, we embed a square lattice of $N \times N$ Ising spins in this rectangle, as sketched in fig. 5.13. Labeling the lattice sites by two indices $i, j \in \{0, 1, \ldots, N-1\}$, the spins $s_x = s_{i,j} = \pm 1$ are located at

$$\phi = 2\pi \frac{2i+1}{2N}\,, \qquad \eta = \frac{\pi}{2}\frac{2j+1}{2N}\,. \tag{5.35}$$

At the top and the bottom row of the lattice the Ising spins are fixed by the boundary

conditions

$$s_{i,j} := \begin{cases} -1 & \text{if } j = 0 \\ \operatorname{sign}\left(\frac{N\phi}{4\pi} - \left|i - \frac{N}{2}\right|\right) & \text{if } j = N-1\,, \end{cases} \tag{5.36}$$

where $\phi = x/L$ is the size of the entangling region.

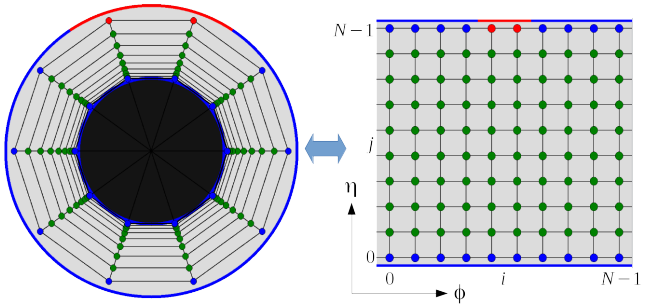

Figure 5.13: BTZ black hole (left) with radial coordinate $\arctan(r/L)$ mapped to conformal coordinates ϕ, η (right) where an Ising model on a square lattice is embedded. The top and the bottom row of spins are fixed according to the respective boundary conditions (red=↑, blue=↓) while the green spins are allowed to fluctuate. Figure by H. Hinrichsen [31].

Each horizontal (angular) bond cuts a vertical line element of a domain wall with $\Delta\phi = 0, \Delta\eta = \pi/2N$, corresponding to the geodesic length $\Delta s \approx L\sec(\eta)\Delta\eta$. Likewise each vertical (radial) bond cuts a horizontal line element $\Delta\phi = 2\pi/N, \Delta\eta = 0$ with the geodesic length $\Delta s \approx T\sec(\eta)\Delta\phi$, where η corresponds to center of the bond. Thus, assigning the coupling constants

$$\begin{aligned} \text{horizontal: } J_{i,j;i+1,j} &:= \frac{\pi L}{2N}\sec\left(\frac{\pi}{2}\frac{2j+1}{2N}\right) \\ \text{vertical: } J_{i,j;i,j+1} &:= \frac{2\pi T}{N}\sec\left(\frac{\pi}{2}\frac{j+1}{N}\right), \end{aligned} \tag{5.37}$$

the energy contribution of a domain wall is approximately proportional to its geodesic length while the total magnetization would reflect the enclosed volume. However, it should be noted that the rotational invariance of the Ising model is broken on a square lattice at low temperatures, preferring domain walls that are aligned with the lattice. As we will see below, this causes the simulated domain wall to deviate slightly from the analytically expected RT surface. Nevertheless, the results from the Ising model can be used as a good approximation which qualitatively reproduce the results derived above.

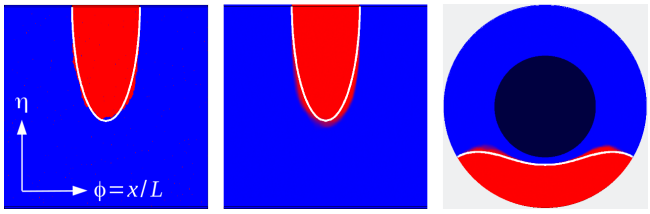

Figure 5.14: Left: Snapshot of a typical configuration of Ising spins on a lattice with 256x256 sites near equilibrium. The white curve marks the theoretically expected RT surface. Center: Magnetization averaged over many independent configurations. Right: Average magnetization mapped back to the Poincaré disk. Figure by H. Hinrichsen [31].

Simulation results

In order to find the equilibrium configuration of the Ising model numerically, we use a standard heat bath dynamics at very low temperature. First we measure the entanglement $E(x)$ for a constant mass M and varying subregion size $\phi = x/L$. In the Ising model the entanglement is given by the energy difference

$$E(x) \approx -\frac{1}{2} \sum_{<x,y>} J_{x;y}(s_x s_y - 1) \tag{5.38}$$

which has to be compared with the exact result

$$\begin{aligned} E_b(x) &= 2 \log\Big[\frac{2L}{\sqrt{M}\epsilon} \sinh\Big(\frac{\sqrt{M}x}{2L}\Big)\Big] \\ E_a(x) &= E(2\pi L - x) + 2\pi\sqrt{M} \end{aligned} \tag{5.39}$$

in the phases a and b. Here ϵ is the cutoff distance of γ_ϵ at the conformal boundary which is expected to scale with the lattice spacing. The transition takes place at a subregion size x^* where $E_a(x^*) = E_b(x^*)$, giving

$$x^* = L\phi^* = -\frac{L}{\sqrt{M}} \log\Big(1 - \tanh(\pi\sqrt{M})\Big). \tag{5.40}$$

As shown in the left panel of fig. 5.15, the numerically estimated entanglement in the two phases reproduces the expected behavior and the two curves intersect accurately at the expected value of x^*, which is marked as a vertical dashed line in the figure.

Next we compute the complexity $\mathcal{C}_{a,b}(x)$ in the two phases. As can be seen in the right panel, the numerical results nicely reproduce the predicted linear law $\mathcal{C}(x) = x/\epsilon + const.$

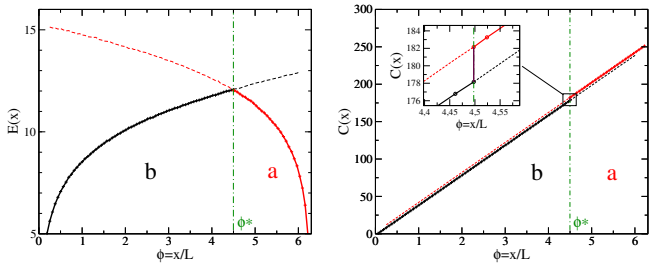

Figure 5.15: Numerical results on a lattice with 200×200 sites for a BTZ black hole with mass $M = 0.1$. Left: Numerically measured entanglement of the two solutions as functions of the subregion size. As can be seen, the lines cross precisely at the theoretically expected transition point, marked by the vertical green dashed line. Right: Corresponding complexity, reproducing the linear law. The inset shows a magnification where the discontinuous jump occurs. Figure by H. Hinrichsen [31].

Both lines are separated at a constant distance, leading to a discontinuous jump of the complexity at the transition. However, the magnitude of the jump $\Delta\mathcal{C} \approx 4.0 \pm 0.3$ is clearly smaller than 2π, reflecting the limitations of the model.

Finally, we repeat the simulation for varying mass M between 0 and 1 for a fixed subregion size. Here one has to take into account that the lattice implicitly determines the cutoff ϵ and that it varies with M. In order to determine ϵ, we compare the integrated bulk volume with the total sum of site volumes on the lattice. Then we subtract the expected influence of the cutoff left and right of the expected transition point. The result is shown in fig. 5.16. As can be seen, the simulations fairly reproduce the finding that the complexity is independent of the mass. At the transition the jump with $\Delta\mathcal{C} = 3.8(3)$ is again smaller than 2π.

So far we cannot explain why $\Delta\mathcal{C}$ deviates from 2π. The deviation could be related to the fact that the use of a square lattice at low Ising temperature breaks the rotational symmetry of the Ising model, so that domain walls aligned with the lattice and diagonal ones behave differently. This is reminiscent of the situation in the MERA, where the minimal cut line is not unique.

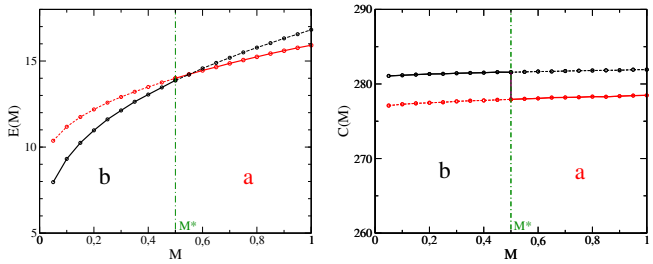

Figure 5.16: Left: Numerically determined entanglement for varying mass measured on a lattice with 120^2 sites and a fixed subregion size $\phi = x/L = 5.31946$ for which the transition is expected to take place at $M = 0.5$. Right: Numerically determined complexity as a function of the mass, where the implicit mass dependence of the cutoff ϵ has been removed (see text), reproducing Fig. 5.12 for $M > 0$. Figure by H. Hinrichsen [31].

5.3.4 Subregion complexity from the CFT

The subregion complexity of [35] comprises a refinement of the holographic "complexity equals volume" (C=V) proposal [103], in the sense that it depends on a choice of entanglement region A, while reducing to the C=V proposal when A is all of space. However, there is as yet no satisfactory independent definition of subregion complexity in field theory, leaving open the question of what, if anything, this quantity tells us about field theory. Section 5.3.3 offered a picture in the tensor network language for how this quantity should be interpreted: as the number of tensors required to compress the information contained in ρ_A to a Hermitian operator acting on a Hilbert space associated to the Ryu-Takayanagi surface.

In this section, we address this problem from a different perspective. Rather than demanding a definition from first principles, we ask instead, how does one *compute* the subregion complexity within field theory? Our proposal is this: for states sufficiently close to the AdS vacuum, the subregion complexity can be computed from the entanglement entropy using the *kinematic space* formalism [133]. In this section we verify this proposal for the simplest case, where the state is the vacuum and the entangling interval is the entire spatial slice.[4] Results for excited states and non-trivial entangling intervals will

[4]Recent work [112,113] has proposed a boundary prescription for reproducing the "complexity equals action" proposal within field theory in terms of the Liouville action, and [113] develops a relationship to

appear in upcoming work [**?**].

The goal of [133] was to derive a CFT expression for the perimeter of an arbitrary bulk region using *kinematic space* $\mathcal{K}$, the space of geodesics of the constant time slice. When the bulk is a weakly curved dual to a large-c CFT, the Ryu-Takayanagi prescription gives a correspondence between points in kinematic space and entangling regions in the CFT. Using the differential entropy of [140], [133] showed that the perimeter can be expressed as the integral over a region in kinematic space, with respect to a measure defined in terms of the entanglement entropy. Here, we extend this result (in the case of vacuum AdS) by expressing the bulk volume in terms of an integral, with respect to an appropriate measure, over a region in $\mathcal{K} \times \mathcal{K}$.

We begin by reviewing the construction of [133]. We then propose an expression for the volume in terms of entanglement entropy, which we apply to pure AdS_3.[5] Evaluating our expression explicitly in the case where the entangling region covers the entire boundary space, we find that it agrees with equation (5.28).

Kinematic space

We write the metric of a spatial slice of vacuum AdS in the form

$$ds^2 = L^2(d\rho^2 + \sinh^2\rho\, d\phi^2)\,, \tag{5.41}$$

related to the coordinates in (5.20) by $\sinh\rho = r/L$. The geodesics are parametrized conveniently by

$$\cos(\alpha) = \tanh(\rho)\cos(\phi - \theta)\,, \quad \alpha \in (0,\pi)\,,\ \theta \in S^1\,, \tag{5.42}$$

where 2α is the opening angle of the geodesic and θ the center of the region subtended by the geodesic (fig. 5.17). Each complete oriented geodesic is specified uniquely by a pair (θ, α), making this a global coordinate system on the kinematic space $\mathcal{K}$. Note that the orientation reversal of the geodesic (θ, α) is $(\pi + \theta, \pi - \alpha)$.

kinematic space. As of yet it is not clear how to generalize this approach to subregion complexity, nor what its explicit relation to our prescription is. This is an interesting direction for future study.

[5] We restrict our attention to pure AdS since the kinematic space has been worked out in great detail. However, there has been recent work on kinematic spaces corresponding to conical defects [141] and black holes [142, 143].

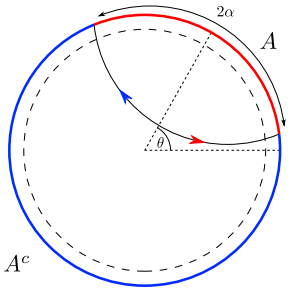

Figure 5.17: Oriented geodesics. We associate the geodesic given by (θ, α) with the entangling region A and the orientation given by the red arrow. The geodesic $(\theta+\pi, \pi-\alpha)$ on the other hand is associated with A^c and the orientation given by the blue arrow. We have chosen the orientation of geodesics in such a way that it matches the one assigned to them in section 5.3.2. Figure by R. Abt [31].

An oriented geodesic in the bulk is naturally associated to an entangling interval (u, v) in the CFT, where

$$u = \theta - \alpha\,, \qquad v = \theta + \alpha\,. \tag{5.43}$$

Flipping the orientation of a geodesic is thus associated with exchanging the entangling region with its complement (fig. 5.17). In the limit $\alpha \to 0$ the geodesic (θ, α) shrinks to a point on the boundary of the spatial slice. We may therefore identify the boundary $(\theta, \alpha = 0)$ of kinematic space with the circle on which the CFT lives. Note that we work with the same metric on the spatial circle as in section 5.3.2, $ds^2_{S^1} = l^2_{\text{CFT}} d\phi^2$.

Our discussion will make extensive use of the concept of a *point curve*, the one-parameter family of geodesics passing through a point. Given a point (ρ, ϕ), its point curve is the set of (θ, α) in $\mathcal{K}$ satisfying (5.42). Each point in the AdS spatial slice is therefore encoded by a point curve in $\mathcal{K}$ (see fig. 5.18).

To recover information about the geometry of AdS requires a geometry on $\mathcal{K}$. The required object is the *density of lines*, which is a volume form on kinematic space [133]

$$\omega = \frac{\partial^2 S}{\partial u \partial v} du \wedge dv = -\frac{1}{2}\partial_\alpha^2 S \, d\theta \wedge d\alpha = \frac{c}{6}\frac{1}{\sin^2(\alpha)} d\theta \wedge d\alpha\,. \tag{5.44}$$

Here, c is the central charge of the dual CFT, while S is the field theory entanglement

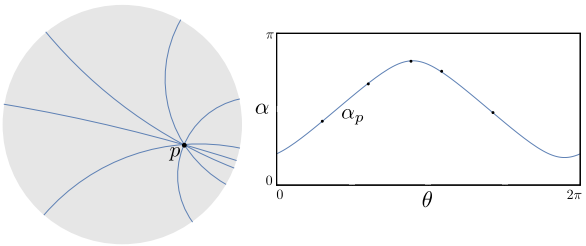

Figure 5.18: Point curves in kinematic space. A given point p in AdS (LHS) is associated with a point curve $\alpha_p(\theta)$ in kinematic space (RHS). This point curve is formed by all geodesics that intersect p. This graphic was generated using [144] with permission of the authors.

entropy on circle of length $2\pi\, l_{\text{CFT}}$ obtained by Cardy and Calabrese [145]

$$\begin{aligned} S &= \frac{c}{3}\log\left(\frac{2l_{\text{CFT}}}{\epsilon}\sin\left(\frac{v-u}{2}\right)\right) \\ &= \frac{c}{3}\log\left(\frac{2l_{\text{CFT}}\sin(\alpha)}{\epsilon}\right). \end{aligned} \tag{5.45}$$

Equipped with the volume form ω, kinematic space now allows us to reconstruct bulk geometric objects from CFT entanglement entropies. This was done in [133] for the length of bulk curves: to any bulk curve γ we can associate a two-dimensional region $\mathcal{G}_\gamma$ of $\mathcal{K}$ consisting of the geodesics intersecting γ. Using the differential entropy of [140], it was shown that the length of γ is proportional to the integral, with respect to the measure ω, of the intersection number of the geodesic with γ. For instance, the geodesic distance $\lambda(p,p')$ between two points p, p' of the spatial slice is given by the integral

$$\frac{\lambda(p,p')}{4G_N} = \frac{1}{4}\int_{\alpha_p \triangle \alpha_{p'}} \omega\,. \tag{5.46}$$

The integration region $\alpha_p \triangle \alpha_{p'}$ is the region bounded by the two point curves $\alpha_p(\theta)$ and $\alpha_{p'}(\theta)$ of the points p and p', respectively, and is comprised of all geodesics intersecting the geodesic arc between p and p' (fig. 5.19).

Of course, our interest in this thesis is in the computation of bulk volumes. In what follows we will illustrate how to compute bulk volumes in terms of chord lengths and therefore, using (5.46) and (5.44), in terms of entanglement entropy.

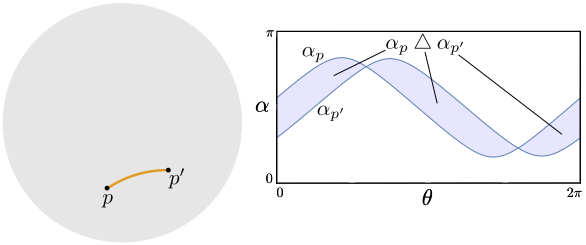

Figure 5.19: The distance between two points p, p' in the bulk (LHS) is given by an integral over the region enclosed by the point curves $\alpha_p, \alpha_{p'}$ (RHS). This graph was generated using [144] with permission of the authors.

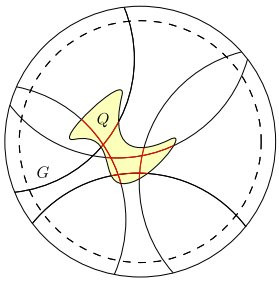

Figure 5.20: In order to obtain the volume of some set Q in terms of kinematic space quantities, we formulate it as an integral over all geodesics G that intersect Q. The chords $G \cap Q$ are red colored. Figure by R. Abt [31].

Bulk volumes at zero temperature

Equation (5.46) is based on the Ryu-Takayanagi formula expressing the length of a geodesic in terms of the entanglement entropy of the corresponding region,

$$\frac{\ell}{4G_N} = S\,, \tag{5.47}$$

so we may also write

$$\omega = -\frac{1}{8G_N}\partial_\alpha^2 \ell \, d\theta \wedge d\alpha\,. \tag{5.48}$$

We compute the volume of a bulk region Q as follows. In analogy with (5.46), we wish to express it as an integral over all geodesics intersecting Q (fig. 5.20). We will see that the correct expression is

$$\frac{vol(Q)}{4G_N} = \frac{1}{2\pi}\int_{\mathcal{G}_Q} \lambda_Q \, \omega\,. \tag{5.49}$$

Here $\mathcal{G}_Q$ is the set of all geodesics $G \in \mathcal{K}$ intersecting Q, while $\lambda_Q(G)$ is the length of the intersection $G \cap Q$ (depicted in red in fig. 5.20). Observe that $\lambda_Q(G)$ is an integral over

$\mathcal{K}$ (see (5.46)). Therefore (5.49) is an integral over $\mathcal{K} \times \mathcal{K}$.

General expressions of this type are known in the integral geometry literature (see *e.g.* chapter 17 of [146]). Let us briefly sketch how to prove (5.49). The first step is to confirm the formula for disks centered at the origin. This can be done via an explicit calculation that we show below. The second step is to verify certain properties of volumes, such as additivity, for the integral on the right hand side of (5.49). They allow us to generalize the validity of (5.49) to arcs of annuli. In the infinitesimal limit we recover the volume element of the (ρ, ϕ) coordinates, allowing us to recover the Riemann integral from (5.49) for arbitrary regions. We will present a more detailed discussion of this proof in future work [**?**].

We now show that (5.49) holds for disks D_K of radius K around the origin (fig. 5.21). The chord length is straightforward to compute and takes the form

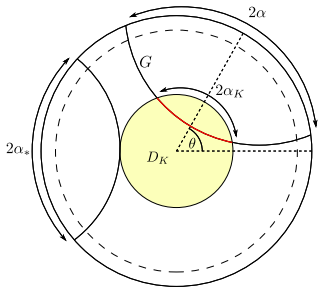

Figure 5.21: To calculate the volume of the disk D_K we need to consider all geodesics G that intersect it. Their opening angle 2α introduces another opening angle $2\alpha_K$ on the boundary of the disk in a natural way. The angle α_* corresponds to a geodesic that is tangential to D_K. Figure by R. Abt [31].

$$\lambda_{D_K}(\theta, \alpha) = L \operatorname{arcosh}\Big(1 + 2\sinh^2(\rho_K)\sin^2(\alpha_K)\Big)\,, \tag{5.50}$$

where $\sinh(\rho_K) = K/L$ and $2\alpha_K$ is the opening angle of the geodesic (θ, α) on the boundary of D_K (fig. 5.21). α_K is related to the boundary angle α via

$$\tanh(\rho_K)\cos(\alpha_K) = \cos(\alpha)\,. \tag{5.51}$$

As we sketched above, to establish (5.49) it suffices to prove

$$vol(D_K) = -\frac{1}{4\pi}\int_0^{2\pi} d\theta \int_{\alpha_*}^{\pi-\alpha_*} d\alpha\, \lambda_{D_K}\partial_\alpha^2 \ell\,, \tag{5.52}$$

where α_* corresponds to a geodesic tangent to the boundary of D_K (fig. 5.21). Geodesics with a smaller opening angle do not intersect D_K and therefore do not contribute. This α_* is given by (5.51) with α_K set to zero,

$$\tanh(\rho_K) = \cos(\alpha_*)\,. \tag{5.53}$$

It is convenient to express (5.52) as an integral over α_K. Using

$$\partial_\alpha^2 \ell \; d\alpha = \partial_{\alpha_K}^2 \lambda_{D_K} d\alpha_K \tag{5.54}$$

leads to

$$\begin{aligned} vol(D_K) &= -\frac{1}{4\pi}\int_0^{2\pi} d\theta \int_{\alpha_*}^{\pi-\alpha_*} d\alpha\, \lambda_{D_K} \partial_\alpha^2 \ell \\ &= -\frac{1}{2}\int_0^{\pi} d\alpha_K \lambda_{D_K} \partial_{\alpha_K}^2 \lambda_{D_K} \\ &= 2\pi L^2 \Big(\sqrt{1+\frac{K^2}{L^2}} - 1\Big)\,, \end{aligned} \tag{5.55}$$

reproducing the well-known result for the volume of the disk D_K and thereby confirming (5.52).

As a special case of (5.52), (5.55) can be directly compared to the complexity of the entire CFT circle (5.28) that we derived using the Gauss-Bonnet theorem. Since the scalar curvature R is constant, the expression (5.18) for complexity is proportional to the volume of the time slice. This complexity is computed by (5.55) with K set to the cutoff radius $r_\epsilon = L\, l_{\text{CFT}}/\epsilon$:

$$\begin{aligned} \mathcal{C}(\text{circle}) &= -\frac{1}{2} R\; vol(D_{r_\epsilon}) \\ &= \frac{2G_N}{\pi L^2}\int_{\mathcal{G}_{D_{r_\epsilon}}} \lambda_{D_{r_\epsilon}} \omega \\ &= 2\pi\Big(\frac{l_{\text{CFT}}}{\epsilon} - 1\Big) + \mathcal{O}(\epsilon)\,. \end{aligned} \tag{5.56}$$

This successfully reproduces the complexity computed in (5.28).

We can now combine the volume formula (5.49) with the formula for distances (5.46) to obtain a volume formula for any region Q in terms of entanglement entropy. To do so we apply (5.46) to the chord length λ_Q:

$$\begin{aligned} \frac{vol(Q)}{4G_N^2} =& \frac{1}{2\pi}\int_{\mathcal{G}_Q}\Big(\int_{\alpha_p \triangle \alpha_{p'}} \omega\Big)\omega \\ =& \frac{1}{8\pi}\int_{\mathcal{G}_Q} d\theta d\alpha \int_{\alpha_p\triangle\alpha_{p'}} d\theta' d\alpha' \partial_\alpha^2 S(\alpha)\partial_{\alpha'}^2 S(\alpha')\;. \end{aligned} \tag{5.57}$$

Here $p(\theta, \alpha)$ and $p'(\theta, \alpha)$ are the points where the geodesic (θ, α) intersects the boundary of Q. Note that we have assumed that each geodesic intersects the boundary of Q exactly twice, so that (5.57) holds only for Q convex.

Equation (5.57) is the main result of this section. It computes the volume of any convex region Q, and thus reproduces the subregion complexity upon setting $Q = \Sigma$ (which is always convex). Therefore, (5.57) constitutes an explicit expression for the holographic subregion complexity purely in terms of CFT quantities, namely entanglement entropies.

We emphasize that this result is not the end of the story. While (5.57) will reproduce the volume of any convex bulk region, determining a valid integration region without knowledge of the bulk region it corresponds to is in general a difficult problem. Fortunately, in the case of an entangling region, which is bounded by geodesics, this problem is considerably simplified. Explicitly verifying the general formula (5.26) is an interesting problem, whose details will be presented in upcoming work. More generally, it would be helpful to understand this problem in the case of finite temperature and for time slices of non-constant curvature.

Mutual complexity

The quantities we have been mostly investigating have some degree of arbitrariness, which is very familiar from entanglement entropy: the UV cutoff dependence. One way of getting rid of this dependence and define a UV finite object is to define *relative* or *mutual* quantities. Mutual information is one of them. Given two subregions A and B, the **mutual information** is defined by

$$I(A|B) \equiv S(A) + S(B) - S(AB) \tag{5.58}$$

This is a very important observable in information theory.

In the case of subregion complexity, it is very natural to define an analogous quantity. We dub this **mutual subregion complexity**, and define it in the obvious way:

$$\Delta C(A|B) \equiv C(AB) - C(A) - C(B) \tag{5.59}$$

The interpretation of this quantity in holography is very nice and intuitive. It measures how much more complex it is to compress the density matrix ρ_{AB} than to construct

individually ρ_A and ρ_B by separate. The signs are chosen such that ΔC in (5.59) is non-negative. This is simply because the product state $\rho_A \otimes \rho_B$ is a particular case of the general ρ_{AB} which generically doesn't factorise. From the bulk point of view, this is due to a property of the RT surfaces known as *entanglement wedge nesting* [147, 148]. This is the statement that, if $A \subseteq B$ or more precisely if the domain of dependence of A is contained in that of B, then the entanglement wedge of A is contained in that of B. For our purposes, the entanglement wedge can be thought of as the region Σ discussed above.

The difference in bulk volumes in (5.59) is depicted in Fig.5.22. In the tensor network, it counts the (finite) amount of gates needed to compress $\rho_A \otimes \rho_B$ into ρ_{AB}. We will perform this calculation in MERA explicitly in Section 5.4.

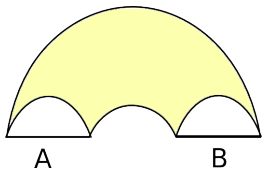

Figure 5.22: Depiction of the mutual complexity $\Delta C(A|B)$ defined in (5.59).

One very interesting question is how exactly does one compute the mutual complexity in the CFT. Although we ignore the procedure, this is a very well posed problem that could be addressed in a concrete way, thus shedding light over a difficult-to-get-a-handle topic as complexity. Indeed, given a reduced density matrix over some set of regions $\{A_i\}$, $\Delta C(\{A_i\})$ essentially measure the number of direct product that exist in the density matrix $\rho(\{A_i\})$. Therefore, we see that it is a *separability* problem [149]. We leave these inquiries for further investigation.

5.4 Counting gates in AdS/MERA

The results of this section are based on still unpublished work in collaboration with J. Erdmenger, P. Fries and H. Hinrichsen.

In Section 5.2 we studied subregion complexity by using a random tensor network model. Although this provides new insight into the problem, one could wonder wether a more direct measurement is possible for comparison. This is indeed the case that we consider in this section. From the point of view of the AdS/MERA perspective, it is very natural to associate the subregion volume to simply *counting* gates in the MERA network. This has several benefits. First, the problem of the set of gates doesn't arise, since the gate set is fixed: we only consider disentanglers and isometries. Second, the calculation is in principle completely straightforward: given a subregion on the boundary layer of the network, how many gates are contained within the minimal cut line?

This is not as naive a question as it seems, and there are two reasons for it. The first reason is that, although not emphasised in the literature, minimal cut lines (geodesics) in MERA **are not unique**. Actually, they are very far from being unique. Indeed, the number of minimal lines (their degeneracy) actually diverges as we increase the size of the selected interval. The spectrum of lines actually has a quite interesting structure which we will explore in detail below. For now, the problem at hand is to understand how to *define* the subregion complexity $\sim$ gate counting in the network. If the minimal cut line is not unique but instead we have a family of minimal lines, which one should we choose in order to count the gates it encloses?

In Fig. 5.23 we illustrate this problem. Even a small interval of 10 sites possesses $\mathcal{O}(10^2)$ different minimal cut lines, all of the same length, but generically containing a different number of enclosed tensors.

The second reason is that MERA is not translationally invariant: if we move both endpoints with the length of the interval fixed, the network geometry probed by the minimal paths varies, and we get a different family of geodesics. If we move them far enough we will indeed come back to the same configuration, due to the discrete scale invariance of the graph.

We propose to deal with these two problems by one simple prescription: we define the complexity as obtained by *averaging* the number of enclosed tensors over all minimal

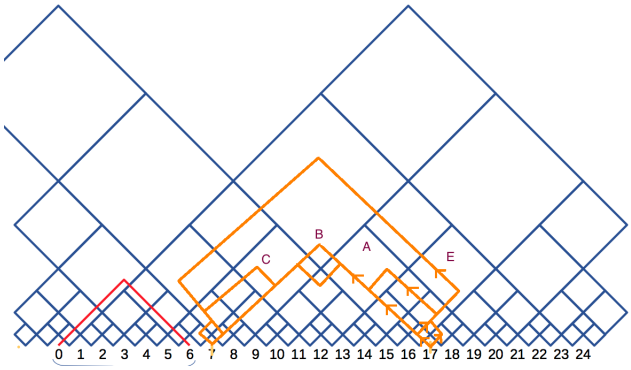

Figure 5.23: Degeneration of minimal cut lines for an interval in MERA. Any combinations of segments respecting the direction indicated by the arrows constitutes a minimal path.

lines, which includes all geodesics for any endpoints with a fixed interval length. This prescription is motivated by the physics we already discussed in the Random Tensor Network model. In that case, the minimal line - the domain wall separating opposite spins - is also not unique. All of them contribute in the partition function, and the key point is that they all come weighted by the same Boltzmann factor, namely $e^{-|\gamma|}$ where $|\gamma|$ is the length of the wall. In other words, one must perform a path integral of the form

$$C_{\text{MERA}}(n) := \frac{\int_n \mathcal{D}\gamma_{\text{min}} V(\gamma_{\text{min}})}{\int_n \mathcal{D}\gamma_{\text{min}}} \tag{5.60}$$

where n is the length of the interval, γ_{min} a minimal cut line and $V(\gamma)$ the number of gates enclosed by γ. The integral $\int_n$ indicates a sum over all minimal paths that connect two points separated by n sites. With this setup in mind, let us recall that the exact gravity result for the subregion complexity is

$$C = \frac{x}{\epsilon} - \pi \tag{5.61}$$

where x is the length of the entangling region and ϵ a UV cutoff. The most natural identification between the AdS and the MERA variables is to set $n \sim x/\epsilon$: the number of lattice points should be proportional to the size of the region. However, we have not been able to determine the exact proportionally constant. Notice that there is **no logarithmic** divergence $\sim \log(n)$. It is this scaling that we aim at reproducing this scaling behaviour.

To illustrate the method, consider again the case shown in Fig. 5.23, with the endpoints fixed. We have chosen a particularly symmetric configuration, such that we are

able to perform analytic calculations. Amongst all the minimal lines, two are special: γ^+ and γ^- are defined as the geodesics that enclose the largest and smallest number of gates $V(\gamma^+)$ and $V(\gamma^-)$ respectively.

Consider an interval as in the figure with $n = 2^N$ sites for some large N. Let $a_k^\pm$ be the number of tensors trapped at each layer, starting from $k = 0$ as the first row of disentanglers. Then, it is easy to see that they satisfy the recursion relations,

$$a_{2k}^\pm = \frac{1}{2} a_{2k-1} \quad , \quad a_{2k+1}^\pm = a_{2k}^\pm \pm 1 \tag{5.62}$$

The calculation simplifies if we count pairs of layers, i.e.

$$b_k^\pm \equiv a_{2k}^\pm + a_{2k+1}^\pm = 2a_{2k}^\pm \pm 1 \tag{5.63}$$

Then the recurrence relation for b_k becomes,

$$\begin{aligned} b_{k+1}^\pm &= 2a_{2k+2}^\pm \pm 1 \\ &= 2 \cdot \frac{1}{2} a_{2k+1}^\pm \pm 1 \\ &= \frac{1}{2} \left(b_k^\pm \pm 3 \right) \end{aligned}$$

This recurrence relation is easily solved. One must provide the initial condition $b_0^\pm = n \pm 1$ at the boundary of the graph. Then, the solution is

$$b_k^\pm = \pm 3 + \frac{n \mp 2}{2^k} \tag{5.64}$$

Now comes a technical point: from the figure we see that this law will remain valid as we move upwards along the network, until we hit the value $a_{2K+2} = 3$, for some K. After that, there always comes a row of two isometries and then one final disentangler at the tip. But since b_k counts bay pairs of layers, it is convenient to use the analytic law (5.64) up until a_{2K+1}, and then add 'by hand' the last 6 gates. Notice that since $2K + 2$ is even, $a_{2K+2} = 3 = \frac{1}{2} a_{2K+1} \;\Rightarrow\; a_{2K+1} = 6$.

For γ^+, we have then $a_{2K^+}^+ = 5$, and thus we sum until $b_{K^+}^+ = 5 + 6 = 11$. For γ_-, we have then $a_{2K^-}^- = 7$, so we sum until $b_{K^-}^- = 7 + 6 = 13$. This gives two equations that determine $K^\pm$,

$$b_{K^+}^+ = 3 + \frac{n-2}{2^{K^+}} = 11 \tag{5.65}$$

$$\Rightarrow \; 2^{K^+} = \frac{2^N - 2}{2^3} = \frac{2^{N-1} - 1}{2^2} \tag{5.66}$$

$$\Rightarrow \; K^+ = \log_2 \left(2^{N-1} - 1 \right) - 2 \tag{5.67}$$

And similarly for γ_-,

$$b^-_{K^-} = -3 + \frac{n+2}{2^{K^-}} = 13 \tag{5.68}$$

$$\Rightarrow \; 2^{K^-} = \frac{2^N+2}{2^4} = \frac{2^{N-1}+1}{2^3} \tag{5.69}$$

$$\Rightarrow \; K^- = \log_2\left(2^{N-1}+1\right) - 3 \tag{5.70}$$

We find that the number of gates $V(\gamma_\pm)$ enclosed by the geodesics $\gamma_\pm$ satisfy

$$V(\gamma_\pm) = 6 + \sum_{k=0}^{K^\pm} b^\pm_k \tag{5.71}$$

$$= 6 + \sum_{k=0}^{K^\pm} \left(\pm 3 + \frac{n \mp 2}{2^k}\right) \tag{5.72}$$

$$= 6 \pm 3\left(K^\pm + 1\right) + (n \mp 2)\sum_{k=0}^{K^\pm} \frac{1}{2^k} \tag{5.73}$$

Here we must pause to make our point. We expect that, if any matching between the tensor network and the AdS side is possible, it should in any case occur in the limit of large intervals $n = 2^N \gg 1$. But in this limit it is clear from (5.67) and (5.70) that $K^\pm \sim \pm\log(n)$. This contribution is precisely the subleading divergence that we should not have. Happily, it turns out that the same logarithmic divergence appears for both γ^+ and γ^- but with the **opposite sign**.

As argued above, the key step is then to compute the *average* value, where the subleading divergences cancel:

$$2\overline{V} \equiv V(\gamma_+) + V(\gamma_-) \tag{5.74}$$

$$= 12 + 3\left(K^+ - K^-\right) + (n+2)\sum_{k=0}^{K^+} \frac{1}{2^k} + (n-2)\sum_{k=0}^{K^-} \frac{1}{2^k} \tag{5.75}$$

Here we see that

$$K^+ - K^- = 1 + \log_2\left(\frac{2^{N-1}-1}{2^{N-1}+1}\right) \tag{5.76}$$

and thus contains no extra finite terms in the limit $n = 2^N \to \infty$. However, the sums still contain finite terms. Indeed, we have

$$n\sum_{k=0}^{K^\pm} \frac{1}{2^k} = n\left(2 - \frac{1}{2^{K^\pm}}\right) \tag{5.77}$$

which gives

$$n\left(2-\frac{8}{n-2}\right)\to 2n-8 \quad , \ \gamma_+ \tag{5.78}$$

$$n\left(2-\frac{16}{n+2}\right)\to 2n-16 \quad , \ \gamma_- \tag{5.79}$$

Since we have taken into account all finite contributions, we can take the limit $n = 2^N \to \infty$ safely, yielding

$$2\overline{V} = 12+3+4n-24 = 4n-9 \tag{5.80}$$

Thus, the average number of gates contained, taking into account only the lines that contain the maximum and minimum number of tensors is

$$\overline{V}(n) = 2n-\frac{9}{2} \tag{5.81}$$

In order to attempt a more precise matching with the results of the gravity side, there is still the issue of the overall normalisation, which we have not solved in this work. Nevertheless, (5.81) is a very interesting result. An educated guess would be simply $n = x/\epsilon$. Then, the constant term we get from MERA is $9/4$ which is not far from the exact value π.

5.5 Outlook

In this thesis we took steps toward understanding the properties of subregion complexity in CFT_2 from three points of view: the original holographic proposal of [35], the definition and study of a tensor network analogue, and a prescription for computing it directly within CFT_2.

Within gravity, we studied a modified "topological complexity" proposal. Using the fact that for locally hyperbolic spaces, the curvature $R = -2/L^2$ is constant, we rewrote the holographic volume proposal as an integral of the curvature scalar. Such a definition of complexity density may be reflective of the loss of degrees of freedom along an RG flow.

For the case of $\mathrm{AdS}_3/\mathrm{CFT}_2$, the new form is readily evaluated using the Gauss-Bonnet theorem, giving a simple universal formula (5.26) valid for an arbitrary number of entangling intervals and at any temperature. Particularly interesting was the change in

complexity during transitions between topologically distinct RT surfaces. At these transitions, the subregion complexity jumps by a discrete quantity proportional to the Euler characteristic of a bulk region bounded by geodesics. In particular, the jump comes in integral multiples of a basic unit (2π in our normalization), irrespective of the geometry of the entangling region or black hole temperature. Surprisingly, our result also implies that complexity in the black hole background is independent of the size of the black hole, and hence of temperature.

Interesting questions for the future include generalizing this approach to higher dimensions; understanding subregion complexity using the optimization approach of [112–114, 150]; relating our approach with the holographic renormalization properties of the different proposals for complexity [107, 151]; and studying subregion complexity in time-dependent systems [121].

Turning to tensor network states, we proposed that their subregion complexity should be understood as the number of local tensors required to build the map embedding the the Hilbert space cut by the RT surface in the Hilbert space of the entangling region A. The observed jumps in holographic subregion complexity are then understood to arise from qualitative jumps in the form of the optimal compression of ρ_A to a Hilbert space of smaller dimension. We studied this complexity for the random tensor networks of [36] in the presence of a black hole using its map to an Ising model. Using numerical computations we reproduce the discontinuous jump of subregion complexity in this approach, although our numerical value $\Delta\mathcal{C} = 4.0 \pm 0.3$ differs from the gravity result $\Delta\mathcal{C} = 2\pi$. We leave it as an interesting question for future research to track down the origin of this discrepancy. Reassuringly, fig. 5.16 displays independence on temperature to a good approximation. The non-vanishing but small slope is another limitation of this model deserving further investigation.

Finally, we gave a prescription for computing the subregion complexity directly in CFT based on the kinematic space formalism. Our prescription expresses complexity as an integral built from entanglement entropies. We showed that, at zero temperature, our formula coincides with the gravity result, and verifyied the computation explicitly in the case $A = S^1$. If the subregion complexity proposal of [35] provides a useful measure of the complexity of the reduced density matrix, our results suggest a deeper relationship be-

tween complexity and entanglement. To investive this relation further, it will be necessary to gain a deeper understanding of the field theory interpretation of subregion complexity. Another interesting generalization is to extend our prescription to finite temperature by working with kinematic space for black hole geometries.

It is promising that we find coinciding results for the subregion complexity in concrete examples from three perspectives — gravity, tensor networks, and CFT — and we are optimistic that we will see more progress along these lines in the near future.

Chapter 6

Black holes with running couplings in AdS_3

6.1 Asymptotic safety for quantum gravity

In the preceding sections of this thesis we have focused a on a particular approach of quantization, namely a special area of string theory - the AdS/CFT duality. Although this is likely the most popular approach, there exist many other which are very interesting by themselves [152–168] (for a review see [169]). In this Chapter, we will focus on another well known alternative, called Asymptotic Safety, after its first proposal by Weinberg [170]. Even though many approaches to quantum gravity are very different, most of them have the common feature that the resulting effective action of gravity acquires a scale dependence. This means that the couplings appearing in the quantum- effective action (such as Newtons coupling G_0, or the cosmological term Λ_0) become scale dependent quantities ($G_0 \to G_k$, $\Lambda_0 \to \Lambda_k$). There is quite some evidence that this scaling behavior is in agreement with Weinberg's Asymptotic Safety program [37, 171–177].

Let us quickly review the big picture of this proposal [178]. The idea is that, although gravity in more than two dimensions is not **perturbatively** renormalizable, Weinberg argued that it might be **non-perturbatively** renormalizable, and thus the UV completion of Einstein gravity might hit a non trivial but well defined, finite UV fixed point. In order to test this, one uses the Functional Renormalization Group technique [178]. As in perturbative QFT, one defines an effective action Γ_k. This represents the 'effective'

action that we see at the scale k, which contains in principle an infinite series of allowed couplings $g_\alpha(k)$ which flow with k. In this sense, $\Gamma_k[\{g_\alpha(k)\}]$ describes a curve in 'theory space', the space of all possible Hamiltonians, spanned by their coupling constants.

The difference with the usual QFT effective action is that now there's an extra RG scale k such that Γ_k contains the functional integral of all fields with momenta p larger than k, and no contribution from the fields with momenta p lower than k. In practice, this is implemented by adding an extra 'mass term' to the action, containing an IR cutoff function $\mathcal{R}_k(p^2)$:

$$I_k[\phi] = \frac{1}{2}\int_p \phi_p \mathcal{R}_k(p^2)\phi_{-p} \tag{6.1}$$

where we have generically called the fields ϕ (in gravity these would include the metric). The IR cutoff function is to a large extend arbitrary, but it must satisfy: i) $\mathcal{R}_k \to 0$ as $k \to 0$ to recover the standard 1PI action in the deep IR, ii) $\mathcal{R}_k(p^2)$ goes quickly to zero for $p \gg k$, so as to leave the momenta above k untouched, iii) $\mathcal{R}_k(p^2) \approx k^2$ for $p^2 \ll k^2$ which freezes these modes by giving them a very large mass. This defines a scale dependent generating functional

$$Z_k[J] = \int [d\phi] \exp\left(-I[\phi] - I_k[\phi] + \int_p J\phi_p\right) \equiv \exp\left(-W_k[J]\right) \tag{6.2}$$

where S is the bare action, J a source for the field ϕ and W_k the scale-dependent generator of connected diagrams. And via the usual Legendre transformation, this defines a scale-dependent effective action

$$\Gamma_k[\phi_c] = W_k[J] - S_k[\phi_c] - \int_x J\phi_c \tag{6.3}$$

where ϕ_c is the classical or average field $\phi_c = \delta W_k[J]/\delta J$. Then, it is not difficult to show that the effective action satisfies the **Wetterich equation**:

$$\partial_k \Gamma_k = \frac{1}{2}\mathrm{Tr}\left[\partial_k \mathcal{R}_k \left(\mathcal{R}_k + \Gamma_k^{(2)}\right)^{-1}\right] \tag{6.4}$$

where $\Gamma^{(2)}$ refers to the second functional derivative with respect to the fields, and the trace simply refers to summing over all momenta. Since the cutoff function is given, (6.4) provides a first order differential equation for Γ_k that in principle doesn't rely on any perturbation theory, and can be directly solved provided an initial condition. Notice that

However, in practice it is not easy to solve, so one resorts to a truncation method on the couplings. Suppose we expand the effective action in a complete set of basis functionals ('action terms') P_α,

$$\Gamma_k[\phi] = \sum_{\alpha=1}^{\infty} g_\alpha(k) P_\alpha[\phi] \tag{6.5}$$

For instance, one term could be $P_1[\phi] = \int (\partial\phi)^2$, i.e. a kinetic term, etc. Now, by expanding the P_α in terms of their beta functions β_α, the Wetterich equation (6.4) can be rewritten as

$$k\partial_k g_\alpha(k) = \beta_\alpha\left(g_1, g_2, \ldots\right) \tag{6.6}$$

Provided initial conditions, these equations completely determine the evolution of all the couplings $g_\alpha(k)$, which fixes a curve in space and determines the UV behaviour - wether there's a fixed point or not. However, in practice this is impossible since (6.6) consist of an infinite set of coupled differential equations. In order to get a finite system, one truncates the series as $\alpha = 1, 2, \ldots, P$ and solves the P coupled equations numerically.

A particularly important result in this direction was due to Reuter and Saueressig [174]. They considered the 'Einstein truncation', in which the only two couplings allowed to run are Newton's constant (the Planck scale) and the cosmological constant. The result is plotted in Fig. 6.1. The arrows point in the IR direction, and we clearly see the presence of a UV fixed point, which moreover is an attractor, such that all initial data with positive G_k flow towards it. Although very appealing, this result is not decisive, since improvement of the truncation might imply that other couplings in parameter space blow up.

6.2 Black holes in $\mathbf{AdS}_3$ asymptotic safety

The effective action and running couplings in three dimensions have been studied in [180,181]. In any case, scale dependent couplings can be expected to produce differences to classical general relativity, such as modifications of classical black hole backgrounds [182–202].

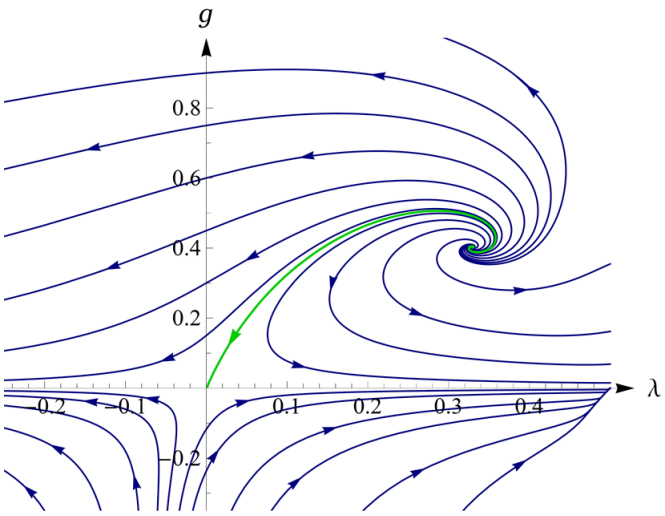

Figure 6.1: RG flow $3+1$ in space g, λ, for the Einstein-truncation. The arrows point towards the IR. The non gaussian UV fixed point is clearly exhibited. Fig. from Andreas Nink, [179].

6.2.1 The setup

In this thesis the possible effects of scale dependence on the black hole in three dimensional gravity will be investigated in the light of the effective action approach. We will use the scale-field method applied to the Einstein-Hilbert truncation, which allows to derive generalized Einstein equations for the case of scale dependent couplings [40, 203–205]. The theoretical uncertainty concerning the functional form of the scale dependence of G_k and Λ_k will be avoided. Instead, the most general stationary spherically symmetric solution without angular momentum, which is in agreement with the common "null energy condition" for the effective stress energy tensor, will be derived. It is further shown that this solution corresponds also to the most general case which is in agreement with the "Schwarzschild relation" $g_{tt} = -1/g_{rr}$.

The chapter is organized as follows: In subsection 6.2.2 the concept of effective action with scale dependent couplings is reviewed. In section 6.3 those techniques will be used to derive and discuss a new black hole solution in three dimensions with scale dependent couplings. In subsection 6.3.1 the "null energy condition" for the effective stress energy tensor is formulated and its connection to the "Schwarzschild relation" is reviewed. The solution is presented in subsection 6.3.2, in subsection 6.3.4 the asymptotic behavior of

the solution is discussed, the horizon structure is analyzed in subsection 6.3.5, and the thermodynamic properties are discussed in subsection 6.3.6. Results are summarized in section 6.4.

6.2.2 Scale dependent couplings and scale setting

This subsection summarizes the equations of motion for the scale dependent space-times in three dimensions. The notation and scale setting procedure is according to [40, 203–206].

The scale dependent effective action is

$$\Gamma(g_{\mu\nu}, k) = \int d^3x \sqrt{-g} \frac{(R - 2\Lambda_k)}{G_k}. \tag{6.7}$$

By varying (6.7) with respect to the metric field one obtains

$$G_{\mu\nu} = -g_{\mu\nu}\Lambda_k + 8\pi G_k T_{\mu\nu}. \tag{6.8}$$

The effective stress energy tensor $T_{\mu\nu}$ contains the actual matter contribution $T^m_{\mu\nu}$ and a contribution $\Delta t_{\mu\nu}$ induced by the possible coordinate dependence of G_k [40]

$$T_{\mu\nu} = T^m_{\mu\nu} - \frac{1}{8\pi G_k} \Delta t_{\mu\nu}, \tag{6.9}$$

where

$$\Delta t_{\mu\nu} = G_k \left(g_{\mu\nu}\Box - \nabla_\mu \nabla_\nu\right) \frac{1}{G_k}. \tag{6.10}$$

By varying (6.7) with respect to the scale-field $k(x)$ one obtains the algebraic equations

$$\left[R \frac{\partial}{\partial k}\left(\frac{1}{G_k}\right) - 2\frac{\partial}{\partial k}\left(\frac{\Lambda_k}{G_k}\right)\right] = 0. \tag{6.11}$$

The above equations of motion are consistently complemented by the Bianchi identity, reflecting invariance under coordinate transformations

$$\nabla^\mu G_{\mu\nu} = 0. \tag{6.12}$$

6.3 Scale dependent non-spinning solution

Let us now turn to solving the system of equations (6.8-6.12) assuming a stationary space-time with rotational symmetry and no angular momentum. The most general line element

in agreement with this symmetry is

$$ds^2 = -f(r)\,dt^2 + g(r)\,dr^2 + r^2 d\phi^2. \tag{6.13}$$

Apart from the two functions $f(r)$ and $g(r)$, the system has to be solved for the scale field $k(r)$. In principle this is possible, as soon as the functional form of the scale dependent couplings G_k and Λ_k is known, for example from some Functional Renormalisation Group (FRG) equation. Those functions have been calculated by using various methods and approximations. However, it has up to now not been possible to obtain an exact and scheme independent expression of the effective average action. Therefore, the functional form of Λ_k and G_k is subject to very large theoretical uncertainties. This problem is aggravated by the fact that most functional forms of Λ_k and G_k are either only valid in the UV or in the IR. Given those drawbacks we will proceed with a method that has been previously applied in four dimensions [40, 203–205]: The first step is to realize that the only appearance of the scale field $k(r)$ is within the couplings and that for any solution of the system the functions Λ_k and G_k will inherit a radial dependence from $k(r)$. Thus, one might try to solve the system for $\{f(r),\, g(r),\, \Lambda(r),\, G(r)\}$ (instead of solving for $\{f(r),\, g(r),\, k(r)\}$). However, since one dealt one unknown function $k(r)$ for two unknown functions $\Lambda(r)$ and $G(r)$, the system is underdetermined. In order to obtain a determined system again one has to impose an additional condition.

6.3.1 The null energy condition

The most common type of conditions in classical general relativity are energy conditions [207–209], where one typically distinguishes between the dominant, weak, strong, and null condition. The less restrictive of those conditions is the null energy condition, which states that for a null vector field l^ν the matter stress energy tensor satisfies

$$T^m_{\mu\nu} l^\mu l^\nu \geq 0. \tag{6.14}$$

Since we are interested in black hole solutions it is crucial to note that the energy condition (6.14) is actually necessary for the proof of fundamental black hole theorems such as the no hair theorem [210] or the second law of black hole thermodynamics [211]. Therefore, if one is looking for black hole solutions that are in agreement with those two fundamental

theorems, it is natural to impose that appearance of scale dependence does not spoil or alter this property for the effective stress energy tensor

$$T_{\mu\nu}l^\mu l^\nu \stackrel{!}{=} T^m_{\mu\nu}l^\mu l^\nu \geq 0. \tag{6.15}$$

A physical interpretation of this condition is that one imposes that not even a light-like observer can observe a difference between the energy density due to the presence of matter and the effective energy density due to the combined matter and scale dependence effects. The relation (6.15) holds if one maintains the standard matter condition (6.14) and one further imposes that the extra contribution to the stress tensor (6.10) induced by the variation of the couplings satisfies

$$\Delta t_{\mu\nu}l^\mu l^\nu = 0. \tag{6.16}$$

In a spherically symmetric setting one can solve this condition for the scale dependent coupling (6.13) without the use of the equations of motion (6.8) giving

$$G(r) = a\left[\int_{r_0}^{r}\sqrt{f(r')\cdot g(r')}\;dr'\right]^{-1}, \tag{6.17}$$

where a and r_0 are constants. The next step consists in finding the metric functions $f(r)$ and $g(r)$ which appear in this integral. This can be achieved by a straight forward argument following Jacobson [212]: one can choose the null vector field to be $l^\mu = \left\{\sqrt{g}, \sqrt{f}, 0\right\}$. Combining the equations of motion (6.8) for this vector field with the condition (6.15) gives in regions without external matter ($T^m_{\mu\nu} = 0$)

$$R_{\mu\nu}l^\mu l^\nu = (f\cdot g)'\frac{1}{2rg} = 0 \tag{6.18}$$

and thus $f \sim 1/g$. By making use of time reparametrization invariance, this allows to write $f(r) = 1/g(r)$, which corresponds to the so called Schwarzschild relation. It is interesting to note that this common relation further ensures that the radius coordinate is an affine parameter on the radial null geodesics [212]. With this relation the line element is

$$ds^2 = -f(r)\,dt^2 + f(r)^{-1}\,dr^2 + r^2 d\phi^2 \tag{6.19}$$

and the equations of motion can be completely solved for the three functions $\{f(r),\, \Lambda(r),\, G(r)\}$.

6.3.2 A non-trivial solution for scale dependent couplings

Based on (6.15) one finds that the equations (6.8) are solved by

$$G(r) = \frac{G_0^2}{G_0 + \epsilon r(1+G_0 M_0)}, \tag{6.20}$$

$$f(r) = f_0(r) + 2M_0 G_0 \left(\frac{G_0}{G(r)} - 1\right)\left[1 + \left(\frac{G_0}{G(r)} - 1\right)\ln\left(1 - \frac{G(r)}{G_0}\right)\right], \tag{6.21}$$

$$\begin{aligned}\Lambda(r) = {} & \frac{-G(r)^2}{\ell_0^2 G_0^2}\left[1 + 4\left(\frac{G_0}{G(r)} - 1\right) + \left(5M_0 G_0 \frac{\ell_0^2}{r^2} + 3\right)\left(\frac{G_0}{G(r)} - 1\right)^2 + \right. \\ & + 6M_0 G_0 \frac{\ell_0^2}{r^2}\left(\frac{G_0}{G(r)} - 1\right)^3 + \\ & \left. + 2M_0 G_0 \frac{\ell_0^2}{r^2}\frac{G_0}{G(r)}\left(3\left(\frac{G_0}{G(r)} - 1\right) + 1\right)\left(\frac{G_0}{G(r)} - 1\right)^2 \ln\left(1 - \frac{G(r)}{G_0}\right)\right],\end{aligned} \tag{6.22}$$

where $G_0, M_0, \ell_0, \epsilon$ are four integration constants. This represents a family of solutions that includes the classical BTZ black hole: the choice of the integration constants was made by demanding that the classical BTZ solution is recovered when one dimensionless constant (labeled ϵ) vanishes. Indeed, one easily verifies that

$$\lim_{\epsilon\to 0} G(r) = G_0 \quad , \quad \lim_{\epsilon\to 0} f(r) = -G_0 M_0 + \frac{r^2}{\ell_0^2} \quad , \quad \lim_{\epsilon\to 0}\Lambda(r) = -\frac{1}{\ell_0^2} \tag{6.23}$$

which justifies the naming of the constants ($G_0, M_0, \Lambda_0 = -1/\ell_0^2$) in terms of their meaning in the absence of scale dependence. The connection between the new solution and the BTZ solution is given in terms of the difference between the "running" $G(r)$ and the fixed G_0. One further verifies the transition to empty AdS_3 space for the classical "mass gap" relation $M_0 \to -\frac{1}{G_0}$

$$\lim_{M_0\to -1/G_0} G(r) = G_0 \quad , \quad \lim_{M_0\to -1/G_0} f(r) = 1 + \frac{r^2}{\ell_0^2} \quad , \quad \lim_{M_0\to -1/G_0}\Lambda(r) = -\frac{1}{\ell_0^2}$$

Note that in this limit, all dependence on ϵ vanishes. Thus, AdS_3 constitutes the appropriate vacuum of the theory, which is invariant under perturbations due to the running of the couplings controlled by ϵ. In terms of the RG flow, this suggests that AdS would be a fixed point of the RG group. Note further that M_0 is the mass of the black hole only if $\epsilon \to 0$, while for $\epsilon \neq 0$ it is much harder to determine the mass. We will come back to this point at the end of section 6.3.

Since the constant ϵ controls the strength of the new scale dependence effects, in some

cases it is useful to treat it as small expansion parameter

$$\begin{aligned} G(r) &= G_0 - \epsilon \cdot (1 + G_0 M_0) r + \mathcal{O}(\epsilon^2), \\ f(r) &= -G_0 M_0 + \frac{r^2}{\ell_0^2} + 2\epsilon \cdot M_0 (1 + G_0 M_0) r + \mathcal{O}(\epsilon^2), \\ \Lambda(r) &= -\frac{1}{\ell_0^2} - \epsilon \cdot \frac{2r}{\ell_0^2 G_0} (1 + G_0 M_0) + \mathcal{O}(\epsilon^2). \end{aligned} \tag{6.24}$$

In figure 6.2 the lapse function $f(r)$ is shown for different values of ϵ in comparison to the classical BTZ solution.

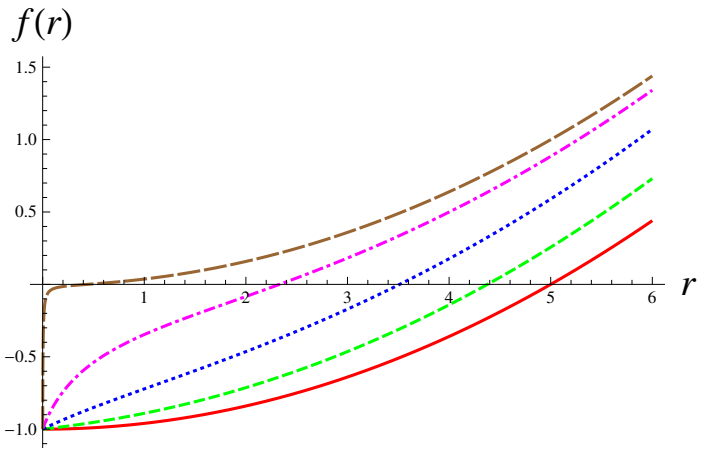

Figure 6.2: Radial dependence of the lapse function $f(r)$ for $\ell_0 = 5$, $G_0 = 1$ and $M_0 = 1$. The different curves correspond to the classical case $\epsilon = 0$ solid red line, $\epsilon = 0.02$ short dashed green line, $\epsilon = 0.09$ dotted blue line, $\epsilon = 0.5$ dot-dashed magenta line, and $\epsilon = 100$ long dashed brown line. Plot from [42].

As can be seen in the solution (6.20)-(6.22), one observes that $f(r)$ is monotonically growing for all chosen values of ϵ, that $\lim_{r\to 0} f(r) = -G_0 M_0$ independent of ϵ, and that all functions grow as $\sim r^2$ for large values of r. One further notes that, even though $\lim_{\epsilon\to 0} f(r) = -G_0 M_0 + r^2/\ell_0^2$, the first derivative of $f(r)$ at the origin is strongly dependent on ϵ. As discussed below, the non vanishing of this derivative induced by ϵ produces a curvature singularity at the origin proportional to ϵ.

6.3.3 Curvature singularity

For small radial coordinate a new singularity appears, which is absent in the classical BTZ solution. This can be verified by evaluating for example the invariant Ricci scalar

in the limit of $r \to 0$, where one finds that the leading terms are

$$R = -4M_0\epsilon(1+G_0M_0)\cdot\frac{1}{r} - \left(\frac{6}{\ell_0^2} + 10\frac{M_0}{G_0}(1+G_0M_0)^2\epsilon^2\right) + \mathcal{O}(r^1). \tag{6.25}$$

This quantity is divergent for $\epsilon \neq 0$ and it is finite for $\epsilon = 0$. In particular, when $\epsilon = 0$ one recovers the classical Ricci scalar for BTZ solution $R_{\rm BTZ} = -6/\ell_0^2$. This demonstrates how sensible the curvature singularity of BTZ is. Indeed, only the choice $G_0M_0 + 1 = 0$ renders the origin smooth. Any deviation from it, no matter how small, will produce a singularity at the origin.

In fact there is a natural expectation that this should be the case. The non-rotating BTZ spacetime, although devoid of a curvature singularity at $r = 0$, has a causal singularity there. Moreover, it is well known that the smoothness of the manifold at that point is unstable under the inclusion of matter fields in the dynamics. Now, as we have seen above, the extra contribution (6.10) to the stress tensor induced by the scale dependence of Newton's constant can be thought of as a matter source.

6.3.4 Asymptotics

Concerning the limit $r \to \infty$, the exact solution (6.21) is asymptotically AdS_3: $f(r) \sim \frac{r^2}{\ell_0^2}$ at leading order in r. But although asymptotically the metric behaves as BTZ, neither $\Lambda(r)$ nor $G(r)$ mimic their BTZ analogs. Indeed, $\Lambda(r) = -3/\ell_0^2 = 3\Lambda_0$ at $r \to \infty$. This 'effective' cosmological constant at infinity arises from the extra term in Einstein's equation. Evaluating this term for the solution in the large r regime, one has

$$\Delta t_{\mu\nu}|_{r\to\infty} = \frac{2}{\ell_0^2} g_{\mu\nu}. \tag{6.26}$$

When analyzing such asymptotics one has to be careful since even though ϵ is a small dimensionless parameter, other quantities like $\epsilon r/G_0$ might actually become large at large radial coordinates. On the other hand, it is clear from (6.20) that the behavior of $G(r)$ possesses two very different regimes: for $\epsilon r(1 + M_0G_0) \ll G_0$, it behaves effectively as a constant G_0, while for $\epsilon r(1 + M_0G_0) \gg G_0$ it falls to zero. To consider this latter non-standard regime, one performs an expansion of the lapse function (6.21), where the

smallness parameter is $\frac{G(r)}{G_0} \ll 1$. This yields, at first order,

$$f_{G\ll G_0}(r) \approx \left(\frac{r}{\ell_0}\right)^2 - \frac{2}{3}M_0 G(r)$$
$$= \left(\frac{r}{\ell_0}\right)^2 - \frac{2}{3}M_0 G_0 \frac{G_0}{(1+M_0G_0)\epsilon r}. \tag{6.27}$$

where ℓ_0 remains arbitrary. We shall use this approximation for the analysis of the next sections.

6.3.5 Horizon structure

Horizons are crucial for understanding the structure of a black hole. Unfortunately, the zero of the lapse function (6.21) implies a transcendental equation for r, which can not be solved analytically. We approach this problem in three different ways: First, we study the leading corrections with respect to the classical regime (ϵ small). Second, we focus on a specific region of parameter space that exhibits a particularly interesting strong scale dependence effects, namely $G(r)/G_0 \ll 1$, that display some novel features. Third, those two approaches are compared with a numerical analysis.

- Expansion in $\epsilon \ll 1$: For weak scale dependence one can use the expansion (6.24), for which one finds the horizon

$$r_h|_{\epsilon\ll 1} = \sqrt{G_0 M_0}\ell_0 - \epsilon\ell_0^2 M_0(1+G_0M_0) + \mathcal{O}(\epsilon^2). \tag{6.28}$$

  Unfortunately, an analytic result is again limited to order ϵ. One sees that the scale dependence tends to decrease the apparent horizon radius.

- Expansion in $G(r_h)/G_0 \ll 1$: from (6.20), Newton's coupling evaluated at the horizon will be much smaller than its classical value provided that

$$\epsilon r_h(1+M_0G_0) \gg G_0 \tag{6.29}$$

  In this limit the horizon can be obtained from (6.27). It is the real root of

$$r_h^3|_{G(r)/G_0\ll 1} \approx \frac{2}{3}\frac{M_0 G_0^2 \ell_0^2}{(1+M_0G_0)\epsilon}. \tag{6.30}$$

  For consistency, this must satisfy (6.29), yielding a condition over the parameters:

$$\frac{M_0(1+M_0G_0)^2\epsilon^2\ell_0^2}{G_0} \gg 1 \tag{6.31}$$

A particularly interesting region of the parameter space is $M_0 G_0 \to \infty$. Indeed, the radius of the horizon converges to a finite value,

$$r_h^3|_{G(r)/G_0 \ll 1 \,\&\, M_0 G_0 \gg 1} \approx \frac{2}{3}\frac{G_0 \ell_0^2}{\epsilon} \tag{6.32}$$

for any $\epsilon \ell_0^2 > 0$, as required by (6.31). We thus see the crucial difference with its constant-coupling counterpart: for a fixed cosmological constant, the radius of the horizon remains finite as $M_0 \to \infty$. As we show below, this has important consequences on the thermodynamic properties of the solution (note however that, as $\epsilon \to 0$, the horizon radius becomes unbounded). In the light of this result one should keep in mind that M_0 is only the mass parameter for the classical solution and it is not the actual mass of the black hole. However, in the next section we show that for the particular case when (6.32) is valid, the physical mass indeed diverges as $M_0 \to \infty$, and nevertheless the horizon remains at finite constant distance from the origin.

- Numerical analysis: For given values, the above analytical estimates can be compared with a numerical solution of $f(r) \stackrel{!}{=} 0$. In figure 6.3 the horizon r_h is shown as a function of the classical mass parameter M_0.

One observes that for small M_0, the horizon is in agreement with the classical result. Finally, one notes that for very large values of M_0 the numerical value of the horizon saturates at constant r_h which is given by the horizontal line in accordance with the $G \ll G_0$ approximation (6.30).

6.3.6 Thermodynamics

After having gained knowledge on the horizon structure one can now turn towards the thermodynamic properties of the solution (6.20-6.22). The temperature of a black hole with the metric structure (6.19) is given by

$$T = \frac{1}{4\pi}\frac{\partial f(r)}{\partial r}\bigg|_{r=r_h} . \tag{6.33}$$

Leaving the horizon radius implicit one finds

$$T = \frac{1}{2\pi r}\frac{G_0^2 M_0}{G_0 + r\epsilon(1 + G_0 M_0)}\bigg|_{r=r_h} . \tag{6.34}$$

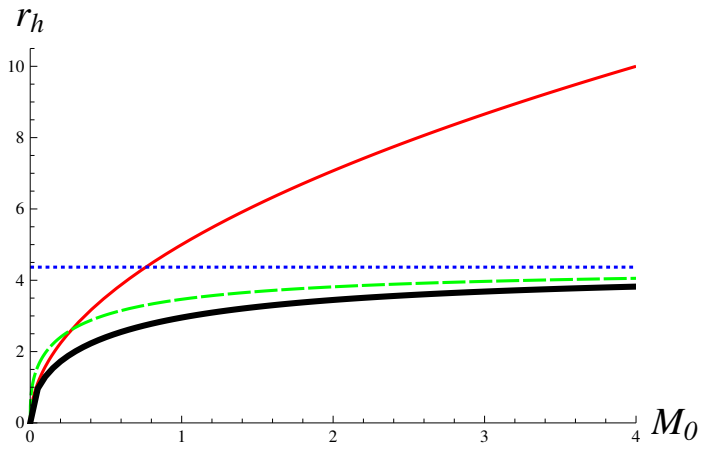

Figure 6.3: Apparent black hole horizon r_h as a function of M_0 for $\ell_0 = 5$, $G_0 = 1$ and $\epsilon = 0.2$. The different curves correspond to the classical case (solid red line) the expansion (6.30) for small G/G_0 (long dashed green line) the expansion (6.32) for small G/G_0 and large $G_0 M_0$ (dotted blue line), and the numerical solution (thick solid black line). The expansion (6.28) for small ϵ is not shown since for the given numerical values it would only be reliable for very small $M_0 < 0.2$. Plot from [42].

Inserting the perturbative value for the horizon radius (6.28) one finds that the $\mathcal{O}(\epsilon)$ corrections to the temperature cancel out and that the leading correction to the classical temperature enters at order ϵ^2

$$T|_{\epsilon \ll 1} = \frac{\sqrt{G_0 M_0}}{2\pi \ell_0} + \mathcal{O}(\epsilon^2). \tag{6.35}$$

The transcendent structure of the solution does not allow to go straight forwardly beyond this $\mathcal{O}(\epsilon)$ approximation. However, in the opposite limit the lapse function becomes polynomial again, and one can again explore the case considered above, (6.29)-(6.32), $G \ll G_0$ and one finds from (6.27) that

$$T|_{G \ll G_0} \approx \frac{1}{4\pi} \left(18 \frac{M_0 G_0^2}{\ell_0^4 (1 + G_0 M_0)\epsilon} \right)^{1/3}, \tag{6.36}$$

so in particular, the temperature of the black hole with fixed ℓ_0 and $M_0 \to \infty$ converges to a constant,

$$T|_{G \ll G_0 \,\&\, G_0 M_0 \gg 1} \approx \frac{1}{4\pi} \left(18 \frac{G_0}{\ell_0^4 \epsilon} \right)^{1/3}. \tag{6.37}$$

for any finite ϵ, ℓ_0. Those analytical results can again be compared to a numerical solution of (6.34). In figure 6.4 the numerical temperature is shown as a function the parameter

M_0 in comparison to the analytical and classical results. One finds that the temperature behavior as a function of M_0 is actually a rescaled version of the horizon radius in figure 6.3. This is a particularity of the three dimensional case. One further sees that for small M_0, the numerical curve of the new solution approaches the behavior of the classical BTZ case. However, in the opposite limit of large M_0 the temperature of the new solution saturates at the values given by the approximations (6.36 and 6.37).

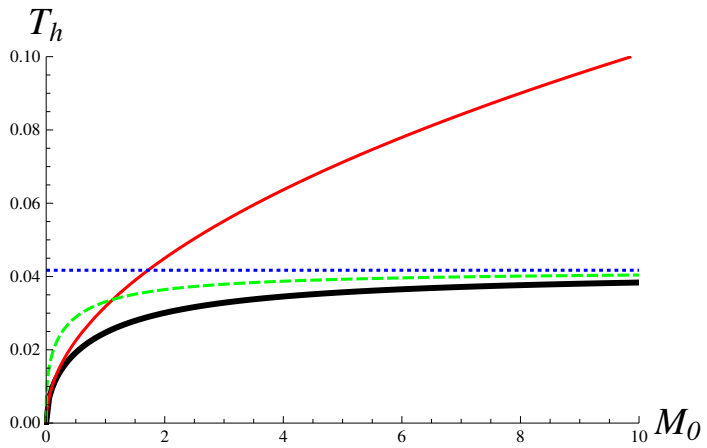

Figure 6.4: Temperature T_h as a function of M_0 for $\ell_0 = 5$, $G_0 = 1$, and $\epsilon = 0.2$. The different curves correspond to the classical case (thin solid red line), the expansion (6.36) for small G/G_0 (dashed green line), the expansion (6.37) for small G/G_0 and large $G_0 M_0$ (dotted blue line), and the numerical solution (thick solid black line). Plot from [42].

Another window for the understanding the thermodynamic properties of a black hole is its entropy. As it is well known from Brans-Dicke theory [213–217], the entropy of black hole solutions in $D+1$ spacetime dimensions with varying Newton's constant is given by

$$S = \frac{1}{4} \oint_{r=r_h} d^{D-1}x \frac{\sqrt{h}}{G(x)}, \tag{6.38}$$

where h_{ij} is the induced metric at the horizon r_h. For the present spherically symmetric solution this integral is trivial. The induced metric for constant t and r slices is simply $ds = r d\phi$ and moreover $G(x) = G(r_h)$ is constant along the horizon. Therefore, the entropy for this solution is

$$S = \frac{2\pi r_h}{4G(r_h)} = \frac{2\pi r_h}{4G_0}\left[1 + \frac{(1+G_0 M_0)\epsilon r_h}{G_0}\right]. \tag{6.39}$$

As expected, the entropy behaves differently in the two regimes highlighted above. Those two regimes can be addressed by the corresponding approximations $\epsilon \ll 1$ or $G \ll G_0$. For

very small scale dependence effects ($\epsilon \ll 1$) one finds that the $\mathcal{O}(\epsilon)$ contribution cancels out which leaves the classical entropy up to subleading corrections

$$S|_{\epsilon \ll 1} = \frac{\pi}{2}\sqrt{\frac{M_0}{G_0}}\ell_0 + \mathcal{O}(\epsilon^2). \tag{6.40}$$

This means that for small black holes, the entropy obeys the holographic principle according to the Bekenstein-Hawking law. This result can also be read directly from (6.39) in the limit of $(1 + G_0 M_0)\epsilon r_h \ll G_0$.

The opposite limit is more interesting. When $(1 + G_0 M_0)\epsilon r_h \gg G_0$ or equivalently (6.31), namely if the parameters satisfy $\frac{M_0(1+M_0G_0)^2\epsilon^2\ell_0^2}{G_0} \gg 1$, the holographic principle is not satisfied and the dominant contribution to the entropy is proportional to the area times the radius, as it can again be seen directly from (6.39). This transition from an "area law" to an "area $\times$ radius law" is a very striking consequence of the simple assumption of allowing for scale dependent couplings. Since our initial input was the condition (6.15), it would be very interesting to analyze this result in future studies in the context of the "Quantum Null Energy Conjecture" [218–222]. By insertion of (6.30) into (6.39) one can obtain the entropy in this limit as

$$S|_{G \ll G_0} \approx \pi \left[\frac{\ell_0^4 M_0^2 (1 + M_0 G_0)\epsilon}{18 G_0^2}\right]^{1/3}. \tag{6.41}$$

Please, note that by considering the case where $M_0 G_0 \gg 1$, the entropy is linear respect to the classical Black Hole mass M_0, and therefore one has:

$$S|_{G \ll G_0 \,\&\, G_0 M_0 \gg 1} \approx \ \pi M_0 \left(\frac{\ell_0^4 \epsilon}{18 G_0}\right)^{1/3}. \tag{6.42}$$

Since the entropy (6.39) is directly given from the knowledge of the horizon radius r_h it is straight forward to implement the graphical analysis of the approximations (6.30, 6.32) in comparison to the numerical result. This is done in figure 6.5. One notes again that the classical behavior is dominant for small M_0, while for large M_0 a different scaling behavior appears, which is given by the approximations (6.41 and 6.42).

Lets now come back to the physical mass of the black hole M. As the discussion above showed, the classical mass parameter M_0 is actually only the mass of the black hole if $G \to G_0$

$$M|_{G \to G_0} = M_0. \tag{6.43}$$

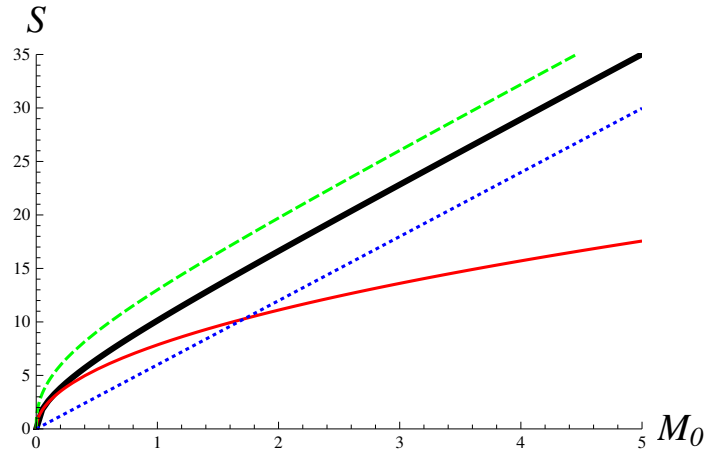

Figure 6.5: Entropy as a function of M_0 for $\ell_0 = 5$, $G_0 = 1$, and $\epsilon = 0.2$. The different curves correspond to the classical case (thin solid red line), the expansion for small G/G_0 (dashed green line), the expansion for small G/G_0 and large $G_0 M_0$ (dotted blue line), and the numerical solution (thick solid black line). Plot from [42].

In general the physical mass differs from the mass parameter, $M \neq M_0$, but it is a very difficult task to express it in a closed form. However, for the non-classical regime $G \ll G_0$ considered above, we posses analytic expressions. What is the actual mass in this regime? This question can be answered by integrating the thermodynamic relation

$$dM = TdS, \tag{6.44}$$

which yields

$$M - m = \frac{1}{4}\left(M_0 + \frac{1}{G_0} - \frac{1}{3G_0}\ln(1 + M_0 G_0)\right) \tag{6.45}$$

where m is a constant of integration independent of M_0, irrelevant for these purposes. This proves the statement claimed earlier, that for fixed values of ϵ, G_0, ℓ_0 the limit of $M_0 \to \infty$ implies, according to (6.45), that the physical mass diverges as $M \sim M_0 \to \infty$, while the horizon converges to the finite value given in (6.32).

6.4 Summary and Conclusion

We have investigate the quantum properties of the BTZ black hole, in the framework of the asymptotic safety approach. The most prominent feature is that it presents certain non-standard properties in the limit of very large mass.

A possible scale dependence of the gravitational coupling introduces an additional contribution to the stress energy tensor of the generalized field equations (6.8). By imposing that the usual "null energy condition" is not modified by this contribution it is shown that in those cases any stationary solution with spherical symmetry necessarily follows the "Schwarzschild relation" $g_{tt} = -1/g_{rr} \equiv f(r)$. Based on this observation an exact spherically symmetric black hole solution for three dimensionally gravity with scale dependent couplings is derived. It is shown that the functional form of $f(r)$, of Newtons coupling $G(r)$, and of the cosmological coupling $\ell(r)$ is completely determined by the field equations. The properties of the solution are analyzed from various perspectives. Particular attention is dedicated to a meaningful interpretation of the integration constants which is given in terms of the classical parameters G_0, ℓ_0, M_0 and one additional constant ϵ, that parametrizes the strength of scale dependence. Asymptotic spacetimes, horizon structure, and black hole thermodynamics are discussed in detail. It is found that the large r asymptotic is AdS_3 and that the $r \to 0$ asymptotic has a singular behavior. It is found that for fixed values of ϵ, G_0, ℓ_0 the horizon radius saturates for $M_0 \to \infty$ to a finite value given by (6.32). Although M_0 is not equal to the physical mass of the black hole in general, in the limit of $G \ll G_0 \,\&\, G_0 M_0 \gg 1$ the physical mass M grows without bound as $M_0 \to \infty$, while the radius of the horizon still converges to (6.32). The analysis of the thermodynamics showed another novel result. Whereas for small black holes, the usual "area law" holds up to order $\mathcal{O}(\epsilon)$, the opposite limit (which occurs when $G(r)$ deviates strongly from G_0) follows an "area $\times$ radius law". This apparent deviation from the holographic principle is probably the most interesting feature of this new black hole solution with scale dependent couplings. Finally, it would be interesting to understand this point further, since it appears that black holes with varying couplings have more entropy - and therefore more quantum microstates - than their constant coupling counterparts.

Chapter 7

Outlook

In this section we end by making more precise some further directions that we suggested in the main text.

7.1 Holographic Renyi entropies

We showed some applications of the holographic Renyi entropies to understand the phase diagram of semiclassical gravity in AdS spaces. One of the most interesting directions is to explore how the constraints coming from information theory determine some general properties of the phase diagram. It is well known that Renyi entropies satisfy the inequalities

$$\begin{aligned} S_n &\geq 0 \\ \partial_n S_n &\leq 0 \\ \partial_n \left(\frac{n-1}{n} S_n \right) &\geq 0 \\ \partial_n \left((n-1) S_n \right) &\geq 0 \\ \partial_n^2 \left((n-1) S_n \right) &\leq 0 \end{aligned}$$

Do these properties tell us some general lesson about the nature and existence of the HP transition? Does the HP transition disappear at any point? And if so, how does that occur? Is there any second order transition?

It would also be interesting to study in more detail the approximations involved in the torus partition function and go beyond the first order expansion, to see if the results

suggested by the naive extrapolation of our equations actually hold or not.

A particularly interesting direction is to understand the possibility of defining Renyi entropies in classical GR without AdS/CFT. This would indeed be very exciting, since it could find much more realistic applications within asymptotically flat or de Sitter spacetimes. The main difficulty to be overcome is to understand how to perform the replica trick in the bulk, without doing reference to the conformal boundary.

7.2 Higher spin black holes

We showed that already the spin-4 black hole has an intricate grand canonical phase diagram. At this level, an obvious question that we did not address was the exact meaning of the second order phase transition. As we know, this implies the emergence of an extra Virasoro symmetry that does not come from the original CFT symmetry but rather from a fine tuning of the potentials. On the other hand, we should also study the partition function of the higher spin CFT directly in order to exhibit, in the $c \gg 1$ regime, the same phase transitions. Moreover, the HP higher spin transition should appear as the natural generalisation of the modular invariance of the higher spin partition function.

More generally, it would be very interesting to perform the same systematic analysis that we did but for the algebra hs[λ] instead of $sl(4)$. In the case of $sl(2N)$, we expect to find phase transitions up to order N. Understanding the physics of these black holes would be very exciting.

7.3 Holographic complexity

We showed how holographic subregion complexity can be understood from its topological properties in AdS_3. It would be very interesting to further pursue the connection with compression algorithms, in particular in relation to Shannon's source coding theorem, and Schumacher's quantum version of it. These theorems give an estimate on the size of the compressed 'file' in terms of the original source, but they don not directly give a measure of how complex it is to actually perform the compression.

Although we showed a clear connection between the bulk AdS volume and the number of gates in the MERA network, this line requires further investigation. Indeed, the discrete

nature of MERA puts a limit on how close one can get with this proposal. It should be studied if better results can be achieved by using other networks, for instance the HaPPY code [223] or related graphs.

Our results concerning the Random tensor network approach leave a quite intriguing possible direction. We showed that volume complexity can be mapped to the magnetisation of the Ising model in the bulk. However, we only studied the $c \to \infty$ limit of this relation. However, it has been conjectured that the saturation of the growth of complexity should come from quantum fluctuations of the slice as it probes the region close to the singularity for a long time. This could be an analogue to the Faulkner-Lewkowycz-Maldacena result for the subleading terms in the holographic entanglement entropy,

$$S_{boundary} = \frac{\langle A \rangle}{4G} + S_{bulk} + \mathcal{O}(G) \tag{7.1}$$

Therefore, a more in-depth analysis of the finite temperature magnetisation of the spin system could shed some light on this fascinating question.

7.4 Black holes with running couplings

We exhibited the properties of black hole spacetimes in which G and Λ are allowed to have spacetime variations. A very important future work concerns checking how this approach contrasts with other quantum gravity results, namely AdS/CFT.

Also from the purely Asymptotic safety perspective, we should investigate how do our exact solutions relate to the scale-setting proposals present in the literature. Moreover, even without scale-setting, how do our black holes fit in the bigger picture of Einstein truncation? Since the RG flows are known, do these constrain in any way our solutions?

7.5 Further thoughts

In this these we have presented several aspects of the quantum properties of black holes in AdS_3.

As we saw, higher spin theories in lower dimensions exhibit a very interesting structure. Either we detect higher spin particles experimentally or not, this subject is a very interesting one to explore. If we do detect them in the near future, then there's no need

to explain the importance of this analysis. But even if experimental physics would rule them out in some way, it would still be of fundamental importance to understand exactly why is this the case in our universe.

One of the main lessons of this thesis is to acknowledge the great relevance that quantum information theory concepts have developed in recent years. Although until now the community has focused mostly in bipartite entanglement (mainly entanglement entropies), it is remains an open question to understand more sophisticated measures of entanglement on the boundary CFT and how are they related to the geometry in the bulk. As we saw, another concept new in holography and even classical gravity has been that of computational complexity. This remains largely an unexplored territory, even in QFT, where progress has just started to appear very recently, and only for non interacting theories. Moreover, it seems that Renyi entropies could have a much more important role to play, even in classical gravity. Generalising the classical theorems by Hawking and Penrose to their Renyi versions would be a fascinating area to explore. Certainly, one of the most interesting developments to follow in the next years will be this connection between quantum information and gravity.

Finally, the case for a possible UV completion of quantum gravity via a non-trivial fixed point is a possibility that should definitely be investigated further. If correct, this would point high energy physics and quantum gravity in a very different direction as has been the mainstream stringy-oriented fashion in the last decades.

Appendix A

Generalising $sl(N, \mathbb{R})$: the hs[λ] algebra

In this Appendix we summarise the construction of the hs[λ] algebra. Recall that this was relevant in the AdS_3/CFT_2 higher spin duality of Chapter 4. We follow the discussion by Mathias Gaberdiel presented at the ICTS Advanced Strings School 2015 [224].

As we already previewed, the HS theory on the gravity side is supposed to be constructed in terms of a very particular algebra called hs[λ]. We are all familiar with $sl(N)$ when N is a natural number: in the fundamental representation, this algebra contains the set of all $N \times N$ matrices of unit determinant. Is there a way to generalise this notion to *continuum* real values of $\lambda = N$?

In order to understand this algebra one must first introduce the notion of an *associative algebra*. This will be defined as

$$\frac{U(sl(2))}{\langle C^2 - \frac{1}{4}(\lambda^2 - 1)\mathbb{1}\rangle} \tag{A.1}$$

Here $U(sl(2))$ stands for the *universal enveloping* algebra of $sl(2)$. This is quotiented by the Casimir squared. Let us go step by step explaining the ingredients.

We start from the familiar $sl(2)$: we can represent the algebra by the three generators $L_\pm, L_0$ already introduced in 4.21.

In rough terms, the idea of a universal enveloping algebra is the following. Starting from a Lie algebra g (in this case $sl(2)$), we can construct an auxiliary *associative algebra* $\mathcal{A}$ such that the symplectic operation of the bracket in g corresponds simply to the

commutator $xy - yx$ in $\mathcal{A}$. Although in general there are many ways to perform this embedding, there exist a 'largest' $\mathcal{A}$, and this is defined as the universal enveloping algebra of g. One important point is that, in $\mathcal{A}$, the elements corresponding to the basis in g (i.e. the elements associated to the three generators $L_{0,\pm}$) satisfy the same commutation relations as the algebra does, *but no other relations*. What does this mean?

A neat way of describing the associative algebra is in terms of 'words'. In the example of $sl(2)$, the associative algebra will be composed of all the 'words' that one could write down using only three letters: L_0, L_+, L_-. Suppose we call these letters A, B, C respectively. Then, consider the set of words of arbitrary length, e.g. $A, BB, CBAACAC \ldots$. Next we use the commutation relations between the letters to bring any word to an canonical form, where all the A's go first, then all B's and then all C's. Then, one can associate two words by simple placing one after the other, and bringing it again into the canonical form.

The phrase above saying that in the enveloping algebra the letters satisfy no 'extra' relations means that, we cannot construct the enveloping algebra from the explicit generators $L_{0,\pm}$ since they will obey some other unwanted relations. For example, $L_0^2, L_0^4, \ldots \sim \mathbb{1}$, but we do not want the words $AA, AAAA, \ldots$ to collapse to the empty word! We wish to keep them as non trivial independent words. This implies that the enveloping algebra cannot be constructed simply using the elements of the original algebra, hence the idea of constructing 'words'. Operating in this way one can construct a (infinite) list of all possible words.

Finally there's the quotient by the Casimir. This simply means that, whenever we encounter a string of letters corresponding to the Casimir (which for $sl(2)$ is the well known total angular momentum operator $L_0^2 - \frac{1}{2}(J_+J_- + J_-J_+)$), we replace it by $\frac{\lambda^2-1}{4}$. Why would the number λ matter, if its multiplying an identity? That's because it will not in general appear as a global factor but rather as a relative factor between different words that are being identified. So different λ's will not change the vector space but they *will* change the commutators between elements.

In this way we get an infinite set of elements which serve as a basis for $U(sl(2))$. Any arbitrary unordered word can be written as linear combination of these basis vectors. Moreover, this algebra is equipped with a commutator and a multiplication of elements,

which is simply concatenating and ordering. Here's a list of the first few elements,

# of letters	words	# of elements
0	1	1
1	A,B,C	3
2	AA,AB,AC,CC,BC,BB	5
	⋮	

How does hs[λ] emerge from this construction? It turns out that every time we have an associative Lie algebra, we can construct a Lie algebra out of it: define the commutator in the Lie algebra as the commutator but *evaluate* it in the associative algebra. For $sl(2)$, the Lie algebra constructed in this way takes the form of a direct sum,

$$\mathbb{C} \oplus hs[\lambda] \tag{A.2}$$

The first term is a the trivial algebra corresponding to the subspace of 'no word'. All the rest, that is, the Lie algebra that is constructed by taking all non-trivial words and their commutators (evaluated in the associative algebra) is known as the hs[λ] algebra!

So finally: what is the relation between hs[λ] and $sl(N)$? Let us avoid very long formulas and state the result. One can compute the commutators of words of any length with other words of any other length, and write the result in the basis of hs[λ]. Now, and this is the key point, the values of the commutators depend on the value of λ as mentioned before. And in the case that λ is a natural number, many cancellations occur that produce the emergence of an *ideal* (a subspace such that the commutator of anyone else with someone in that subspace belongs to the subspace). More concretely, for $\lambda = N \in \mathbb{N}$, all generators with at least N letters form an ideal: their commutators with any generator with strictly less than N letters contains only words with at least N letters. But whenever we have a Lie algebra containing an ideal, we can quotient out that ideal to produce a subalgebra. For $\lambda = N$, this subalgebra is precisely $sl(N)$!

For example, for $\lambda = 2$, all words with two or more letters become an ideal; once we get rid of the ideal we are simply left with the three 1-letter words: that is precisely $sl(2)$! For $\lambda = 3$, all words with at least three letters form an ideal that we quotient out, and we are left with the three 1-letter words plus the five 2-letter words: together, they form $sl(3)$. An so on.

Bibliography

[1] G. Aad *et al.*, "Observation of a new particle in the search for the Standard Model Higgs boson with the ATLAS detector at the LHC," *Phys. Lett.*, vol. B716, pp. 1–29, 2012.

[2] S. Chatrchyan *et al.*, "Observation of a new boson at a mass of 125 GeV with the CMS experiment at the LHC," *Phys. Lett.*, vol. B716, pp. 30–61, 2012.

[3] B. P. e. a. Abbott, "Observation of gravitational waves from a binary black hole merger," *Phys. Rev. Lett.*, vol. 116, p. 061102, Feb 2016.

[4] B. P. e. a. Abbott, "Gw170817: Observation of gravitational waves from a binary neutron star inspiral," *Phys. Rev. Lett.*, vol. 119, p. 161101, Oct 2017.

[5] F. Englert and R. Brout, "Broken symmetry and the mass of gauge vector mesons," *Phys. Rev. Lett.*, vol. 13, pp. 321–323, Aug 1964.

[6] P. W. Higgs, "Broken symmetries, massless particles and gauge fields," *Phys. Lett.*, vol. 12, pp. 132–133, 1964.

[7] P. W. Higgs, "Broken symmetries and the masses of gauge bosons," *Phys. Rev. Lett.*, vol. 13, pp. 508–509, Oct 1964.

[8] A. Einstein, "Über Gravitationswellen," *Sitzungsberichte der Königlich Preußischen Akademie der Wissenschaften (Berlin), Seite 154-167.*, 1918.

[9] J. A. Wheeler and K. W. Ford, "Geons, Black Holes, and Quantum Foam: A Life in Physics," 1998.

[10] K. Schwarzschild, "Über das Gravitationsfeld eines Massenpunktes nach der Einsteinschen Theorie," *Sitzungsberichte der Königlich Preußischen Akademie der Wissenschaften (Berlin), 1916, Seite 189-196*, 1916.

[11] J. D. Bekenstein, "Black holes and entropy," *Phys. Rev. D*, vol. 7, pp. 2333–2346, Apr 1973.

[12] S. W. Hawking, "Particle Creation by Black Holes," *Commun. Math. Phys.*, vol. 43, pp. 199–220, 1975. [,167(1975)].

[13] S. W. Hawking, "Black hole explosions," *Nature*, vol. 248, pp. 30–31, 1974.

[14] G. W. Gibbons and S. W. Hawking, "Action Integrals and Partition Functions in Quantum Gravity," *Phys. Rev.*, vol. D15, pp. 2752–2756, 1977.

[15] S. W. Hawking and D. N. Page, "Thermodynamics of Black Holes in anti-De Sitter Space," *Commun. Math. Phys.*, vol. 87, p. 577, 1983.

[16] A. H. Guth, "Inflationary universe: A possible solution to the horizon and flatness problems," *Phys. Rev. D*, vol. 23, pp. 347–356, Jan 1981.

[17] A. D. Linde, "Inflationary Cosmology," *Lect. Notes Phys.*, vol. 738, pp. 1–54, 2008.

[18] Ya. B. Zel'dovich, A. Krasinski, and Ya. B. Zeldovich, "The Cosmological constant and the theory of elementary particles," *Sov. Phys. Usp.*, vol. 11, pp. 381–393, 1968. [Usp. Fiz. Nauk95,209(1968)].

[19] S. M. Carroll, "The Cosmological constant," *Living Rev. Rel.*, vol. 4, p. 1, 2001.

[20] M. Hobson, G. Efstathiou, and A. Lasenby, *General Relativity: An Introduction for Physicists*. Cambridge University Press, 2006.

[21] A. Castro, E. Hijano, A. Lepage-Jutier, and A. Maloney, "Black Holes and Singularity Resolution in Higher Spin Gravity," *JHEP*, vol. 01, p. 031, 2012.

[22] R. Penrose, "Gravitational collapse: The role of general relativity," *Riv. Nuovo Cim.*, vol. 1, pp. 252–276, 1969. [Gen. Rel. Grav.34,1141(2002)].

[23] P. Hayden and J. Preskill, "Black holes as mirrors: Quantum information in random subsystems," *JHEP*, vol. 09, p. 120, 2007.

[24] J. Polchinski, "The Black Hole Information Problem," in *Proceedings, Theoretical Advanced Study Institute in Elementary Particle Physics: New Frontiers in Fields and Strings (TASI 2015): Boulder, CO, USA, June 1-26, 2015*, pp. 353–397, 2017.

[25] D. Marolf, "The Black Hole information problem: past, present, and future," *Rept. Prog. Phys.*, vol. 80, no. 9, p. 092001, 2017.

[26] K. Papadodimas and S. Raju, "Black Hole Interior in the Holographic Correspondence and the Information Paradox," *Phys. Rev. Lett.*, vol. 112, no. 5, p. 051301, 2014.

[27] S. Ryu and T. Takayanagi, "Holographic Derivation of Entanglement Entropy from the anti de Sitter Space/Conformal Field Theory Correspondence," *Physical Review Letters*, vol. 96, p. 181602, May 2006.

[28] T. Hartman and J. Maldacena, "Time Evolution of Entanglement Entropy from Black Hole Interiors," *JHEP*, vol. 05, p. 014, 2013.

[29] L. Susskind, "Entanglement is not enough," *Fortsch. Phys.*, vol. 64, pp. 49–71, 2016.

[30] J. M. Maldacena, "The Large N limit of superconformal field theories and supergravity," *Int. J. Theor. Phys.*, vol. 38, pp. 1113–1133, 1999. [Adv. Theor. Math. Phys.2,231(1998)].

[31] R. Abt, J. Erdmenger, H. Hinrichsen, C. M. Melby-Thompson, R. Meyer, C. Northe, and I. A. Reyes, "Topological Complexity in AdS_3/CFT_2," *Fortsch. Phys.*, vol. 66, no. 6, p. 1800034, 2018.

[32] A. Lewkowycz and J. Maldacena, "Generalized gravitational entropy," *JHEP*, vol. 08, p. 090, 2013.

[33] X. Dong, "The Gravity Dual of Renyi Entropy," *Nature Commun.*, vol. 7, p. 12472, 2016.

[34] M. Baados, G. Dring, A. Faraggi, and I. Reyes, "Phases of higher spin black holes: Hawking-Page, transitions between black holes and a critical point," *Phys. Rev.*, vol. D96, no. 4, p. 046017, 2017.

[35] M. Alishahiha, "Holographic Complexity," *Phys. Rev.*, vol. D92, no. 12, p. 126009, 2015.

[36] P. Hayden, S. Nezami, X.-L. Qi, N. Thomas, M. Walter, and Z. Yang, "Holographic duality from random tensor networks," *JHEP*, vol. 11, p. 009, 2016.

[37] S. Weinberg, "General Relativity: An Einstein centenary survey," *CambridgeUniversity Press.*, vol. chapter 16, pp. 790–831, 1979.

[38] S. Weinberg, "Asymptotically Safe Inflation," *Phys. Rev.*, vol. D81, p. 083535, 2010.

[39] B. L. Nelson and P. Panangaden, "Scaling behavior of interacting quantum fields in curved spacetime," *Phys. Rev. D*, vol. 25, pp. 1019–1027, Feb 1982.

[40] M. Reuter and H. Weyer, "Renormalization group improved gravitational actions: A Brans-Dicke approach," *Phys. Rev.*, vol. D69, p. 104022, 2004.

[41] M. Baados and I. A. Reyes, "A short review on Noethers theorems, gauge symmetries and boundary terms," *Int. J. Mod. Phys.*, vol. D25, no. 10, p. 1630021, 2016.

[42] B. Koch, I. A. Reyes, and . Rincn, "A scale dependent black hole in three-dimensional spacetime," *Class. Quant. Grav.*, vol. 33, no. 22, p. 225010, 2016.

[43] P. A. M. Dirac, "Generalized hamiltonian dynamics," *Proceedings of the Royal Society of London. Series A, Mathematical and Physical Sciences*, vol. 246, no. 1246, pp. 326–332, 1958.

[44] T. Regge and C. Teitelboim, "Role of Surface Integrals in the Hamiltonian Formulation of General Relativity," *Annals Phys.*, vol. 88, p. 286, 1974.

[45] J. Polchinski, "Dirichlet Branes and Ramond-Ramond charges," *Phys. Rev. Lett.*, vol. 75, pp. 4724–4727, 1995.

[46] M. Ammon and J. Erdmenger, *Gauge/gravity duality*. Cambridge: Cambridge University Press, 2015.

[47] H. Nastase, *Introduction to the ADS/CFT Correspondence*. Cambridge University Press, 2015.

[48] E. Witten, "Anti-de Sitter space and holography," *Adv. Theor. Math. Phys.*, vol. 2, pp. 253–291, 1998.

[49] S. Deser, R. Jackiw, and G. 't Hooft, "Three-Dimensional Einstein Gravity: Dynamics of Flat Space," *Annals Phys.*, vol. 152, p. 220, 1984.

[50] A. Achucarro and P. Townsend, "A Chern-Simons Action for Three-Dimensional anti-De Sitter Supergravity Theories," *Phys.Lett.*, vol. B180, p. 89, 1986.

[51] E. Witten, "(2+1)-Dimensional Gravity as an Exactly Soluble System," *Nucl.Phys.*, vol. B311, p. 46, 1988.

[52] J. D. Brown and M. Henneaux, "Central charges in the canonical realization of asymptotic symmetries: an example from three dimensional gravity," *Communications in Mathematical Physics*, vol. 104, no. 2, pp. 207–226, 1986.

[53] M. Banados, C. Teitelboim, and J. Zanelli, "The Black hole in three-dimensional space-time," *Phys. Rev. Lett.*, vol. 69, pp. 1849–1851, 1992.

[54] S. Carlip, "The (2+1)-Dimensional black hole," *Class. Quant. Grav.*, vol. 12, pp. 2853–2880, 1995.

[55] S. Aminneborg, I. Bengtsson, S. Holst, and P. Peldan, "Making anti-de Sitter black holes," *Class. Quant. Grav.*, vol. 13, pp. 2707–2714, 1996.

[56] A. Strominger, "Black hole entropy from near horizon microstates," *JHEP*, vol. 02, p. 009, 1998.

[57] T. Hartman, C. A. Keller, and B. Stoica, "Universal Spectrum of 2d Conformal Field Theory in the Large c Limit," *JHEP*, vol. 09, p. 118, 2014.

[58] C. E. Shannon, "A mathematical theory of communication," *Bell System Technical Journal*, vol. 27, no. 3, pp. 379–423.

[59] A. Rnyi, "On measures of entropy and information," in *Proceedings of the Fourth Berkeley Symposium on Mathematical Statistics and Probability, Volume 1: Contributions to the Theory of Statistics*, (Berkeley, Calif.), pp. 547–561, University of California Press, 1961.

[60] M. Rangamani and T. Takayanagi, "Holographic Entanglement Entropy," *Lect. Notes Phys.*, vol. 931, pp. pp.–, 2017.

[61] D. V. Fursaev, "Proof of the holographic formula for entanglement entropy," *JHEP*, vol. 09, p. 018, 2006.

[62] H. Maxfield, S. Ross, and B. Way, "Holographic partition functions and phases for higher genus Riemann surfaces," *Class. Quant. Grav.*, vol. 33, no. 12, p. 125018, 2016.

[63] E. Witten, "Anti-de Sitter space, thermal phase transition, and confinement in gauge theories," *Adv. Theor. Math. Phys.*, vol. 2, pp. 505–532, 1998. [,89(1998)].

[64] A. Maloney and E. Witten, "Quantum Gravity Partition Functions in Three Dimensions," *JHEP*, vol. 02, p. 029, 2010.

[65] B. Chen, J.-B. Wu, and J.-j. Zhang, "Short interval expansion of Rnyi entropy on torus," *JHEP*, vol. 08, p. 130, 2016.

[66] C. Fronsdal, "Massless fields with integer spin," *Phys. Rev. D*, vol. 18, pp. 3624–3629, Nov 1978.

[67] S. Coleman and J. Mandula, "All possible symmetries of the s matrix," *Phys. Rev.*, vol. 159, pp. 1251–1256, Jul 1967.

[68] S. Weinberg, "Phenomenological Lagrangians," *Physica*, vol. A96, no. 1-2, pp. 327–340, 1979.

[69] M. A. Vasiliev, "Consistent equation for interacting gauge fields of all spins in (3+1)-dimensions," *Phys. Lett.*, vol. B243, pp. 378–382, 1990.

[70] I. R. Klebanov and A. M. Polyakov, "AdS dual of the critical O(N) vector model," *Phys. Lett.*, vol. B550, pp. 213–219, 2002.

[71] S. Giombi and X. Yin, "The Higher Spin/Vector Model Duality," *J. Phys.*, vol. A46, p. 214003, 2013.

[72] M. R. Gaberdiel and R. Gopakumar, "An AdS3 Dual for Minimal Model CFTs," *Phys. Rev.*, vol. D83, p. 066007, 2011.

[73] A. Achucarro and P. K. Townsend, "A Chern-Simons Action for Three-Dimensional anti-De Sitter Supergravity Theories," *Phys. Lett.*, vol. B180, p. 89, 1986.

[74] E. Witten, "(2+1)-Dimensional Gravity as an Exactly Soluble System," *Nucl. Phys.*, vol. B311, p. 46, 1988.

[75] M. Banados, "Three-dimensional quantum geometry and black holes," *AIP Conf.Proc.*, vol. 484, pp. 147–169, 1999.

[76] A. Campoleoni, S. Fredenhagen, S. Pfenninger, and S. Theisen, "Asymptotic symmetries of three-dimensional gravity coupled to higher-spin fields," *JHEP*, vol. 11, p. 007, 2010.

[77] M. Henneaux and S.-J. Rey, "Nonlinear $W_{infinity}$ as Asymptotic Symmetry of Three-Dimensional Higher Spin Anti-de Sitter Gravity," *JHEP*, vol. 12, p. 007, 2010.

[78] M. R. Gaberdiel and T. Hartman, "Symmetries of Holographic Minimal Models," *JHEP*, vol. 05, p. 031, 2011.

[79] R. Gopakumar.

[80] J. D. Bekenstein, "Black holes and entropy," *Physical Review D*, vol. 7, no. 8, p. 2333, 1973.

[81] J. M. Bardeen, B. Carter, and S. W. Hawking, "The four laws of black hole mechanics," *Communications in Mathematical Physics*, vol. 31, no. 2, pp. 161–170, 1973.

[82] S. W. Hawking, "Particle creation by black holes," *Communications in mathematical physics*, vol. 43, no. 3, pp. 199–220, 1975.

[83] G. W. Gibbons and S. W. Hawking, "Action integrals and partition functions in quantum gravity," *Physical Review D*, vol. 15, no. 10, p. 2752, 1977.

[84] M. Gutperle and P. Kraus, "Higher spin black holes," *Journal of High Energy Physics*, vol. 2011, no. 5, pp. 1–24, 2011.

[85] J. R. David, M. Ferlaino, and S. P. Kumar, "Thermodynamics of higher spin black holes in 3D," *JHEP*, vol. 11, p. 135, 2012.

[86] B. Chen, J. Long, and Y.-N. Wang, "Phase Structure of Higher Spin Black Hole," *JHEP*, vol. 03, p. 017, 2013.

[87] A. Chowdhury and A. Saha, "Phase Structure of Higher Spin Black Holes," *JHEP*, vol. 02, p. 084, 2015.

[88] M. Ferlaino, T. Hollowood, and S. P. Kumar, "Asymptotic symmetries and thermodynamics of higher spin black holes in AdS3," *Phys. Rev.*, vol. D88, p. 066010, 2013.

[89] B. F. Whiting and J. W. York, Jr., "Action Principle and Partition Function for the Gravitational Field in Black Hole Topologies," *Phys. Rev. Lett.*, vol. 61, p. 1336, 1988.

[90] M. Bañados, A. Castro, A. Faraggi, and J. I. Jottar, "Extremal higher spin black holes," *Journal of High Energy Physics*, vol. 4, p. 77, 2016.

[91] M. Bañados, R. Canto, and S. Theisen, "The action for higher spin black holes in three dimensions," *Journal of High Energy Physics*, vol. 2012, no. 7, pp. 1–20, 2012.

[92] C. Bunster, M. Henneaux, A. Perez, D. Tempo, and R. Troncoso, "Generalized Black Holes in Three-dimensional Spacetime," *JHEP*, vol. 05, p. 031, 2014.

[93] A. Perez, D. Tempo, and R. Troncoso, "Higher spin black hole entropy in three dimensions," *JHEP*, vol. 04, p. 143, 2013.

[94] J. de Boer and J. I. Jottar, "Thermodynamics of higher spin black holes in AdS_3," *JHEP*, vol. 01, p. 023, 2014.

[95] J. Prost, *The physics of liquid crystals*. No. 83, Oxford university press, 1995.

[96] D. Andrienko, "Introduction to liquid crystals," *IMPRS school, Bad Marienberg*, 2006.

[97] X. Zheng and P. Palffy-Muhoray, "Maier-saupe theory in four dimensions," *Physical Review E*, vol. 83, no. 4, p. 041702, 2011.

[98] A. Chamblin, R. Emparan, C. V. Johnson, and R. C. Myers, "Holography, thermodynamics and fluctuations of charged AdS black holes," *Phys. Rev.*, vol. D60, p. 104026, 1999.

[99] M. A. Nielsen, "A geometric approach to quantum circuit lower bounds," *Quantum Information and Computation*, vol. 6, pp. 213–262, May 2006.

[100] M. A. Nielsen, "A geometric approach to quantum circuit lower bounds," 2005.

[101] A. Yu. Kitaev, "Fault tolerant quantum computation by anyons," *Annals Phys.*, vol. 303, pp. 2–30, 2003.

[102] M. A. Nielsen, M. R. Dowling, M. Gu, and A. C. Doherty, "Quantum computation as geometry," *Science*, vol. 311, no. 5764, pp. 1133–1135, 2006.

[103] L. Susskind, "Computational Complexity and Black Hole Horizons," *Fortsch. Phys.*, vol. 64, pp. 44–48, 2016. [Fortsch. Phys.64,24(2016)].

[104] A. R. Brown, D. A. Roberts, L. Susskind, B. Swingle, and Y. Zhao, "Complexity, action, and black holes," *Phys. Rev.*, vol. D93, no. 8, p. 086006, 2016.

[105] R. A. Jefferson and R. C. Myers, "Circuit complexity in quantum field theory," 2017.

[106] S. Chapman, M. P. Heller, H. Marrochio, and F. Pastawski, "Towards Complexity for Quantum Field Theory States," 2017.

[107] D. Carmi, R. C. Myers, and P. Rath, "Comments on Holographic Complexity," *JHEP*, vol. 03, p. 118, 2017.

[108] G. Vidal, "Class of quantum many-body states that can be efficiently simulated," *Phys. Rev. Lett.*, vol. 101, p. 110501, Sep 2008.

[109] B. Swingle, "Entanglement Renormalization and Holography," *Phys. Rev.*, vol. D86, p. 065007, 2012.

[110] B. Czech, L. Lamprou, S. McCandlish, and J. Sully, "Tensor Networks from Kinematic Space," *JHEP*, vol. 07, p. 100, 2016.

[111] N. Bao, C. Cao, S. M. Carroll, A. Chatwin-Davies, N. Hunter-Jones, J. Pollack, and G. N. Remmen, "Consistency conditions for an AdS multiscale entanglement renormalization ansatz correspondence," *Phys. Rev.*, vol. D91, no. 12, p. 125036, 2015.

[112] M. Miyaji, T. Takayanagi, and K. Watanabe, "From path integrals to tensor networks for the AdS/CFT correspondence," *Phys. Rev.*, vol. D95, no. 6, p. 066004, 2017.

[113] B. Czech, "Einstein Equations from Varying Complexity," *Phys. Rev. Lett.*, vol. 120, no. 3, p. 031601, 2018.

[114] P. Caputa, N. Kundu, M. Miyaji, T. Takayanagi, and K. Watanabe, "Liouville Action as Path-Integral Complexity: From Continuous Tensor Networks to AdS/CFT," *JHEP*, vol. 11, p. 097, 2017.

[115] S. Ryu and T. Takayanagi, "Holographic derivation of entanglement entropy from AdS/CFT," *Phys. Rev. Lett.*, vol. 96, p. 181602, 2006.

[116] A. Almheiri, X. Dong, and D. Harlow, "Bulk Locality and Quantum Error Correction in AdS/CFT," *JHEP*, vol. 04, p. 163, 2015.

[117] F. Pastawski, B. Yoshida, D. Harlow, and J. Preskill, "Holographic quantum error-correcting codes: Toy models for the bulk/boundary correspondence," *JHEP*, vol. 06, p. 149, 2015.

[118] M. Van Raamsdonk, "Building up spacetime with quantum entanglement," *Gen. Rel. Grav.*, vol. 42, pp. 2323–2329, 2010. [Int. J. Mod. Phys.D19,2429(2010)].

[119] C. M. Papadimitriou, *Computational complexity*. Reading, Massachusetts: Addison-Wesley, 1994.

[120] A. R. Brown and L. Susskind, "The Second Law of Quantum Complexity," 2017.

[121] D. Carmi, S. Chapman, H. Marrochio, R. C. Myers, and S. Sugishita, "On the Time Dependence of Holographic Complexity," 2017.

[122] K.-Y. Kim, C. Niu, R.-Q. Yang, and C.-Y. Zhang, "Check proposals of complexity by time dependent thermofield double states," 2017.

[123] E. Bakhshaei, A. Mollabashi, and A. Shirzad, "Holographic Subregion Complexity for Singular Surfaces," 2017.

[124] P. Roy and T. Sarkar, "On subregion holographic complexity and renormalization group flows," 2017.

[125] S. Banerjee, J. Erdmenger, and D. Sarkar, "Connecting Fisher information to bulk entanglement in holography," 2017.

[126] M. Miyaji, T. Numasawa, N. Shiba, T. Takayanagi, and K. Watanabe, "Distance between Quantum States and Gauge-Gravity Duality," *Phys. Rev. Lett.*, vol. 115, no. 26, p. 261602, 2015.

[127] M. Alishahiha and A. Faraji Astaneh, "Holographic Fidelity Susceptibility," 2017.

[128] W.-C. Gan and F.-W. Shu, "Holographic complexity: A tool to probe the property of reduced fidelity susceptibility," *Phys. Rev.*, vol. D96, no. 2, p. 026008, 2017.

[129] M. Flory, "A complexity/fidelity susceptibility g-theorem for $AdS_3/BCFT_2$," *JHEP*, vol. 06, p. 131, 2017.

[130] O. Ben-Ami and D. Carmi, "On Volumes of Subregions in Holography and Complexity," *JHEP*, vol. 11, p. 129, 2016.

[131] K. Hashimoto, N. Iizuka, and S. Sugishita, "Time Evolution of Complexity in Abelian Gauge Theories - And Playing Quantum Othello Game -," 2017.

[132] R.-Q. Yang, "A Complexity for Quantum Field Theory States and Application in Thermofield Double States," 2017.

[133] B. Czech, L. Lamprou, S. McCandlish, and J. Sully, "Integral Geometry and Holography," *JHEP*, vol. 10, p. 175, 2015.

[134] T. Hartman, "Entanglement Entropy at Large Central Charge," 2013.

[135] T. Faulkner, "The Entanglement Renyi Entropies of Disjoint Intervals in AdS/CFT," 2013.

[136] V. Balasubramanian, B. D. Chowdhury, B. Czech, and J. de Boer, "Entwinement and the emergence of spacetime," *JHEP*, vol. 01, p. 048, 2015.

[137] G. Evenbly and G. Vidal, "Tensor network states and geometry," *Journal of Statistical Physics*, vol. 145, pp. 891–918, Nov 2011.

[138] G. Evenbly and G. Vidal, "Tensor network renormalization," *Phys. Rev. Lett.*, vol. 115, p. 180405, Oct 2015.

[139] D. Stanford and L. Susskind, "Complexity and Shock Wave Geometries," *Phys. Rev.*, vol. D90, no. 12, p. 126007, 2014.

[140] M. Headrick, R. C. Myers, and J. Wien, "Holographic Holes and Differential Entropy," *JHEP*, vol. 10, p. 149, 2014.

[141] J. C. Cresswell and A. W. Peet, "Kinematic Space for Conical Defects," 2017.

[142] J.-d. Zhang and B. Chen, "Kinematic Space and Wormholes," *JHEP*, vol. 01, p. 092, 2017.

[143] C. T. Asplund, N. Callebaut, and C. Zukowski, "Equivalence of Emergent de Sitter Spaces from Conformal Field Theory," *JHEP*, vol. 09, p. 154, 2016.

[144] B. Czech, L. Lamprou, S. McCandlish, and J. Sully, "Kinematic_and_real_space.nb," 2015. packaged with arXiv:1505.05515 [hep-th].

[145] P. Calabrese and J. Cardy, "Entanglement entropy and conformal field theory," *J. Phys.*, vol. A42, p. 504005, 2009.

[146] L. A. Santaló, *Integral Geometry and Geometric Probability*. Massachusetts: Addison-Wesley Publishing Company, 1976.

[147] B. Czech, J. L. Karczmarek, F. Nogueira, and M. Van Raamsdonk, "The Gravity Dual of a Density Matrix," *Class. Quant. Grav.*, vol. 29, p. 155009, 2012.

[148] C. Akers, J. Koeller, S. Leichenauer, and A. Levine, "Geometric Constraints from Subregion Duality Beyond the Classical Regime," 2016.

[149] A. Peres, "Separability criterion for density matrices," *Phys. Rev. Lett.*, vol. 77, pp. 1413–1415, 1996.

[150] P. Caputa, N. Kundu, M. Miyaji, T. Takayanagi, and K. Watanabe, "Anti-de Sitter Space from Optimization of Path Integrals in Conformal Field Theories," *Phys. Rev. Lett.*, vol. 119, no. 7, p. 071602, 2017.

[151] D. Carmi, "More on Holographic Volumes, Entanglement, and Complexity," 2017.

[152] J. A. Wheeler, "On the Nature of quantum geometrodynamics," *Annals Phys.*, vol. 2, pp. 604–614, 1957.

[153] S. Deser and B. Zumino, "Consistent Supergravity," *Phys. Lett.*, vol. B62, p. 335, 1976.

[154] C. Rovelli, "Loop quantum gravity," *Living Rev. Rel.*, vol. 1, p. 1, 1998.

[155] L. Bombelli, J. Lee, D. Meyer, and R. Sorkin, "Space-Time as a Causal Set," *Phys. Rev. Lett.*, vol. 59, pp. 521–524, 1987.

[156] A. Ashtekar, "Gravity and the quantum," *New J. Phys.*, vol. 7, p. 198, 2005.

[157] A. D. Sakharov, "Vacuum quantum fluctuations in curved space and the theory of gravitation," *Sov. Phys. Dokl.*, vol. 12, pp. 1040–1041, 1968. [Gen. Rel. Grav.32,365(2000)].

[158] T. Jacobson, "Thermodynamics of space-time: The Einstein equation of state," *Phys. Rev. Lett.*, vol. 75, pp. 1260–1263, 1995.

[159] E. P. Verlinde, "On the Origin of Gravity and the Laws of Newton," *JHEP*, vol. 04, p. 029, 2011.

[160] M. Reuter, "Nonperturbative evolution equation for quantum gravity," *Phys. Rev.*, vol. D57, pp. 971–985, 1998.

[161] D. F. Litim, "Fixed points of quantum gravity," *Phys. Rev. Lett.*, vol. 92, p. 201301, 2004.

[162] P. Horava, "Quantum Gravity at a Lifshitz Point," *Phys. Rev.*, vol. D79, p. 084008, 2009.

[163] C. Charmousis, G. Niz, A. Padilla, and P. M. Saffin, "Strong coupling in Horava gravity," *JHEP*, vol. 08, p. 070, 2009.

[164] A. Ashtekar, "Asymptotic Quantization of the Gravitational Field," *Phys. Rev. Lett.*, vol. 46, pp. 573–576, 1981.

[165] R. Penrose and W. Rindler, *SPINORS AND SPACE-TIME. VOL. 2: SPINOR AND TWISTOR METHODS IN SPACE-TIME GEOMETRY*. Cambridge University Press, 1988.

[166] A. Connes, "Gravity coupled with matter and foundation of noncommutative geometry," *Commun. Math. Phys.*, vol. 182, pp. 155–176, 1996.

[167] P. Nicolini, "Noncommutative Black Holes, The Final Appeal To Quantum Gravity: A Review," *Int. J. Mod. Phys.*, vol. A24, pp. 1229–1308, 2009.

[168] R. Gambini and J. Pullin, "Consistent discretization and loop quantum geometry," *Phys. Rev. Lett.*, vol. 94, p. 101302, 2005.

[169] C. Kiefer, "Quantum gravity: General introduction and recent developments," *Annalen Phys.*, vol. 15, pp. 129–148, 2005. [Annalen Phys.518,129(2006)].

[170] A. Zichichi, S. (Region), S. (Italy), and M. aitsman le mada, *Understanding the Fundamental Constituents of Matter: Proceedings of the 1976 International School of Subnuclear Physics (NATO-MPI-MRST Advanced Study Institute) Held in Erice, Trapani, Sicily, July 23-August 8, 1976 and Sponsored by the Sicilian Regional Government and the Weizmann Institute of Science*. Subnuclear Series, Plenum Press, 1978.

[171] C. Wetterich, "Exact evolution equation for the effective potential," *Phys. Lett.*, vol. B301, pp. 90–94, 1993.

[172] D. Dou and R. Percacci, "The running gravitational couplings," *Class. Quant. Grav.*, vol. 15, pp. 3449–3468, 1998.

[173] W. Souma, "Nontrivial ultraviolet fixed point in quantum gravity," *Prog. Theor. Phys.*, vol. 102, pp. 181–195, 1999.

[174] M. Reuter and F. Saueressig, "Renormalization group flow of quantum gravity in the Einstein-Hilbert truncation," *Phys. Rev.*, vol. D65, p. 065016, 2002.

[175] P. Fischer and D. F. Litim, "Fixed points of quantum gravity in extra dimensions," *Phys. Lett.*, vol. B638, pp. 497–502, 2006.

[176] R. Percacci, "Asymptotic Safety," 2007.

[177] D. F. Litim, "Fixed Points of Quantum Gravity and the Renormalisation Group," 2008. [PoSQG-Ph,024(2007)].

[178] J. Alexandre, "BUSSTEPP lecture notes: Exact Wilsonian Renormalisation," 2015.

[179] A. Nink, April.

[180] I. G. Avramidi, "Heat kernel and quantum gravity," *Lect. Notes Phys.*, vol. M64, pp. 1–149, 2000.

[181] M. Demmel, F. Saueressig, and O. Zanusso, "Fixed-Functionals of three-dimensional Quantum Einstein Gravity," *JHEP*, vol. 11, p. 131, 2012.

[182] S. Nojiri and S. D. Odintsov, "Effective Lagrangian and static black holes in 2-D dilatonic gravity," *Mod. Phys. Lett.*, vol. A12, pp. 925–936, 1997.

[183] A. Bonanno and M. Reuter, "Quantum gravity effects near the null black hole singularity," *Phys. Rev.*, vol. D60, p. 084011, 1999.

[184] A. Bonanno and M. Reuter, "Renormalization group improved black hole space-times," *Phys. Rev.*, vol. D62, p. 043008, 2000.

[185] A. Bonanno and M. Reuter, "Spacetime structure of an evaporating black hole in quantum gravity," *Phys. Rev.*, vol. D73, p. 083005, 2006.

[186] M. Reuter and E. Tuiran, "Quantum Gravity Effects in Rotating Black Holes," in *Recent developments in theoretical and experimental general relativity, gravitation and relativistic field theories. Proceedings, 11th Marcel Grossmann Meeting, MG11, Berlin, Germany, July 23-29, 2006. Pt. A-C*, pp. 2608–2610, 2006.

[187] B. Koch, "Renormalization group and black hole production in large extra dimensions," *Phys. Lett.*, vol. B663, pp. 334–337, 2008.

[188] T. Burschil and B. Koch, "Renormalization group improved black hole space-time in large extra dimensions," *Zh. Eksp. Teor. Fiz.*, vol. 92, pp. 219–225, 2010. [JETP Lett.92,193(2010)].

[189] K. Falls, D. F. Litim, and A. Raghuraman, "Black Holes and Asymptotically Safe Gravity," *Int. J. Mod. Phys.*, vol. A27, p. 1250019, 2012.

[190] Y.-F. Cai and D. A. Easson, "Black holes in an asymptotically safe gravity theory with higher derivatives," *JCAP*, vol. 1009, p. 002, 2010.

[191] D. F. Litim, "Renormalisation group and the Planck scale," *Phil. Trans. Roy. Soc. Lond.*, vol. A369, pp. 2759–2778, 2011.

[192] P. Nicolini and E. Winstanley, "Hawking emission from quantum gravity black holes," *JHEP*, vol. 11, p. 075, 2011.

[193] D. Becker and M. Reuter, "Running boundary actions, Asymptotic Safety, and black hole thermodynamics," *JHEP*, vol. 07, p. 172, 2012.

[194] D. Becker and M. Reuter, "Asymptotic Safety and Black Hole Thermodynamics," in *Proceedings, 13th Marcel Grossmann Meeting on Recent Developments in Theoretical and Experimental General Relativity, Astrophysics, and Relativistic Field Theories (MG13)*, pp. 2230–2232, 2015.

[195] K. Falls and D. F. Litim, "Black hole thermodynamics under the microscope," *Phys. Rev.*, vol. D89, p. 084002, 2014.

[196] C. Contreras, B. Koch, and P. Rioseco, "Black hole solution for scale-dependent gravitational couplings and the corresponding coupling flow," *Class. Quant. Grav.*, vol. 30, p. 175009, 2013.

[197] B. Koch and F. Saueressig, "Structural aspects of asymptotically safe black holes," *Class. Quant. Grav.*, vol. 31, p. 015006, 2014.

[198] B. Koch, C. Contreras, P. Rioseco, and F. Saueressig, "Black holes and running couplings: A comparison of two complementary approaches," *Springer Proc. Phys.*, vol. 170, pp. 263–269, 2016.

[199] B. Koch and F. Saueressig, "Black holes within Asymptotic Safety," *Int. J. Mod. Phys.*, vol. A29, no. 8, p. 1430011, 2014.

[200] B. Koch and P. Rioseco, "Black Hole Solutions for Scale Dependent Couplings: The de Sitter and the Reissner-Nordström Case," *Class. Quant. Grav.*, vol. 33, p. 035002, 2016.

[201] D. C. Rodrigues, B. Koch, O. F. Piattella, and I. L. Shapiro, "The bending of light within gravity with large scale renormalization group effects," *AIP Conf. Proc.*, vol. 1647, pp. 57–61, 2015.

[202] C. Gonzalez and B. Koch, "Improved Reissner-Nordstrom-(A)dS Black Hole in Asymptotic Safety," 2015.

[203] B. Koch and I. Ramirez, "Exact renormalization group with optimal scale and its application to cosmology," *Class. Quant. Grav.*, vol. 28, p. 055008, 2011.

[204] S. Domazet and H. Stefancic, "Renormalization group scale-setting from the action - a road to modified gravity theories," *Class. Quant. Grav.*, vol. 29, p. 235005, 2012.

[205] B. Koch, P. Rioseco, and C. Contreras, "Scale Setting for Self-consistent Backgrounds," *Phys. Rev.*, vol. D91, no. 2, p. 025009, 2015.

[206] C. Contreras, B. Koch, and P. Rioseco, "Setting the Renormalization Scale in QFT," *J. Phys. Conf. Ser.*, vol. 720, no. 1, p. 012020, 2016.

[207] R. M. Wald, *General Relativity.* Chicago, Usa: Univ. Pr. 491p, 1984.

[208] V. A. Rubakov, "The Null Energy Condition and its violation," *Phys. Usp.*, vol. 57, pp. 128–142, 2014.

[209] M. Parikh and A. Svesko, "Thermodynamic Origin of the Null Energy Condition," 2015.

[210] M. Heusler, "No hair theorems and black holes with hair," *Helv. Phys. Acta*, vol. 69, pp. 501–528, 1996.

[211] J. M. Bardeen, B. Carter, and S. W. Hawking, "The Four laws of black hole mechanics," *Commun. Math. Phys.*, vol. 31, pp. 161–170, 1973.

[212] T. Jacobson, "When is g(tt) g(rr) = -1?," *Class. Quant. Grav.*, vol. 24, pp. 5717–5719, 2007.

[213] T. Jacobson, G. Kang, and R. C. Myers, "On black hole entropy," *Phys. Rev.*, vol. D49, pp. 6587–6598, 1994.

[214] V. Iyer and R. M. Wald, "A Comparison of Noether charge and Euclidean methods for computing the entropy of stationary black holes," *Phys. Rev.*, vol. D52, pp. 4430–4439, 1995.

[215] M. Visser, "Dirty black holes: Entropy as a surface term," *Phys. Rev.*, vol. D48, pp. 5697–5705, 1993.

[216] J. D. E. Creighton and R. B. Mann, "Quasilocal thermodynamics of dilaton gravity coupled to gauge fields," *Phys. Rev.*, vol. D52, pp. 4569–4587, 1995.

[217] G. Kang, "On black hole area in Brans-Dicke theory," *Phys. Rev.*, vol. D54, pp. 7483–7489, 1996.

[218] R. Bousso and N. Engelhardt, "Generalized Second Law for Cosmology," *Phys. Rev.*, vol. D93, no. 2, p. 024025, 2016.

[219] R. Bousso, Z. Fisher, S. Leichenauer, and A. C. Wall, "Quantum focusing conjecture," *Phys. Rev.*, vol. D93, no. 6, p. 064044, 2016.

[220] J. Koeller and S. Leichenauer, "Holographic Proof of the Quantum Null Energy Condition," 2015.

[221] R. Bousso, Z. Fisher, J. Koeller, S. Leichenauer, and A. C. Wall, "Proof of the Quantum Null Energy Condition," *Phys. Rev.*, vol. D93, no. 2, p. 024017, 2016.

[222] Z. Fu and D. Marolf, "Does horizon entropy satisfy a Quantum Null Energy Conjecture?," 2016.

[223] F. Pastawski, B. Yoshida, D. Harlow, and J. Preskill, "Holographic quantum error-correcting codes: Toy models for the bulk/boundary correspondence," *JHEP*, vol. 06, p. 149, 2015.

[224] M. Gaberdiel.